

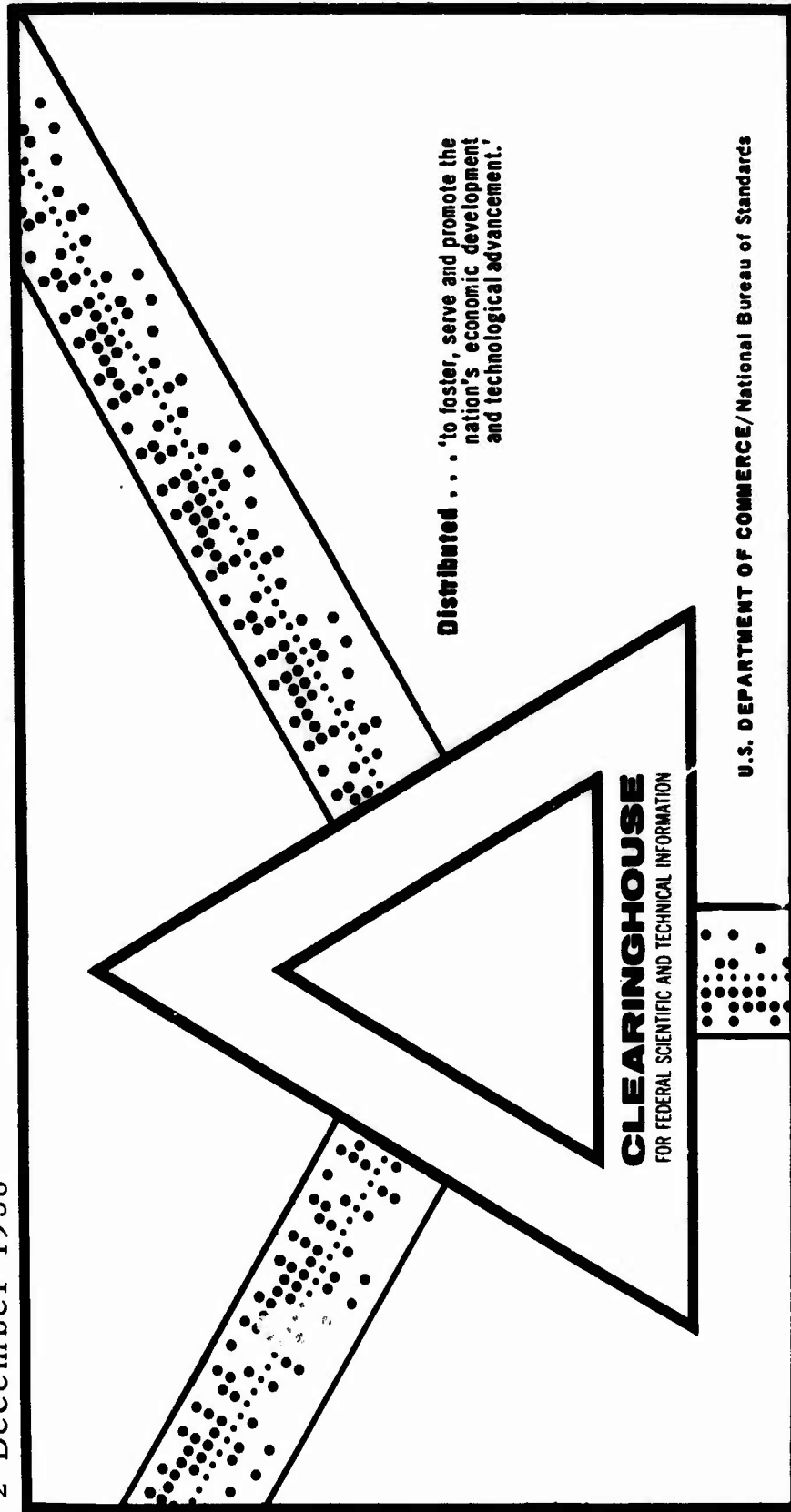
AD 702 233

FRAGMENTATION EFFECTS OF THE 75 mm H. E. SHELL T3 (M48) AS
DETERMINED BY PANEL AND PIT FRAGMENTATION TESTS

N. A. Tolch

Ballistic Research Laboratories
Aberdeen Proving Ground, Maryland

2 December 1938



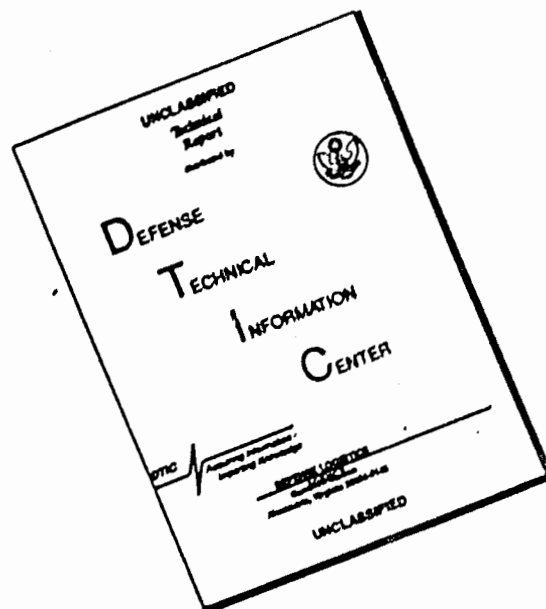
CLEARINGHOUSE
FOR FEDERAL SCIENTIFIC AND TECHNICAL INFORMATION

Distributed . . . to foster, serve and promote the
nation's economic development
and technological advancement.

U.S. DEPARTMENT OF COMMERCE/National Bureau of Standards

This document has been approved for public release and sale.

DISCLAIMER NOTICE



THIS DOCUMENT IS BEST QUALITY AVAILABLE. THE COPY FURNISHED TO DTIC CONTAINED A SIGNIFICANT NUMBER OF PAGES WHICH DO NOT REPRODUCE LEGIBLY.

AD 702233

BRL R 126

BRL

AD

REPORT NO. 126

**FRAGMENTATION EFFECTS OF THE 75MM H. E. SHELL T3 (M48)
AS DETERMINED BY PANEL AND PIT FRAGMENTATION TESTS**

by

N. A. Tolch

December 1938



This document has been approved for public release and sale;
its distribution is unlimited.

Reproduced by the
CLEARINGHOUSE
for Federal Scientific & Technical
Information Springfield Va. 22151

**U.S. ARMY ABERDEEN RESEARCH AND DEVELOPMENT CENTER
BALLISTIC RESEARCH LABORATORIES
ABERDEEN PROVING GROUND, MARYLAND**

81

ACCESSION FOR	
CPSTI	WHITE SECTION <input checked="" type="checkbox"/>
DDG	BUFF SECTION <input type="checkbox"/>
UNANNOUNCED	<input type="checkbox"/>
JUSTIFICATION	
BY	
SECTION NUMBER/WORKLOAD CODES	
REPT.	ANAL. and/or SPECIAL
<input checked="" type="checkbox"/>	<input type="checkbox"/>

Ballistic Research
Laboratory Report No. 126

NAT/emh
Aberdeen Proving Ground, Md.
December 2, 1938

FRAGMENTATION EFFECTS OF THE 75 MM H.E. SHELL T3 (M48)
AS DETERMINED BY PANEL AND PIT FRAGMENTATION TESTS

Project KR 221 - Determination of the fragmentation
effect of the 75 mm H.E. Shell T3

Abstract

By fragmentation firings in semi-circular wood panels, the fragment density was determined as a function of the angle with the axis of the shell, the distance, and the remaining velocity. Considering the fragment densities with regard to the angle with the shell axis, the fragments are concentrated in three main classes, commonly designated as nose, side, and base sprays. With regard to the variable of distance, the densities decrease with the distance, the decrease in total number of hits in the side spray averaging about 55% between the 15 and 120 ft. panels. The general effect of remaining velocity is to reduce the number of fragments in the base spray, to shift the side spray forward, and to increase the number of fragments in the nose spray.

The total number of fragments of a shell recorded in the panel tests is about 5000, while the number of fragments obtained in pit fragmentation tests averaged about 780. It appears that practically all of the fragments recovered in pit tests would be perforating fragments in panel tests.

As determined by the change in the angle of the side spray with change in remaining velocity, the velocity of the perforating fragments due to the explosive charge averaged 2740 f/s. while that of the penetrating fragments was 3030 f/s. It appears that the greater initial velocity of the penetrating fragments is due to their smaller size, or more particularly to their smaller ballistic coefficients.

The general method of evaluating the fragmentation effect of shell in the present program of test consisted of determining the fragment density as a function of three variables, namely, the direction from the

burst, the distance, and the remaining velocity of the shell. From the results of the tests with the 75 mm shell, the method of test, in general, seems to accomplish the desired objective. However, tentative suggestions for improvement are that the number of rounds per shell condition be increased, that the number of conditions of test be decreased, and that firings with shell axis vertical be eliminated except in the 15 ft. panel.

Introduction

The effectiveness of an H. E. Shell is determined by its capacity to produce casualties. Consequently, the fundamental object of a fragmentation program should be to evaluate or measure the capacity of the shell for producing casualties. The general method of evaluation in the present program consisted of determining the fragment density as a function of three variables, the direction from the burst, the distance, and the remaining velocity of the shell. The density as a function of direction was studied by firings in semi-circular panels, thereby cutting out samples symmetrical through 360 deg. normal to the shell axis. The effect of distance was obtained by varying the radius of the panels. The variable of remaining velocity as regards fragment density was measured by bursting the shell within the panels at various remaining velocities.

Having determined the fragment density as a function of the direction, the distance, and the shell velocity, the hits on various distributions of targets may be calculated, the effects of such factors as angle of fall and height of burst becoming matters of computation. However, merely the determination of the number of hits is not sufficient information; it is necessary to know the number of casualty producing hits. For this purpose the kinds of hits on the panels were determined and the hits classed as perforating, penetrating, or denting. The correlation of the kind of hit with respect to its ability to produce a casualty is not as yet as well known as might be desired. While perforating hits on wood panels have been generally accepted as effective, there appears to be need for experiments regarding the ability of various kinds of fragments to produce casualties.

A series of fragmentation firings has been made with the 75 mm T3 shell and the 105 mm M1 shell. The present report deals with the results with the 75 mm shell, the results with the 105 mm shell being reserved for a separate report. Although 75 mm T3 shell were used in the tests, the results may be applied to the 75 mm M48 shell because the two models are identical except for slight differences in the rotating bands.

Suggestions for improvement of the method.

Although the results with the 105 mm M1 shell remain to be reported, a preliminary examination of the data indicate that the differences between the 75 and the 105 mm shell are largely a matter of magnitude rather than kind. Consequently, it appears desirable to make tentative suggestions regarding improvement of the method subject to further revision when all the data have been studied.

The choice of panel radii of 15, 36, 75, and 120 ft. seems to be satisfactory. While the total number of hits per unit solid angle is still appreciable at 120 ft. distance, an increase of panel radius does not seem practical. At great distances from the burst, very high panels are necessary in order to obtain suitable samples sizes. For shell as large as 155 mm it appears to be necessary to eliminate the 15 ft. panel, because there was considerable wear on this panel even with the 105 mm shell.

In general, 5 rounds were used in the panel tests for a given shell condition although in a few instances 2 rounds were used. On study of the data, it appears that a larger number of rounds for a given condition of test is desirable in order to obtain greater precision in measurement of fragment distribution. A minimum of 10 rounds per condition is tentatively recommended.

The remaining velocity of shell used in battle will in most instances be around 800 to 900 f/s, being very rarely less than 700 nor more than 1100 f/s. Consequently, for routine panel tests, it appears that two remaining velocities, for instance 700 and 1100 f/s together with static firings should be sufficient, obtaining intermediate values by interpolation.

Firings with shell axis vertical appear to be useful at 15 ft. distance from the burst where the panel height is sufficient to sample the complete width of the sidespray band. At panel distances greater than 15 ft., firings with shell axis vertical are not recommended because the panels sample only a small portion of the sidespray with respect to the shell axis, although a sample is obtained through 180 deg. perpendicular to the axis.

Results of Pit Fragmentation Tests

Four shells were detonated in the sand pit. In this test, the shells are placed centrally in wood boxes, providing an air space between shell and box. Rounds 1 and 2 were

fired in boxes of such dimensions as to result in a nominal air space of 3 calibers between shell and box although somewhat more at the corners of the box due to its square cross section. Rounds 3 and 4 were fired in boxes giving a nominal air space of 6 calibers. Following detonation of the shell, the fragments are separated from the sand with a hand screen having 4 meshes to the inch, diameter of wire .03 inches, giving square openings of .22 inches on a side. The sizes of the screens used for screening the fragments were measured as to wire diameter and opening with the following average results.

<u>Screen No.</u>	<u>Meshes per inch</u>	<u>Diam. of wire, inches</u>	<u>Size of Opening, Side, inches</u>	<u>Area, sq. in</u>
1	1	.16	.84	.71
2	2	.14	.36	.13
3	3	.10	.23	.053
4	4	.08	.17	.029

It is noted that the openings of the hand screen are slightly larger than those of the No. 4 screen. It appears that the size of openings of the hand screen should be smaller in order to make a true separation of fragments on the No. 4 screen.

The fragments are shaken through the screens with the exception that those fitting the openings rather closely are put through by hand. The purpose of this hand separation is to avoid retaining long fragments on a screen when their sectional dimensions permit them to go through.

In addition to the screen tests the least number of fragments making up 60% of the weight of the empty shell and fuze is determined. In this test, the largest fragments are first picked out, selecting progressively smaller pieces until 60% of the original weight of metal is obtained. This test was used exclusively up till 1925 for pit fragmentation work and since then has been made in conjunction with screen tests so that present day results may be compared with older ones.

The following table shows the data obtained by the pit fragmentation tests:

**Pit Fragmentation Tests of 75 mm T3 Shell from 75 mm
Pack Howitzer Complete Rounds, Shell Lot 2761-3**

Round No.	1	2	3	4
Wt. loaded unfuzed shell	12.50	12.50	12.47	12.53
Fuze (M39 P.D.) Wt., lbs.	2.35	2.35	2.35	2.36
Wt. of TNT charge (ave.) lbs.	1.56	1.56	1.56	1.56
Wt. empty shell & fuze, lbs.	13.29	13.29	13.26	13.33
Fragments caught by following screens:				
Screen No. 1: No.	7	7	5	6
Wt., lbs.	2.073	2.007	1.987	2.104
Screen No. 2: No.	285	244	254	303
Wt., lbs.	8.654	8.668	8.169	8.305
Screen No. 3: No.	252	256	213	300
Wt., lbs.	1.487	1.739	1.807	1.820
Screen No. 4: No.	128	89	171	180
Wt., lbs.	0.246	0.235	0.577	0.399
Through Screen No. 4: No.	114	104	108	89
Wt. lbs.	0.109	0.159	0.231	0.057
No. fragments recovered	786	700	751	878
Wt. " " , lbs.	12.569	12.809	12.772	12.685
% metal recovered	94.6	96.4	96.3	95.2
No. fragments in 60% Wt. Metal	131	117	130	157

As regards the effect of air spacing the tests do not show any significant difference. The explanation appears to be that the difference between 3 and 6 calibers of air space is rather small in fragmentation effect and that a large number of rounds would be required to distinguish between them.

Since the difference in fragmentation effect between the two air spaces appears to be negligible as far as the tests show, the results of the 4 rounds were averaged together. The following table shows the average number and distribution of fragments:

Fragments caught by following screens: (Ave. of 4 rds.)	No. frag- ments	% of total no. of frag- ments	Wt. of frag- ments, lbs.	% of empty shell & fuze
Screen No. 1	6	.8	2.043	15.4
" " 2	272	34.9	8.449	63.6
" " 3	255	32.7	1.713	12.9
" " 4	142	18.2	.364	2.7
Thru Screen No. 4	104	13.4	.139	1.0
	779	100.0	12.708	95.6

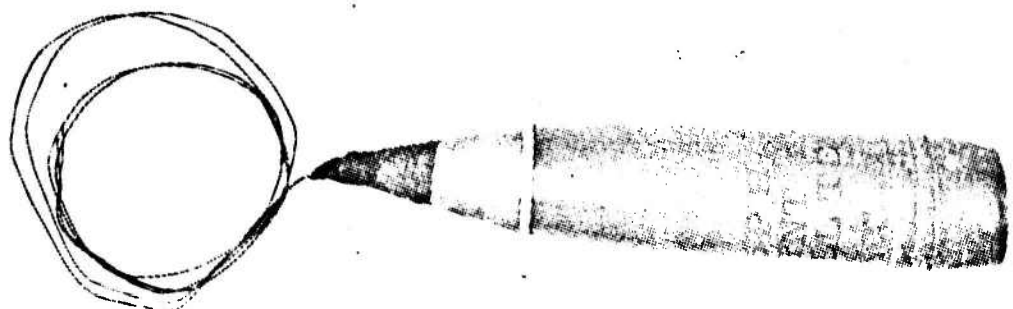
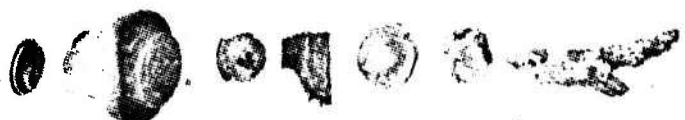
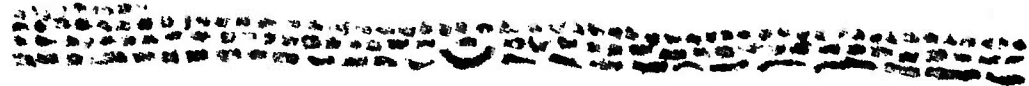
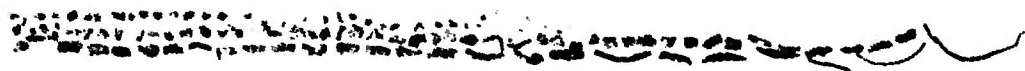
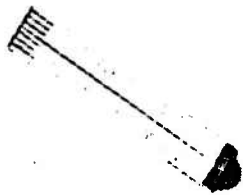
From the above table, about 96% of the weight of metal was recovered in the screen tests. The fragments caught on No. 1 screen are few in number but an appreciable part of the original shell weight, about 15%. These fragments are mostly pieces of fuze. The most numerous and by far the heaviest group of fragments is retained on the No. 2 screen comprising about 35% of the number and 64% of the weight of metal. Thus the fragments caught on screens 1 and 2 make up 79% of the original weight of metal but only 36% of the total number of fragments recovered.

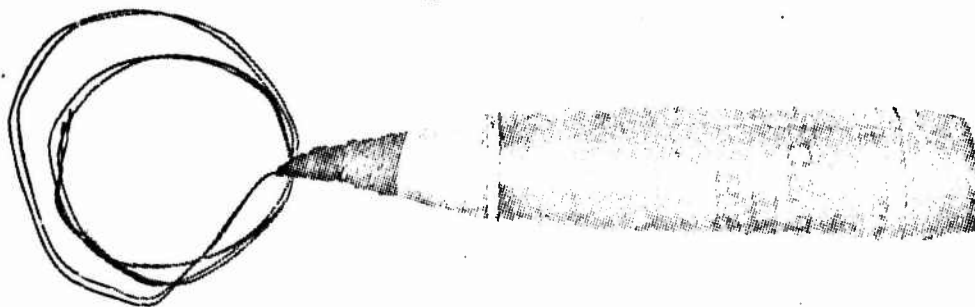
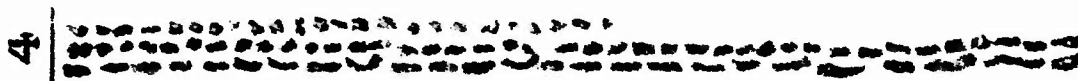
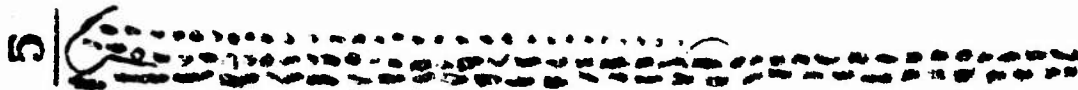
Photographs APG Nos. 34514-17 on pages 7, 8, 9 and 10 show the fragments grouped according to size.

Description of Panel Tests

Four panels designated Panels A, B, C and D having radii of 15, 36, 75, and 120 ft. respectively were used in the tests. They were made out of spruce boards having a nominal thickness of 1". The two layouts of panels on pages 11 and 12 show the arrangement as to length, height, and division into numbered squares. The panels were built in concentric pairs in order to obtain data at two distances from the burst on the same round. Panel D contained about 45° of opening which was sufficient to include the sidespray up to remaining velocities of 1100 f/s. The remaining portion of a semi-circle was not built because of the large amount of material required for a panel at 120 ft. radius and also because the nose and base sprays are, in general, not as important as the side spray. Earth embankments were built within the area inclosed by the panel at heights just sufficient to prevent fragments from ricocheting and striking the panels.

The shell were detonated at the center of the panels at a height midway between the top and bottom with the exception that a few rounds with shell axis vertical were detonated at greater heights in order to hit Panels C and D with the dense part of the side spray. The shell were







ORDNANCE DEPARTMENT
516 1925
67 1925

5

[Illegible text]

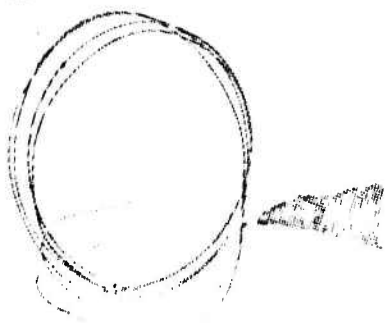
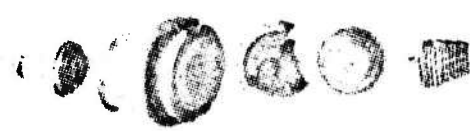
4

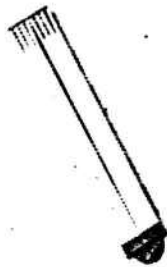
[Illegible text]

3

[Illegible text]

[Illegible text]





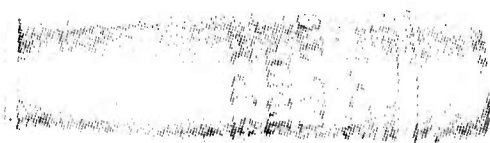
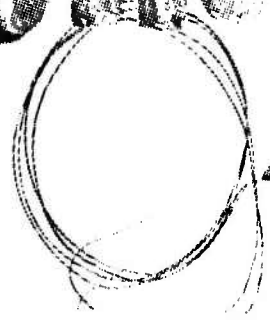
5

.....

.....

.....

.....



PANEL "A"
15 FT. RADIUS 180° ARC

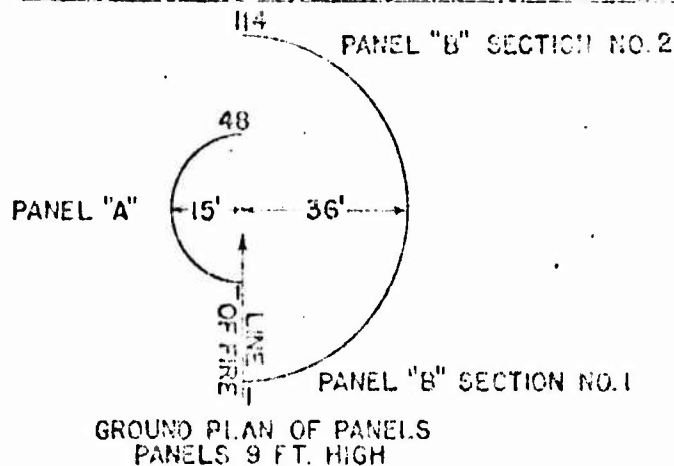
1	4	7	10	13	16	19	22	25	28	31	34	37	40	43	46
2	5	8	11	14	17	20	23	26	29	32	35	38	41	44	47
3	6	9	12	15	18	21	24	27	30	33	36	39	42	45	48

PANEL "B"
SECTION NO. 1
36 FT. RADIUS 90° ARC

1	4	7	10	13	16	19	22	25	28	31	34	37	40	43	46	49	52	55
2	5	8	11	14	17	20	23	26	29	32	35	38	41	44	47	50	53	56
3	6	9	12	15	18	21	24	27	30	33	36	39	42	45	48	51	54	57

PANEL "B"
SECTION NO. 2
36 FT. RADIUS 90° ARC

58	61	64	67	70	73	76	79	82	85	88	91	94	97	100	103	106	109	112
59	62	65	68	71	74	77	80	83	86	89	92	95	98	101	104	107	110	113
60	63	66	69	72	75	78	81	84	87	90	93	96	99	102	105	108	111	114



X = HITS WHICH JUST DENTED WOOD
 □ = HITS WHICH PENETRATED WOOD
 O = HITS WHICH PERFORATED WOOD
 TOTAL X = _____
 TOTAL □ = _____
 TOTAL O = _____

DATE _____
 GUN _____
 RD. NO. _____
 SHELL _____
 POSITION OF SHELL _____

LAYOUT OF PANELS
 AT
 PLATE RANGE
 FOR
 NUMBER, VELOCITY
 AND
 DISTRIBUTION OF FRAGMENTS
 ABERDEEN PROVING GROUND, MD.
 OCT. 28, 1937
 A.P.G. 7303 P.R.

PANEL C
75 FT. RADIUS

1	3	5	7	9	11	13	15	17	19	21	23	25	27	29	31	33	35	37	39
2	4	6	8	10	12	14	16	18	20	22	24	26	28	30	32	34	36	38	40
41	43	45	47	49	51	53	55	57	59	61	63	65	67	69	71	73	75	77	79
42	44	46	48	50	52	54	56	58	60	62	64	66	68	70	72	74	76	78	80

PART 2
PART 1

162 FT.

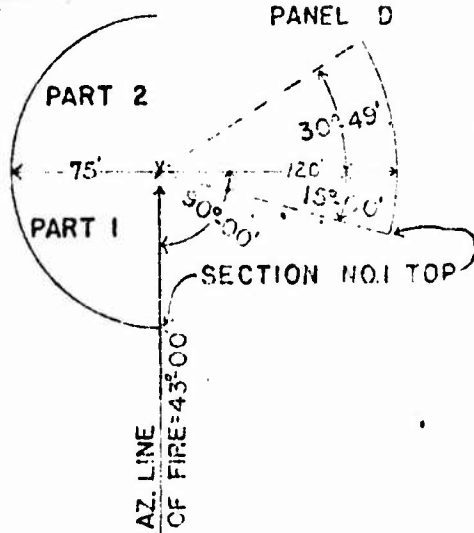
PANEL D
120 FT. RADIUS

1	3	5	7	9	11	13	15	17	19	21	23	25	27	29	31
---	---	---	---	---	----	----	----	----	----	----	----	----	----	----	----

NOT REPRODUCIBLE

PANEL C

PANEL D



GROUND PLAN OF PANELS
PANELS 12 FT. HIGH

DATE _____
GUN _____
RD. NO. _____
SHELL _____
POSITION OF SHELL _____

LAYOUT OF PANELS
AT
PLATE RANGE
FOR
NUMBER, VELOCITY
AND
DISTRIBUTION OF FRAGMENTS

ABERDEEN PROVING GROUND, MD.
APR 28, 1937. A. P. G. 7251 P. R.

fired with axis horizontal and also vertical, statically and at various remaining velocities when burst. The following table shows the conditions under which the rounds were fired:

Position of shell axis	Average remaining velocity when burst, f/s	Number of rounds on Panels A & B	Number of rounds on Panels C & D
Horizontal	0	5	5
Vertical, nose down	0	2	0
" base down	0	3	3
Horizontal	700	5	5
"	1087	5	5
"	1450	2	0
"	1685	2	5
"	2130	2	5

Following the firing of a round, the perforations, penetrations, and dents on each square on the panels were counted. A perforating fragment is defined as one that travels completely through the panel, while a penetrating fragment is one that travels only part way through. A denting fragment is one that merely makes an indentation in the wood without appreciable penetration. The division between penetrations and dents was set at 1/16" classing anything less as dents. The cross-sectional dimensions of the perforations and penetrations were measured, also the depth of the penetrations. Following the collection of the data from the panels, the marks left by the fragments were painted over in order to distinguish them from those of the next round.

Having obtained the kind and number of hits on the panels, the results were expressed in terms of hits per unit solid angle. A unit solid angle is defined as the solid angle subtended by a unit of spherical surface at unit radius. The number of unit solid angles subtended by an area of A sq. yds. at R yds. distance is $\frac{A}{R^2}$. However,

it has been found more convenient to use a smaller unit in fragmentation work. In Aberdeen Proving Ground reports, it has been customary to use 1/100 of the above unit, which makes the unit solid angle in our work equivalent to the solid angle subtended by 1 sq. yd. at 10 yds. distance. Hence, if there are n hits on area A, the hits per unit

solid angle is equal to $\frac{nR^2}{100A}$. Also, if there are σ hits per unit solid angle, the hits per sq. yd. at R yds. distance is equal to $\frac{100\sigma}{R^2}$.

While the unit solid angles are computed on the basis of spherical surfaces, if the radius is large the difference between a plane and spherical surface is negligible. A slight correction for spherical area was made in computing the solid angles for Panel A, but no corrections were necessary for the other panels.

As shown in the layouts, Panels A and B were sub-divided into 3 horizontal rows of squares, while Panels C and D had 2 horizontal rows. For firings with shell axis horizontal, the hits per unit solid angle for each vertical tier of squares were averaged together with the exception that the hits on sections A1 and A3, A46 and A48 were excluded because the base and nose sprays were concentrated in the middle squares at the ends of Panel A. At greater distances from the burst, the base and nose sprays were distributed over greater areas, consequently avoiding the concentration of fragments in one panel section.

Coordinate System

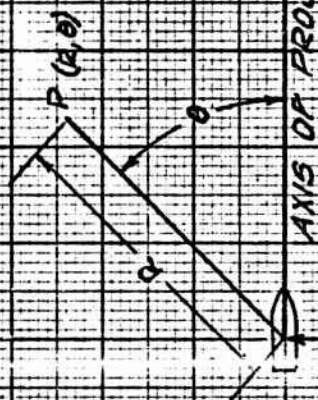
A polar coordinate system was assumed with origin at the center of the panels, plane of the system horizontal and at an elevation midway between the top and bottom of the panels. It is assumed also that the center of gravity of the projectile coincides with the origin, that the shell axis is horizontal, and that the polar axis of the system lies along the extension of the shell axis through the nose end. The diagram on page 15 illustrates the assumed coordinate system. The angles with the axis of the shell mentioned in this report are always measured from the nose end of the shell.

Results of Panel Tests

Plots 1 to 6 show the perforations per unit solid angle on the panels as a function of the angle with the axis of the shell for various remaining velocities when burst. These plots show the usual concentration of fragments into three classes which are designated the base, side, and nose sprays because of their direction of flight and origin within the shell. The space between these main classes is either totally devoid of perforating fragments or greatly reduced in density.

Plots 7 to 12 show the penetrations under various conditions, while Plots 13 to 18 show the dents. The plots of penetrations also show base, side, and nose sprays,

DIAGRAM OF COORDINATE SYSTEM

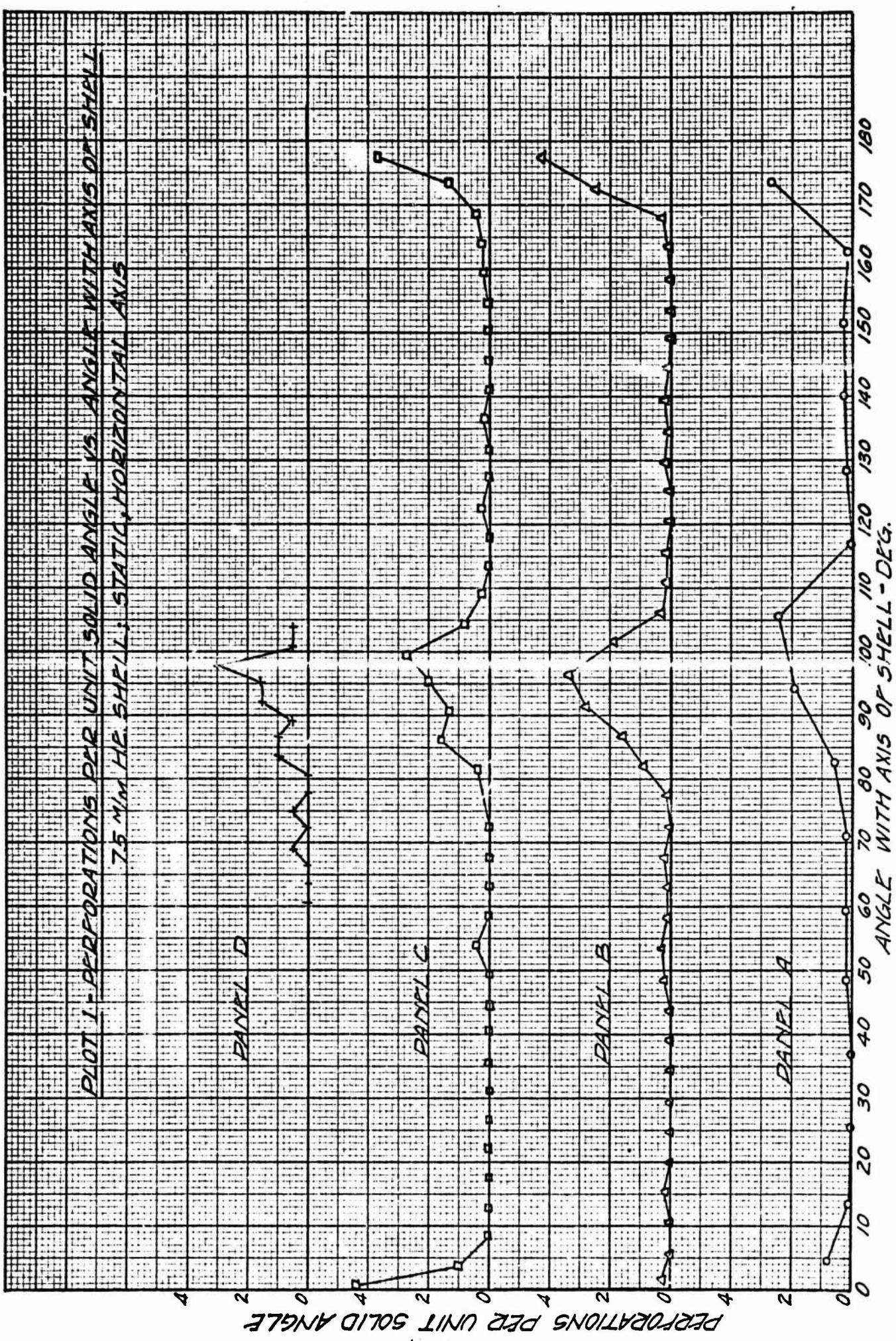


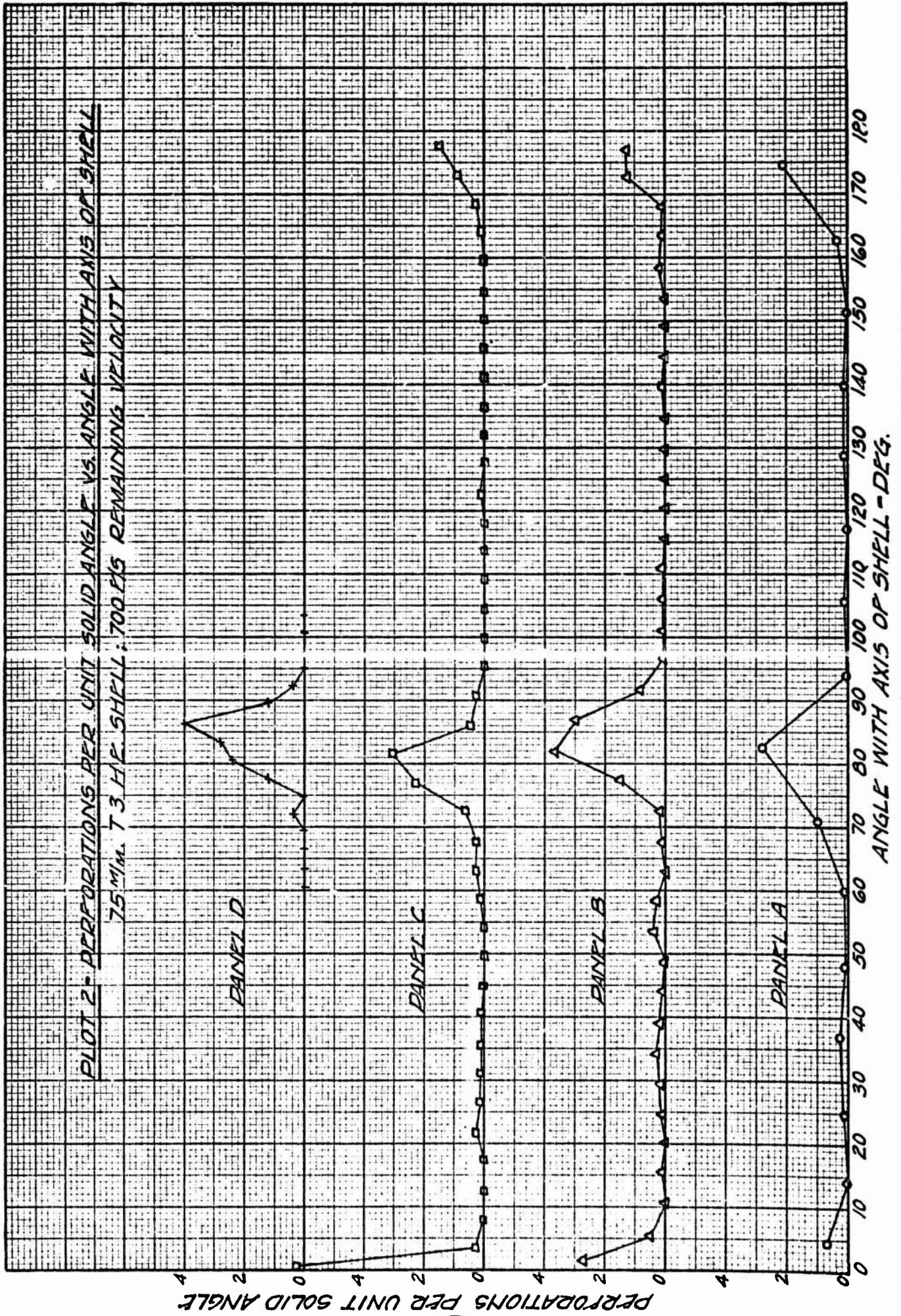
AXIS OF PROJECTIONS

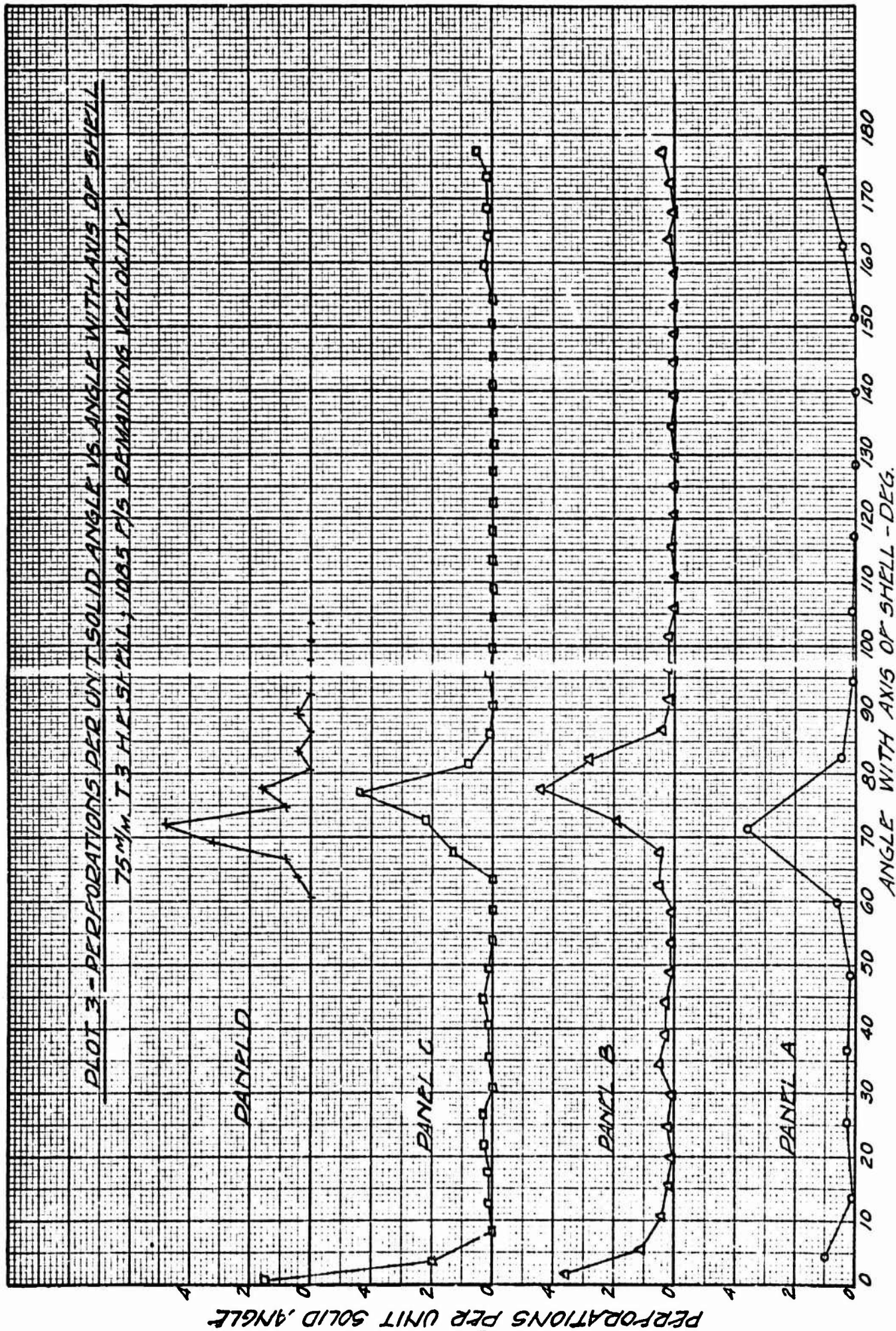
CENTER OF GRAVITY OF PROJECTILE AT ORIGIN
 OF COORDINATE SYSTEM. PLANE OF SYSTEM
 HORIZONTAL.

151

PLOT 1. PERFORATIONS PER UNIT SOLID ANGLE VS. ANGLE WITH AXIS OF SHELL
 7.5 MM. HE. SHELL; STATIC, HORIZONTAL AXIS

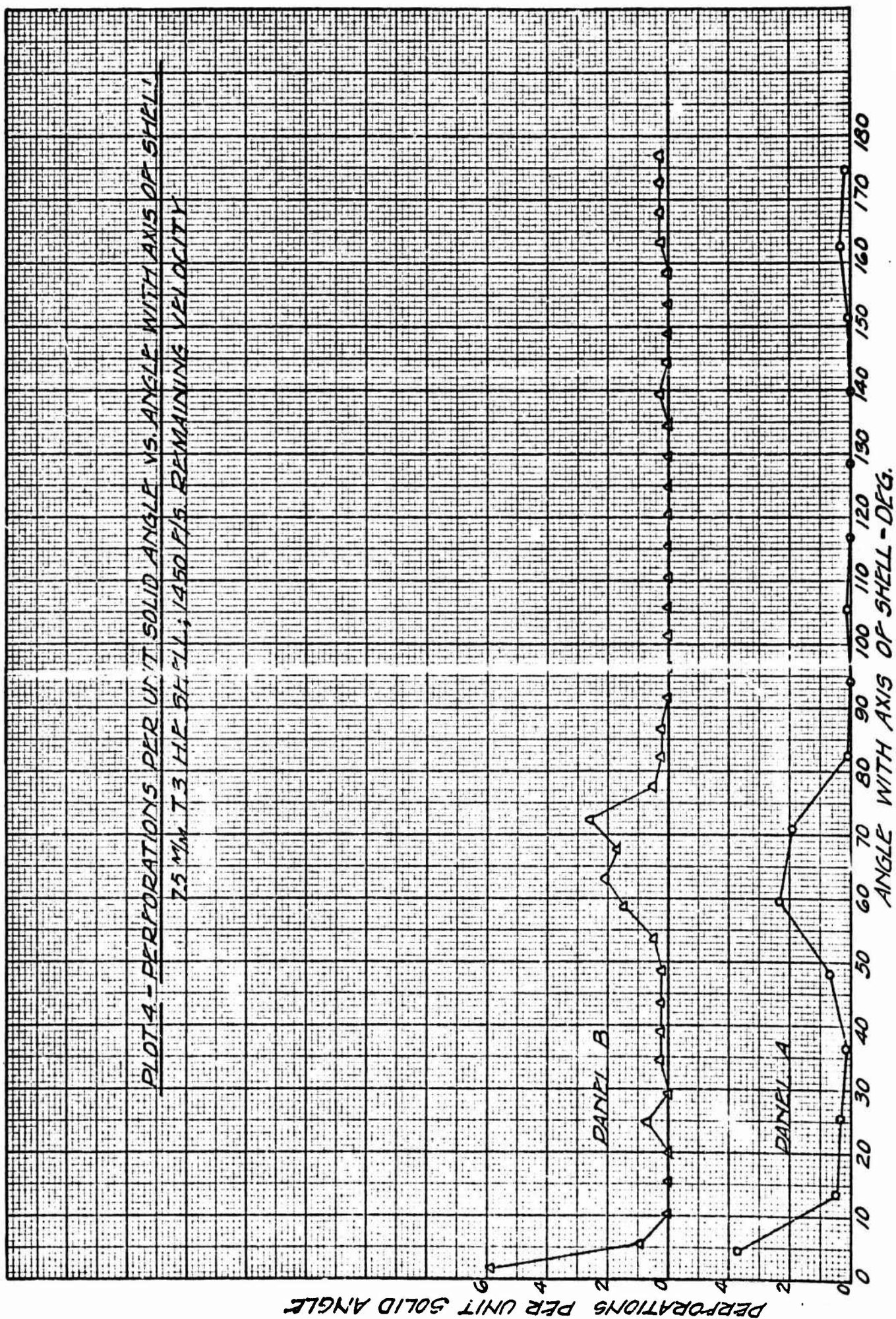


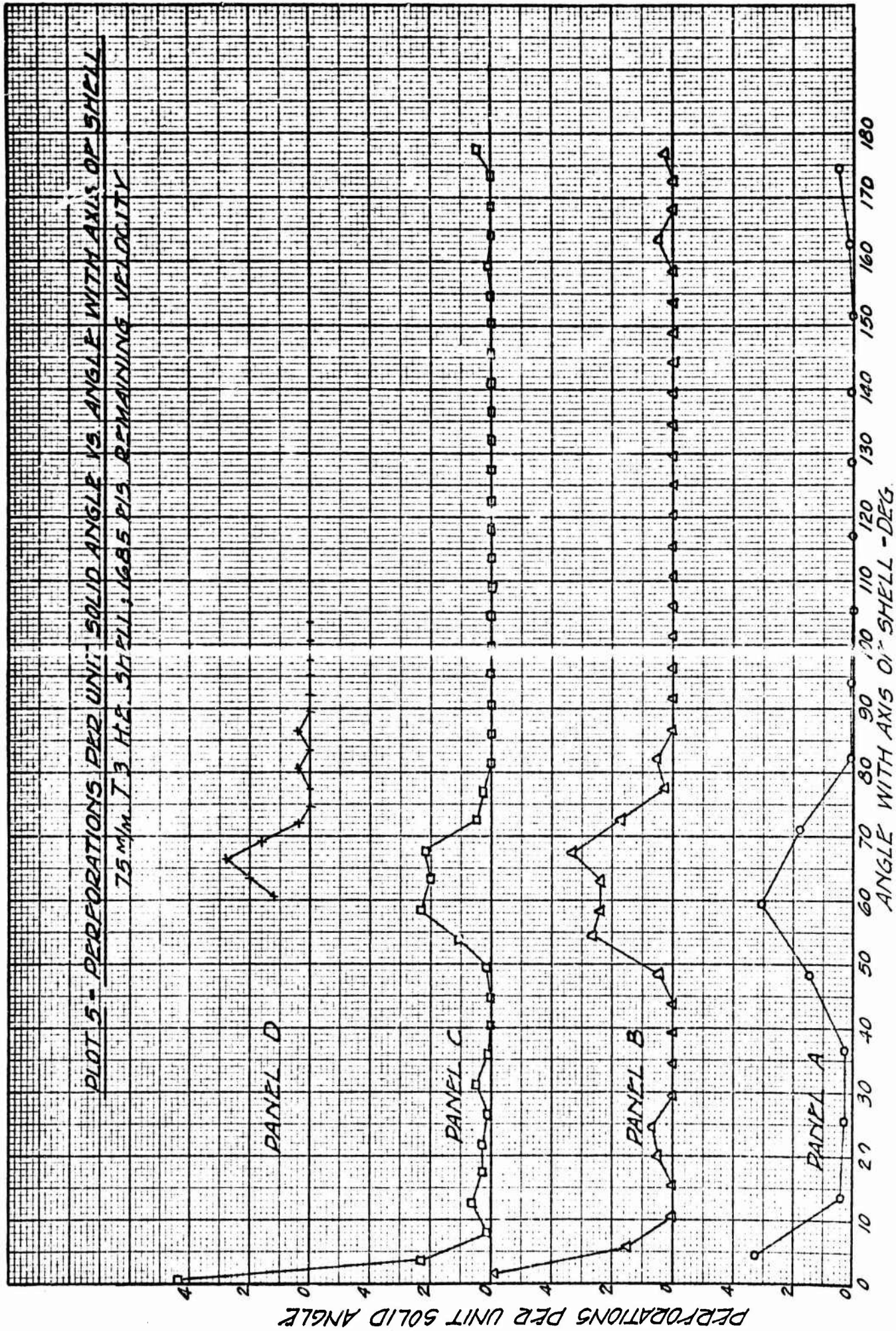


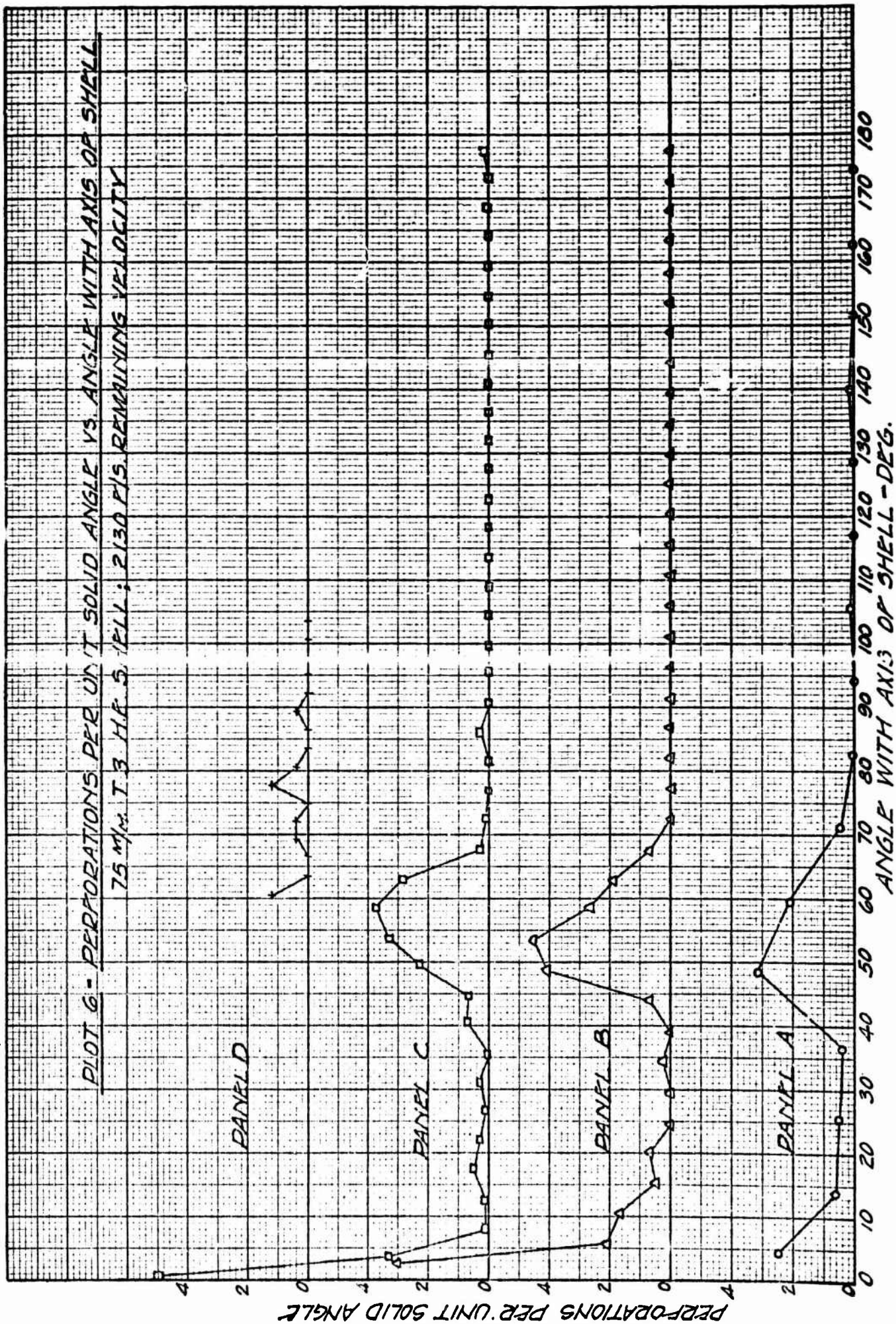


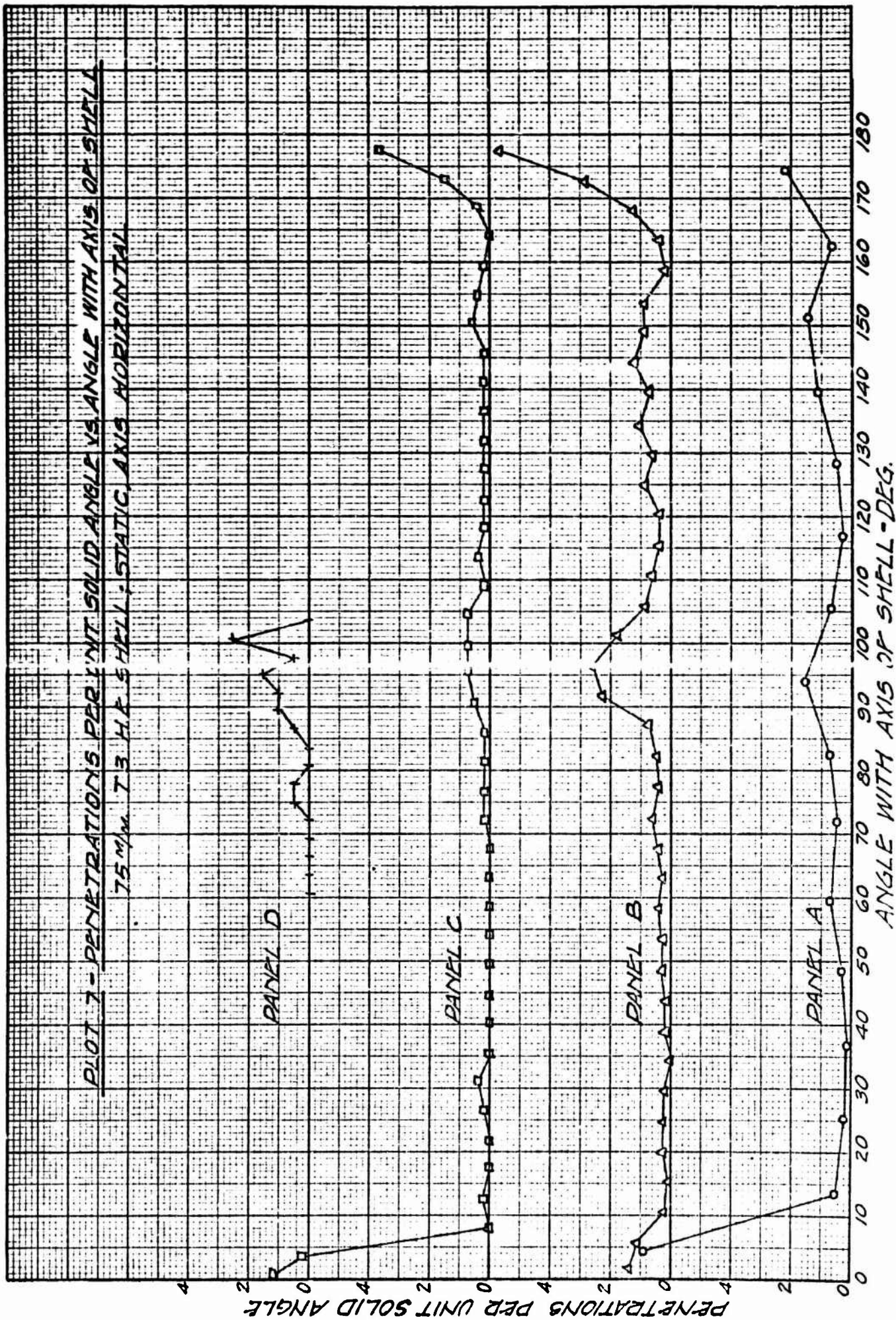
Q 51

PLOT 4 - PERFORATIONS PER UNIT SOLID ANGLE VS. ANGLE WITH AXIS OF SHELL
 75 MM T3 HE SH 511; 1450 F/S. REMAINING VELOCITY

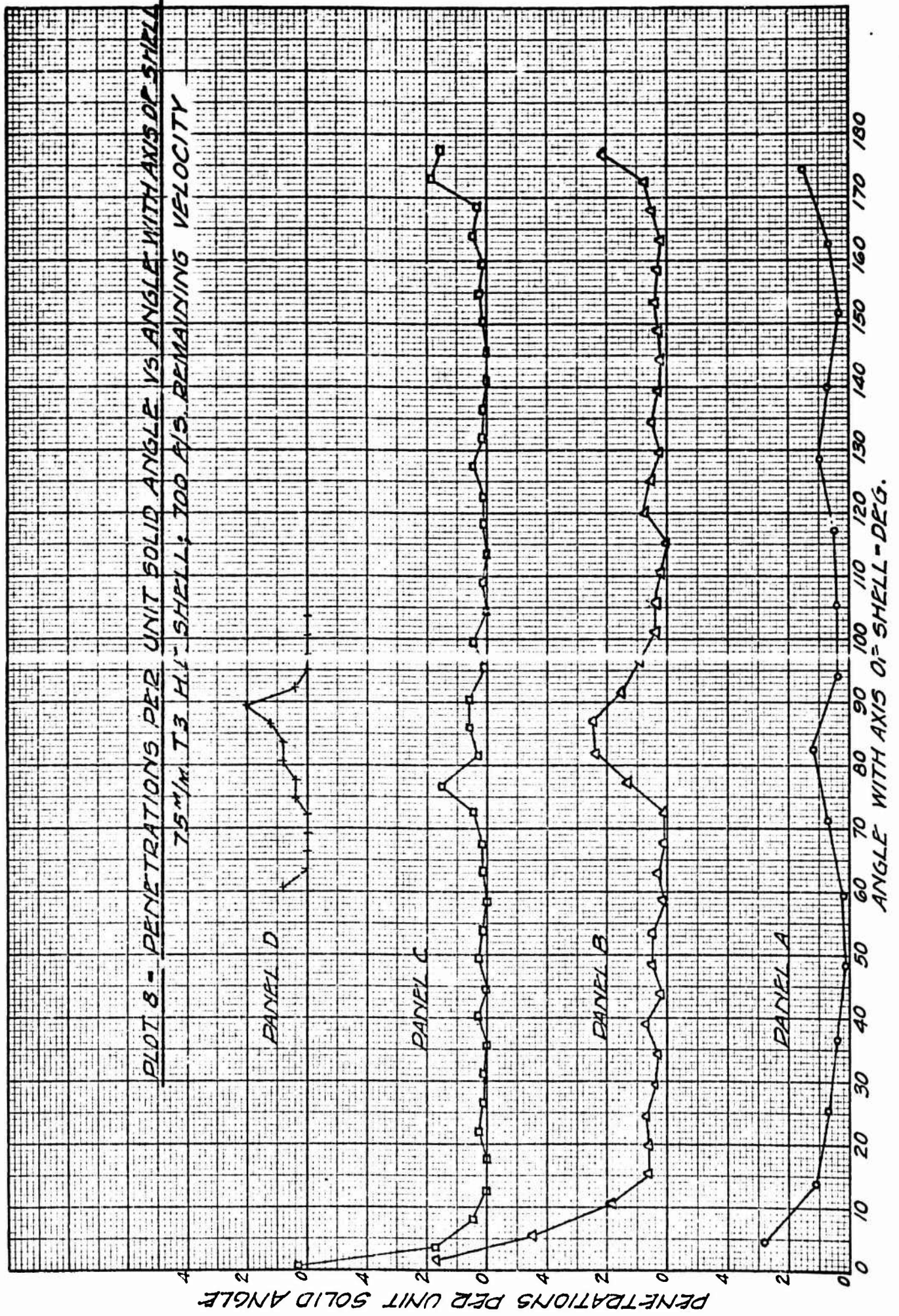








H 51



PLOT 9 - PENETRATIONS PER UNIT SOLID ANGLE VS. ANGLE WITH AXIS OF SHELL
 75 M/M T3 HE SHELL; 108.7 FPS REMAINING VELOCITY

PENETRATIONS PER UNIT SOLID ANGLE

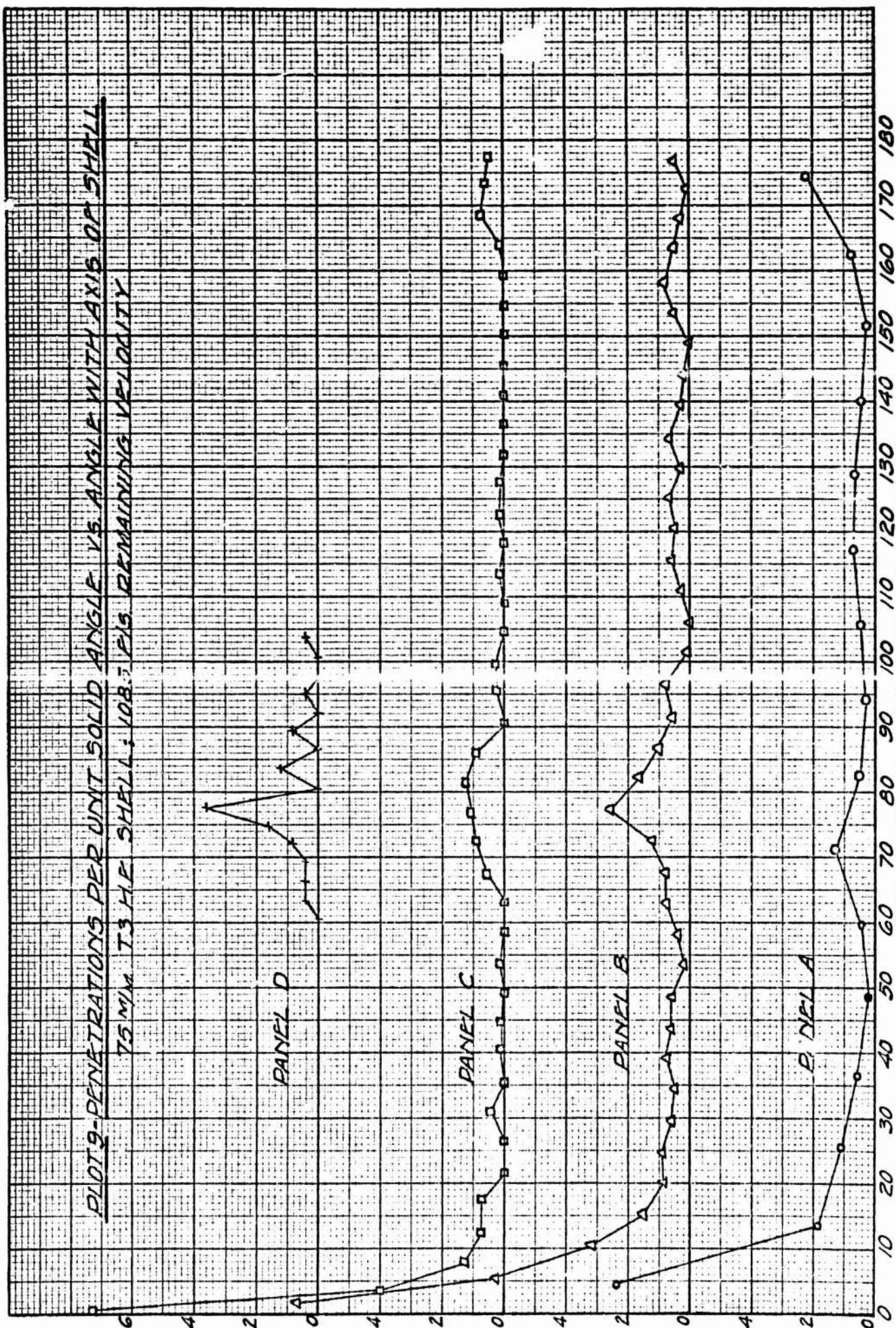
ANGLE WITH AXIS OF SHELL - DEG.

PANEL D

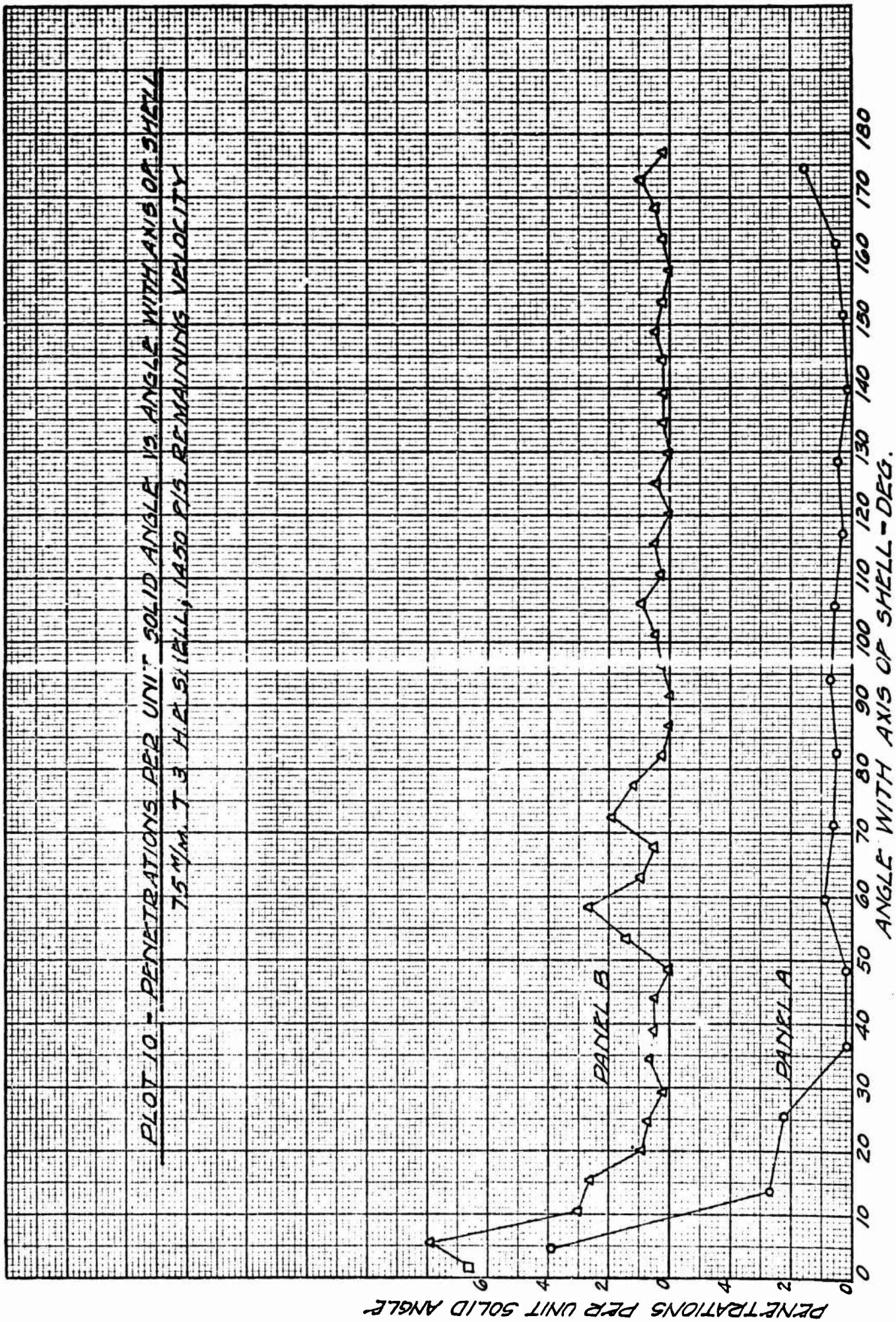
PANEL C

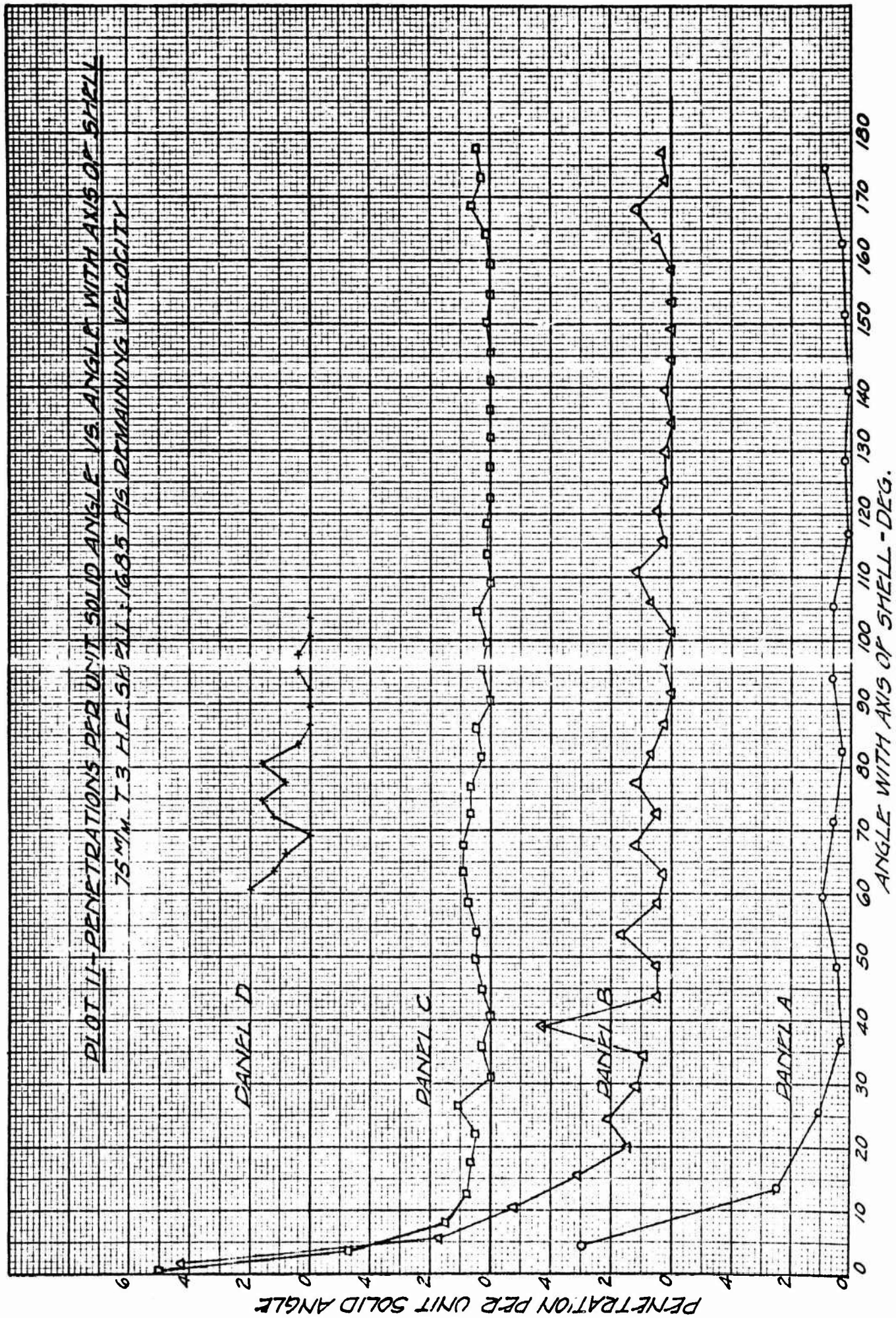
PANEL B

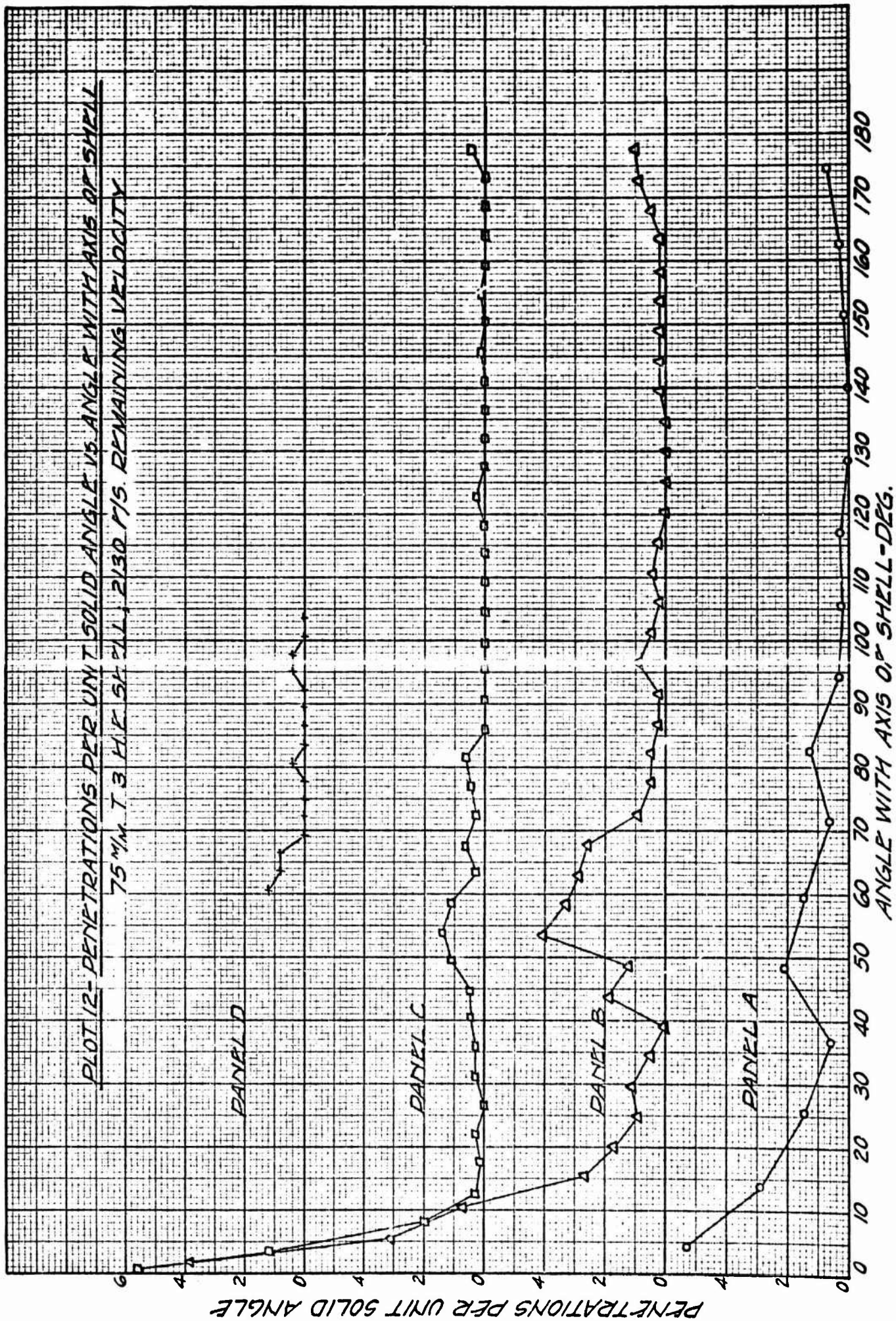
PANEL A



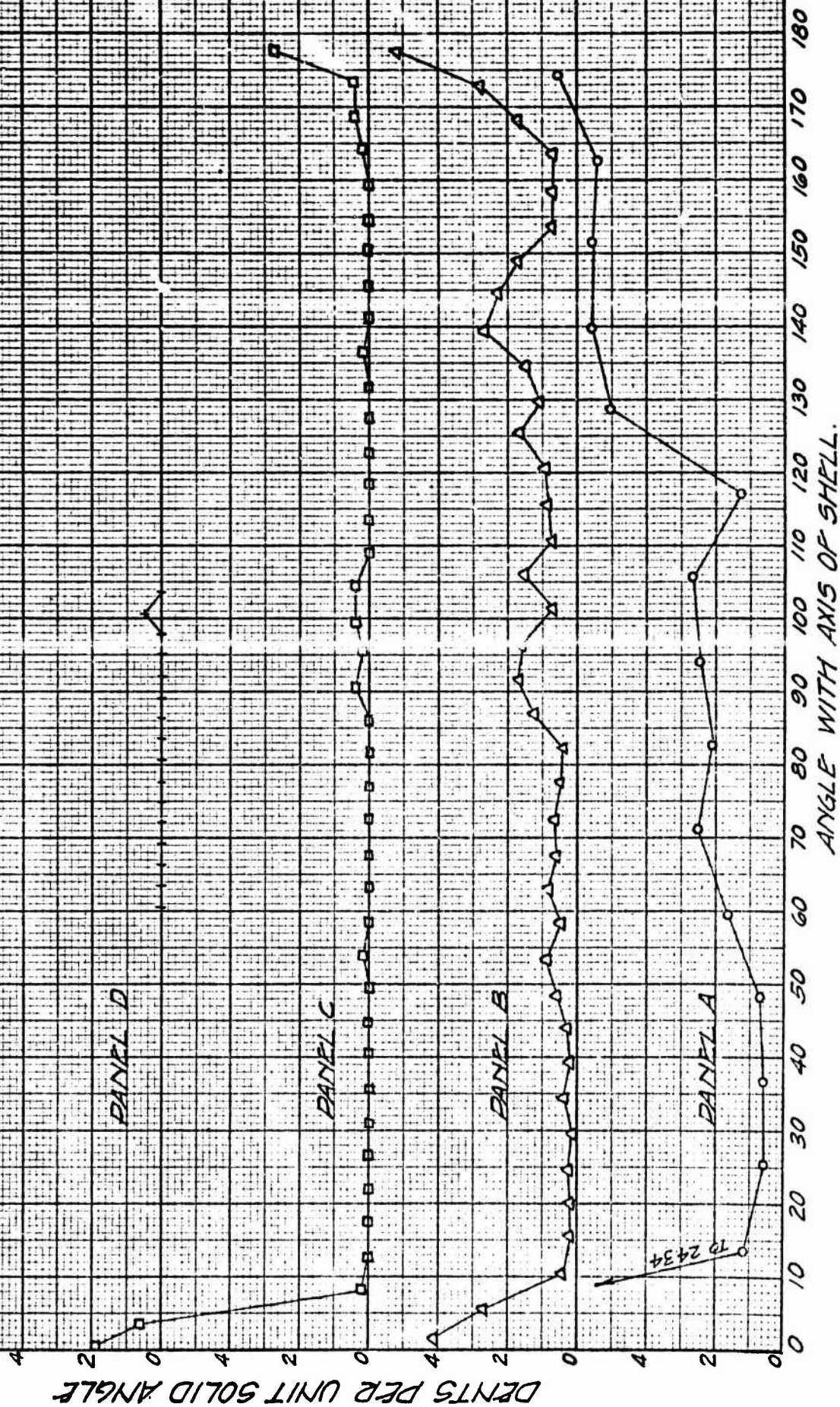
PLOT 10 - PENETRATIONS PER UNIT SOLID ANGLE VS. ANGLE WITH AXIS OF SHELL
75 MM. T-3 H.P. SHELL, 1450 P/S REMAINING VELOCITY







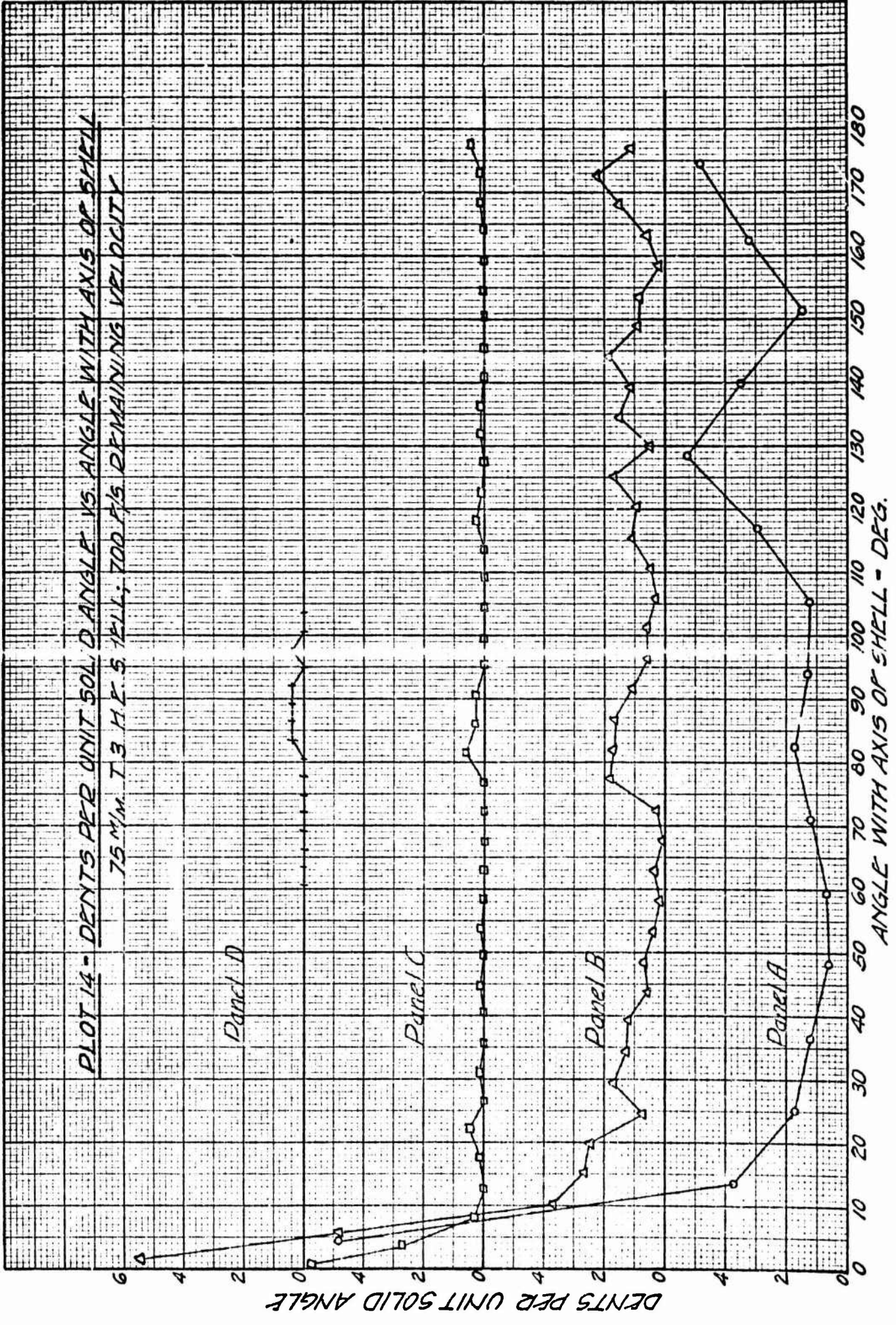
PLOT 13 - DENTS PER UNIT SOLID ANGLE VS. ANGLE WITH AXIS OF SHELL
 75 M/M T-3 H B SHELL; STATIC, AXIS HORIZONTAL



DENTS PER UNIT SOLID ANGLE

ANGLE WITH AXIS OF SHELL

N 15



PLOT 15 DENTS PER UNIT SOLID ANGLE VS. ANGLE WITH AXIS OF SHELL
75 MIN. T3 HE SHELL; 1085 F/S REMAINING VELOCITY

DENTS PER UNIT SOLID ANGLE

ANGLE WITH AXIS OF SHELL - DEG.

TO 282

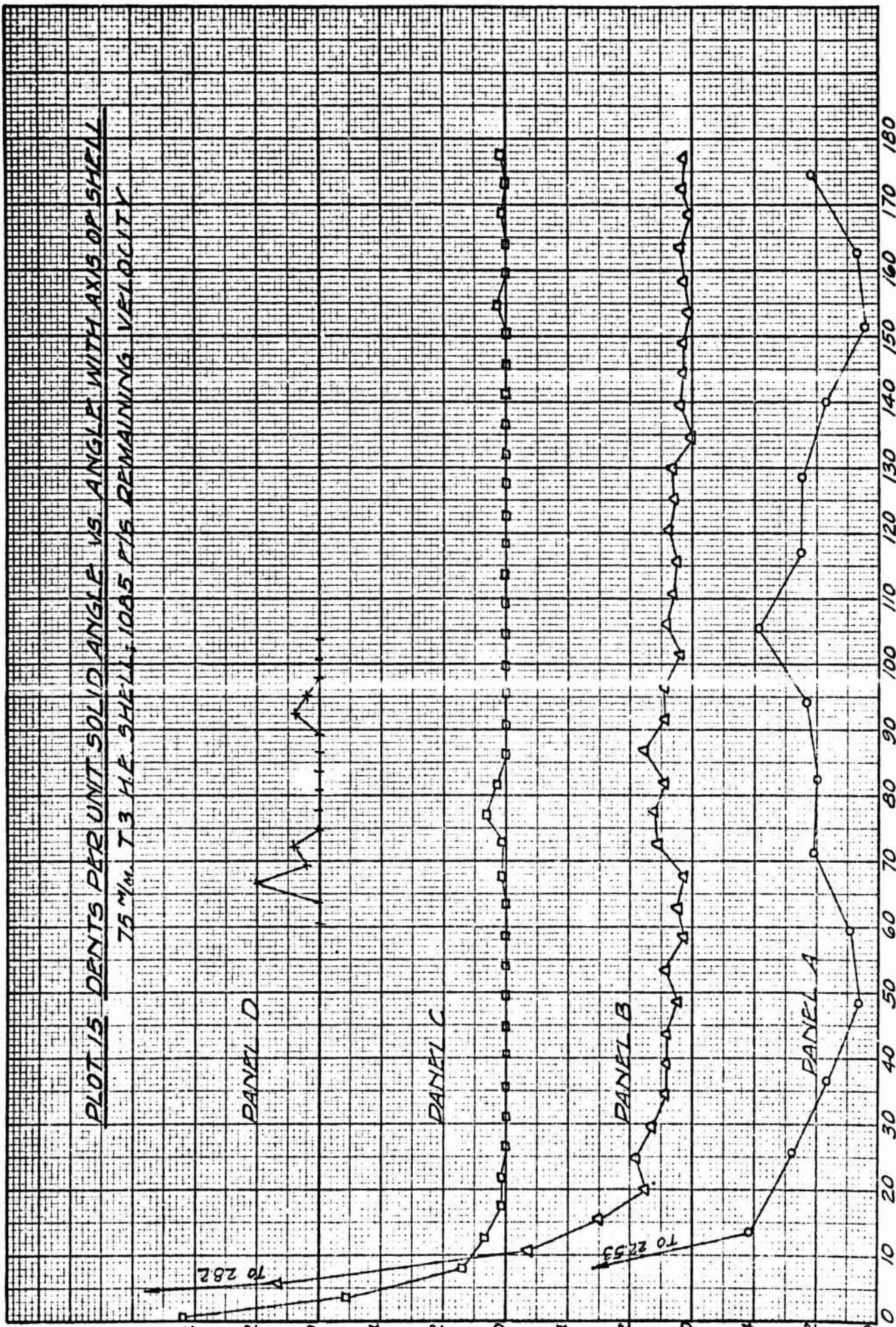
TO 22.53

PANEL D

PANEL C

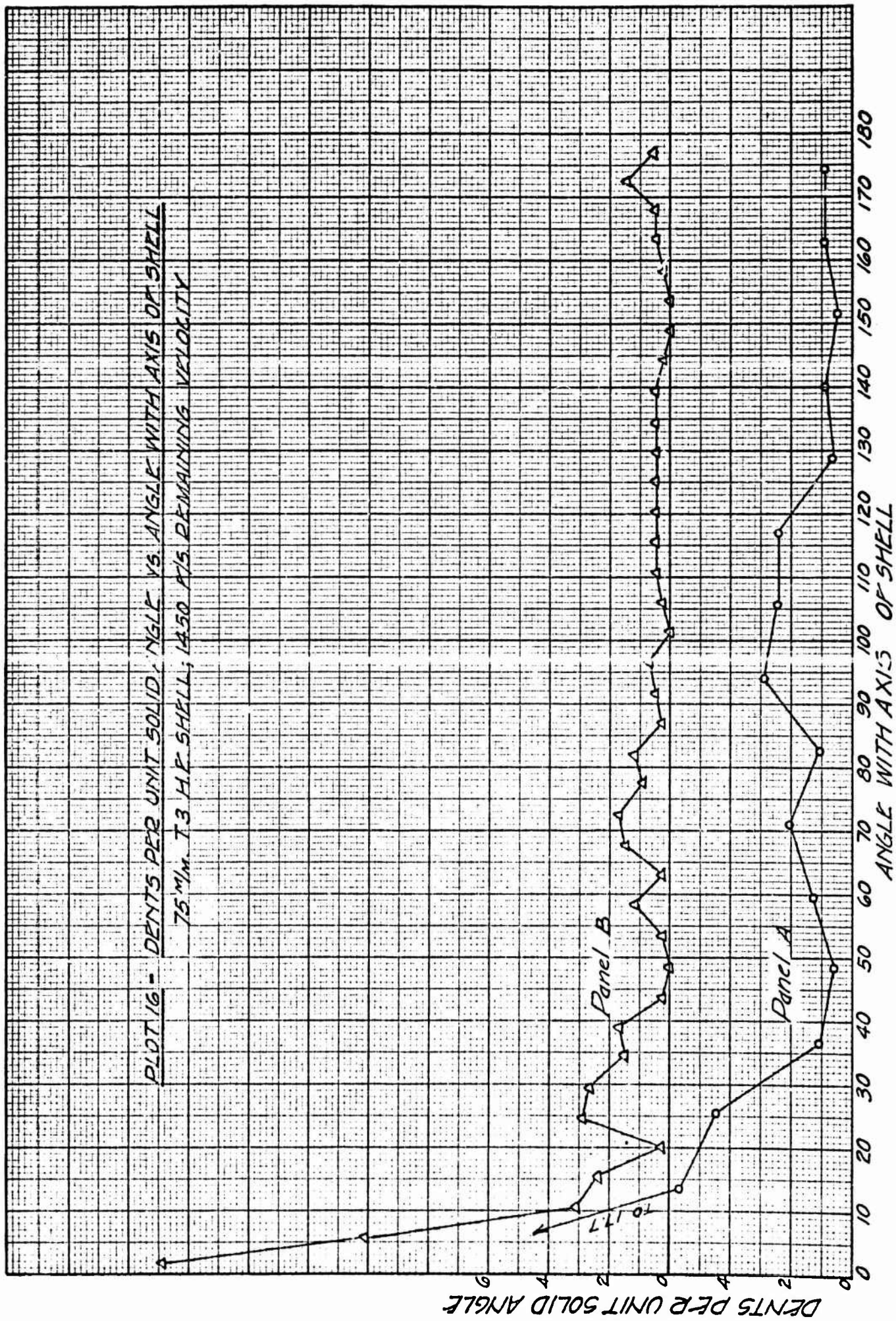
PANEL B

PANEL A

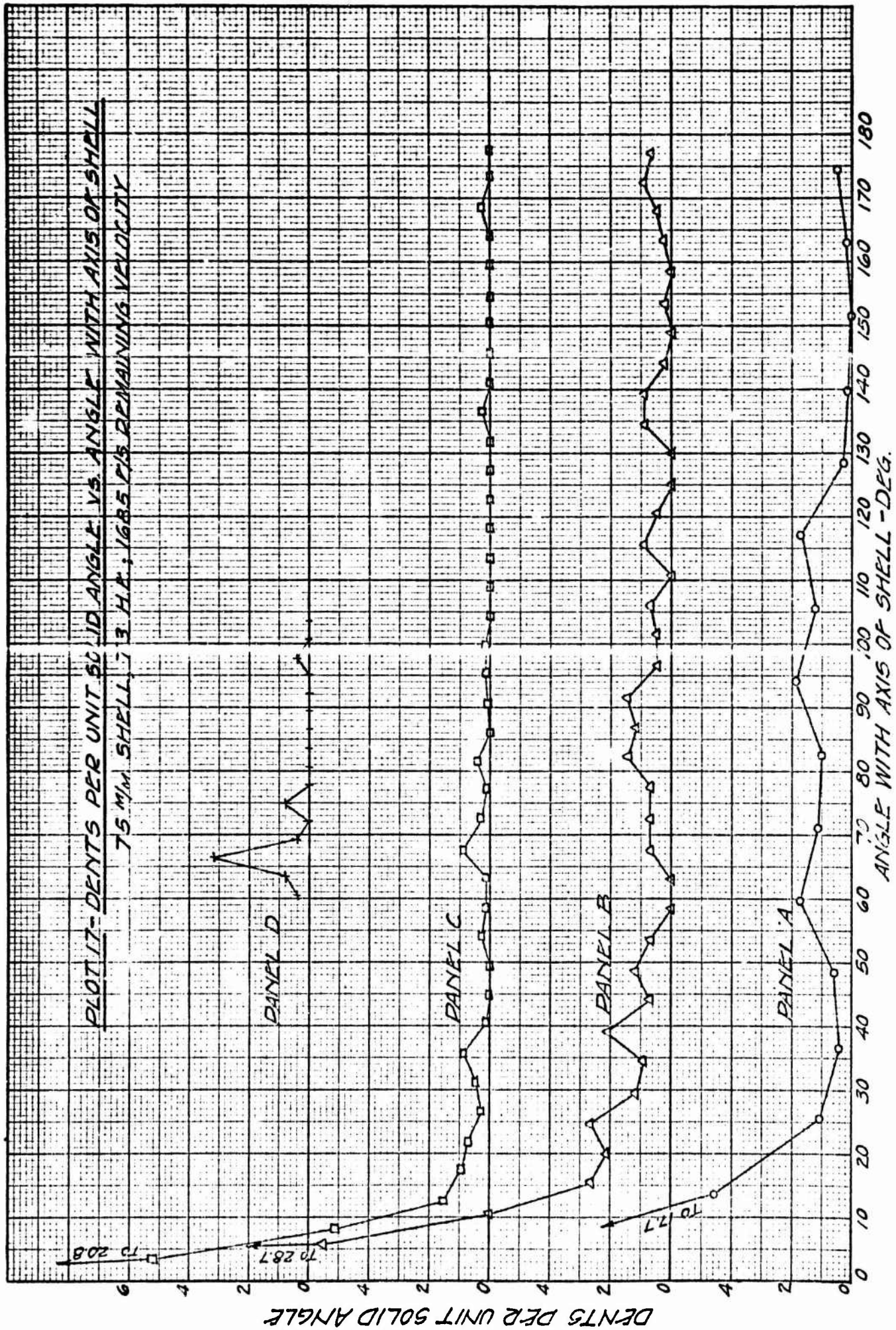


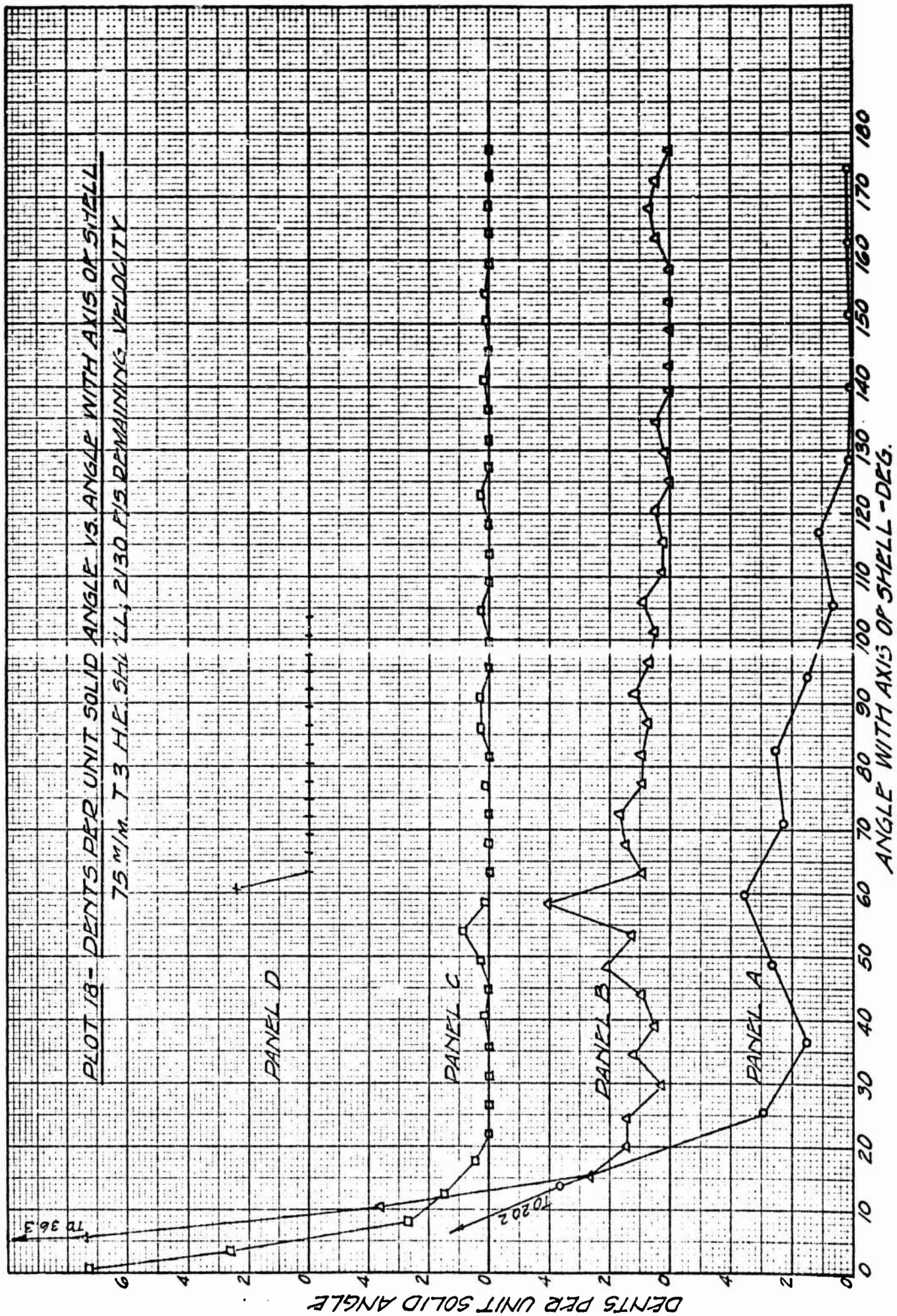
15P

PLOT 16 - DENTS PER UNIT SOLID, NGLE VS. ANGLE WITH AXIS OF SHELL
75 M/M. T3 H.P. SHELL; 1450 F/S. REMAINING VELOCITY



15R





although the side spray is not quite as well defined as that of the perforating fragments. Until they drop out by loss of velocity, the dents appear to be numerous in practically all directions, having no particular concentration into base, side, and nose sprays.

Fragment Density of the Side Spray

Since the fragments lose velocity in flight due to air resistance, their ability to mark the panels decreases with the distance. Also at large distances, the effect of gravity causes some of the fragments to hit the ground before hitting the panels. In order to investigate the loss in density, the hits per unit solid angle were averaged over certain panel areas and arranged in tabular form. For instance, for static firing, the side spray was averaged over 35 deg. of arc, included between 76 and 111 deg. with the shell axis. While 35 deg. of arc. includes somewhat more than the side spray, this angle was purposely selected large in order to make certain that all the sidespray was included. As the sidespray is moved forward due to remaining velocity of the shell it was averaged over 35 deg. of arc, centering the angle about the most dense portion of the sidespray. The same angles were used for the perforations, penetrations and dents. The following table shows the average number of perforations, penetrations, and dents per unit solid angle of the sidespray on the four panels including also the probable errors of the mean.

Number of perforations, penetrations, and dents per unit solid angle of the sidespray.

Average Remain- ing vel. f/s	Angle with axis of shell, deg.	Type of frag- ment	Panel A		Panel B		Panel C		Panel C	
			Ave. No. per u.s.a.	P.E. of Mean	Ave. No. per u.s.a.	P.E. of Mean	Ave. No. per u.s.a.	P.E. of Mean	Ave. No. per u.s.a.	P.E. of Mean
Static	76 to 111	Perf.	1.49	.08	1.47	.10	1.18	.04	.83	.10
700	65 to 100	"	1.25	.07	1.29	.03	.94	.07	1.01	.16
1085	56 to 91	"	1.53	.05	1.41	.08	1.15	.10	1.02	.09
1450	47 to 82	"	1.57	<u>a</u>	1.25	<u>a</u>	-	-	-	-
1685	43 to 78	"	2.05	<u>a</u>	1.79	<u>a</u>	1.11	.08	-	-
2130	36 to 71	"	1.91	<u>a</u>	2.00	<u>a</u>	1.83	.26	-	-
Static	76 to 111	Penet.	.97	.08	1.29	.10	.47	.09	.65	.08
700	65 to 100	"	.76	.08	1.23	.16	.55	.09	.49	.16
1085	56 to 91	"	.75	.05	1.17	.09	.64	.20	.75	.20
1450	47 to 82	"	.62	<u>a</u>	1.19	<u>a</u>	-	-	-	-
1685	43 to 78	"	.70	<u>a</u>	.97	<u>a</u>	.65	.13	-	-
2130	36 to 71	"	1.36	<u>a</u>	2.23	<u>a</u>	.74	.13	-	-
Static	76 to 111	Dents	2.39	.62	1.13	.16	.18	.06	.04	.03
700	65 to 100	"	1.42	.08	1.01	.13	.16	.05	.16	.06
1085	56 to 91	"	1.78	.14	.84	.08	.17	.04	.30	.17
1450	47 to 82	"	1.36	<u>a</u>	.86	<u>a</u>	-	-	-	-
1685	43 to 78	"	1.15	<u>a</u>	.58	<u>a</u>	.26	.08	-	-
2130	36 to 71	"	2.69	<u>a</u>	1.60	<u>a</u>	.20	0	-	-

a two rounds only.

With regard to the perforating fragments of the sidespray, the density decreases with the distance although not as rapidly as might be supposed. For example, the losses in density of perforating fragments between Panels A and D for remaining velocities of zero, 700, and 1085 were 44, 19, and 33% averaging 32%.

As regards the penetrating hits of the sidespray, the density decreases slowly with the distance although there appears to be a significant increase between Panels A and B. While the reason for this increase is not immediately apparent, it is obvious that any increase in penetrating fragments must be accompanied by a corresponding loss of the sum of the perforating and denting fragments.

The density of the denting fragments decreases rapidly with the distance, becoming practically negligible on Panels C and D. Since the loss of perforating and penetrating fragments is sufficient to account for all the denting fragments on Panels C and D it is judged that the denting fragments there obtained were perforating or penetrating fragments closer to the point of burst.

The following table shows the total number of hits of the sidespray per unit solid angle for various remaining velocities:

Total number of hits per unit solid angle in side spray.

Average Remain- ing, Vel. f/s	Angle with axis of shell deg.	Total hits per unit solid angle			
		Panel A	Panel B	Panel C	Panel C
Static	76 to 111	4.85	3.89	1.83	1.52
700	65 to 100	3.43	3.53	1.65	1.66
1085	56 to 91	4.06	3.42	1.96	2.07
1450	47 to 82	3.55	3.30	-	-
1685	43 to 78	3.90	3.34	2.02	-
2130	36 to 71	5.96	5.83	2.77	-

According to the above table, the loss of fragment density between Panels A and D averages about 57%. While there is an apparent gain in density of penetrations between A and B, there is a loss in total number of fragments per unit solid angle for the same panels.

Although it is not evident in the above table it appears that there should be some increase in the average density of the sidespray as the remaining velocity is increased. When fired statically, the sidespray is centered at about 95 deg. with the shell axis, while at 2130 f/s velocity the sidespray is centered at about 55 deg. The effect of this displacement is to crowd the sidespray into a smaller number of solid angles, thus tending to increase the apparent density without increasing the total number.

Fragment density of the base spray

For all practical purposes, the velocity component of the base fragments due to the explosive charge and the velocity component due to the remaining velocity of the projectile have the same line of action, and hence the resultant

fragment velocity is simply the algebraic sum of the two components. Since the two components are of opposite sign, as the remaining velocity becomes large, a great many of the base fragments lose their ability to mark the panels because of their reduced resultant velocity. At very high remaining velocities, the forward component of some of the base fragments may be greater than the rearward component, causing them to travel downrange.

For the base spray the hits per unit solid angle were averaged over the angle with the shell axis included between 162.5 and 180 deg. While this angle is somewhat larger than the half angle of opening of the base spray cone, it was selected large so that all the base fragments would be included. The following tables shows the fragment densities of the base spray as dependent on the remaining velocity and the distance from the burst.

Number of perforations, penetrations, and dents of the base spray per unit solid angle.

Average remain- ing velocity f/s	Type of frag- ment	Panel A		Panel B		Panel C	
		No. per u.s.a.	P.E. of Mean	No. per u.s.a.	P.E. of Mean	No. per u.s.a.	P.E. of Mean
Static	Perf.	1.82	.19	1.93	.14	1.48	.17
700	"	1.51	.19	.75	.12	.77	.09
1085	"	.87	.22	.17	.06	.24	.06
1450	"	.24	<u>a</u>	.24	<u>a</u>	-	-
1685	"	.34	<u>a</u>	.18	<u>a</u>	.12	.06
2130	"	0	<u>a</u>	0	<u>a</u>	.04	.03
Static	Penet.	1.59	.23	2.76	.25	1.49	.39
700	"	1.38	.27	.96	.05	1.08	.29
1085	"	1.89	.26	.34	.07	.53	.22
1450	"	1.29	<u>a</u>	.50	<u>a</u>	-	-
1685	"	.70	<u>a</u>	.57	<u>a</u>	.40	.14
2130	"	.50	<u>a</u>	.71	<u>a</u>	.12	.06
Static	Dents	6.30	1.72	2.76	.25	.96	.32
700	"	4.86	1.40	1.49	.20	.21	.10
1085	"	1.90	.22	.27	.05	.08	.05
1450	"	1.26	<u>a</u>	.76	<u>a</u>	-	-
1685	"	.31	<u>a</u>	.62	<u>a</u>	.08	.04
2130	"	.20	<u>a</u>	.41	<u>a</u>	0	0

a Two rounds only

Considering the base spray on Panel A it appears that the perforations per unit solid angle are reduced by about 50% when the velocity of the shell is changed from static to 1085 f/s. At 1450 f/s remaining velocity, the perforations are reduced about 85%, while at 2130 f/s, they are practically zero.

The penetrations decrease rather slowly on Panel A as the remaining velocity is increased which appears to be due to perforating fragments which become penetrating fragments with increase in remaining velocity. Even at 2130 f/s remaining velocity there are about one third as many penetrations per unit solid angle as when fired statically.

The dents are originally more numerous than the perforations and penetrations, but decrease rapidly when the shell is given some remaining velocity. Between static and 1450 f/s remaining velocity, the loss of perforating and penetrating fragments is about equal to the denting fragments at 1450 f/s so that it is plausible to assume that all of the base denting fragments from static firing never mark the panels when fired at 1450 f/s.

The following table shows the total hits per unit solid angle of the base spray:

Total hits per unit solid angle of the base spray.

Average remaining velocity, f/s	Total hits per unit solid angle		
	Panel A	Panel B	Panel C
Static	9.71	7.45	3.93
700	7.75	3.20	2.06
1085	4.66	.78	.85
1450	2.79	1.50	-
1685	1.35	1.37	.60
2130	.70	1.12	.16

The proportion of base fragments remaining after giving the shell an increment in velocity may be obtained from the above table. Of those striking the panels it is certain that their velocity due to the explosive charge is greater than the velocity due to the remaining velocity of the shell. On this basis, it appears that when the shell is fired statically 80% of the base fragments have a velocity greater than 700 f/s, 48% greater than 1085 f/s, 29% greater than 1450 f/s, 14% greater than 1685 f/s, and 7% greater than 2130 f/s.

Fragment density of the nose spray

With regard to the nose fragments, the velocity component due to the explosive charge and the component due to the remaining velocity of the shell are along approximately the same lines of action and of the same sign, so that the resultant velocity is simply the arithmetic sum of the two components. Consequently the effect of remaining velocity of the shell should be to increase the velocity and range of the nose fragments.

The hits for each type of fragment per unit solid angle were averaged over the angle included between 0 and 17.5 deg. with the axis of the shell. The following table shows the fragment densities of the nose spray for the various conditions of fire:

Number of perforations, penetrations, and dents of the nose spray per unit solid angle.

Average remain- ing vel. f/s	Type of frag- ment	Panel A		Panel B		Panel C	
		Ave. No. per u.s.a.	P.E. of Mean	Ave. No. per u.s.a.	P.E. of Mean	Ave. No. per u.s.a.	P.E. of Mean
Static	Perf.	.37	.06	.10	.05	.55	.07
700	"	.30	.06	.68	.07	.52	.11
1085	"	.59	.08	1.14	.17	1.11	.11
1450	"	1.92	<u>a</u>	1.36	<u>a</u>	-	-
1685	"	1.66	<u>a</u>	1.47	<u>a</u>	1.57	.17
2130	"	1.48	<u>a</u>	2.86	<u>a</u>	1.76	.14
Static	Penet.	3.47	.38	.65	.22	2.19	.77
700	"	2.08	.40	3.31	.17	1.01	.14
1085	"	5.02	.83	5.39	.45	2.62	.26
1450	"	6.60	<u>a</u>	5.06	<u>a</u>	-	-
1685	"	5.74	<u>a</u>	7.20	<u>a</u>	2.69	.36
2130	"	5.17	<u>a</u>	8.00	<u>a</u>	3.32	.38
Static	Dents	12.25	1.22	1.67	.49	2.34	1.19
700	"	9.94	1.05	7.97	.94	1.20	.28
1085	"	13.28	1.89	11.16	.66	2.62	.44
1450	"	11.50	<u>a</u>	7.40	<u>a</u>	-	-
1685	"	12.18	<u>a</u>	10.57	<u>a</u>	6.29	.87
2130	"	14.80	<u>a</u>	15.45	<u>a</u>	4.35	.90

a Two rounds only.

While the fragment densities of the nose spray are rather erratic and the probable errors of the mean large, certain general trends are evident. The perforations per unit solid angle increase markedly with increase in remaining velocity which appears to be due to some of the penetrating hits becoming perforating hits. Also, there are about as many perforations on Panel C as on Panel A indicating that the range of the fragments is increased due to remaining velocity.

Some gain in penetrating hits is evident with increase in remaining velocity which is no doubt due to some of the largest denting fragments becoming penetrating hits.

As near as may be judged from the data, the denting hits are approximately constant as the remaining velocity is increased. It appears that some of the denting fragments become penetrating fragments with increase in shell velocity and hence the number of dents would be reduced a certain amount. However, as shown in Plot 13 giving the dents per unit solid angle for static firing, there are a certain amount of dents in all directions from the burst. Consequently those immediately adjacent to the selected angle of the nose spray, namely 0 to 17.5 deg., would be displaced into the nose spray zone by shell velocity thus augmenting the number.

The average number of perforations, penetrations, and dents per unit solid angle for the nose spray were added together for the various conditions of fire and are listed in the following table:

Total number of hits in the nose spray per unit solid angle.

Average remain- ing vel. f/s	Total hits per unit solid angle.		
	Panel A	Panel B	Panel C
Static	16.09	2.42	5.08
700	12.32	11.96	2.72
1085	18.89	17.69	6.35
1450	20.02	13.82	-
1685	19.58	19.24	10.55
2130	21.45	26.31	9.43

From the results of the above table, there seems to be some gain in the density of hits in the nose spray with increase in shell velocity which is probably due to the displacement of some of the fragments adjacent to the selected angle of nose spray into the nose spray zone. While there is a considerable reduction in total number of fragments with the distance from the burst, the proportion of hits obtained on Panel C with the high remaining velocities indicates that the shell velocity had an appreciable effect on the range of the fragments.

Fragment Density with Shell Axis Vertical

When the shell are fired with axis horizontal, the fragments are sampled through 180 deg. of arc with respect to the shell axis, while in the transverse direction the width of the sample is the angle subtended by the height of the panel to the point of burst. Panel A subtends about 33 deg. of arc, B about 14 deg., C about 9 deg., and D about 6 deg. It is thus apparent that with horizontal firings the side spray is completely sampled in the sense that a cross section is obtained but the size of the sample is rather small varying from 33/360 to 6/360 of the total.

With shell axis vertical, conditions are reversed. On a given panel, the side spray is sampled through 180 deg. normal to the shell axis while with respect to the angle with the shell axis, the size of the sample is limited by the angle subtended by the panel height, varying from 33 to 6 deg. Since the fragment density within the sidespray band is a function of the angle with the axis of the shell, reaching a maximum near the middle of the band and decreasing to practically zero at the edges, it is apparent that either all the sidespray band or symmetrical portions of it must be sampled in order to obtain the fragment density as a function of the distance from the burst. With vertical firings it does not appear practical to sample all of the sidespray band at very great distances from the burst. An angle of 35 deg. was used in averaging the density of the sidespray for horizontal firings, although 25 deg. would include most of it. Assuming even 25 deg. of width, a panel 50 ft. high at 120 ft. distance would be required, which is impractical. Also, unless panels are especially built for the purpose, it is not possible to match symmetrical portions of the sidespray on the various panels.

In view of the conditions mentioned, firings with shell axis vertical were made in Panels A and B at a height midway between the top and bottom of the panels. Under

these conditions, Panel A samples all of the width of the sidespray band since it subtends 33 deg. of arc. Then for Panels C and D, the shell were elevated to a height 18 ft. above the bottom of the panels, base of the shell down. At this height, the middle of the sidespray band should hit the upper row of squares on Panel C and near the center of Panel D. Thus, all of the width of the sidespray band was sampled on Panel A and also the most dense portions on Panels A, B, C and D, although not strictly symmetrical portions.

Plots 19 and 20 show for shell axis vertical the perforations per unit solid angle on Panels A and B as a function of the horizontal angle from zero azimuth. Zero azimuth is defined for axis vertical firings as the horizontal line from the point of burst to the ends of the panels at Sections A1, B1, or C1. The values obtained on Panel A are smoother than those on Panel B, which appears to be largely due to the fact that a square on Panel A subtends about 6 times the solid angle of one on B.

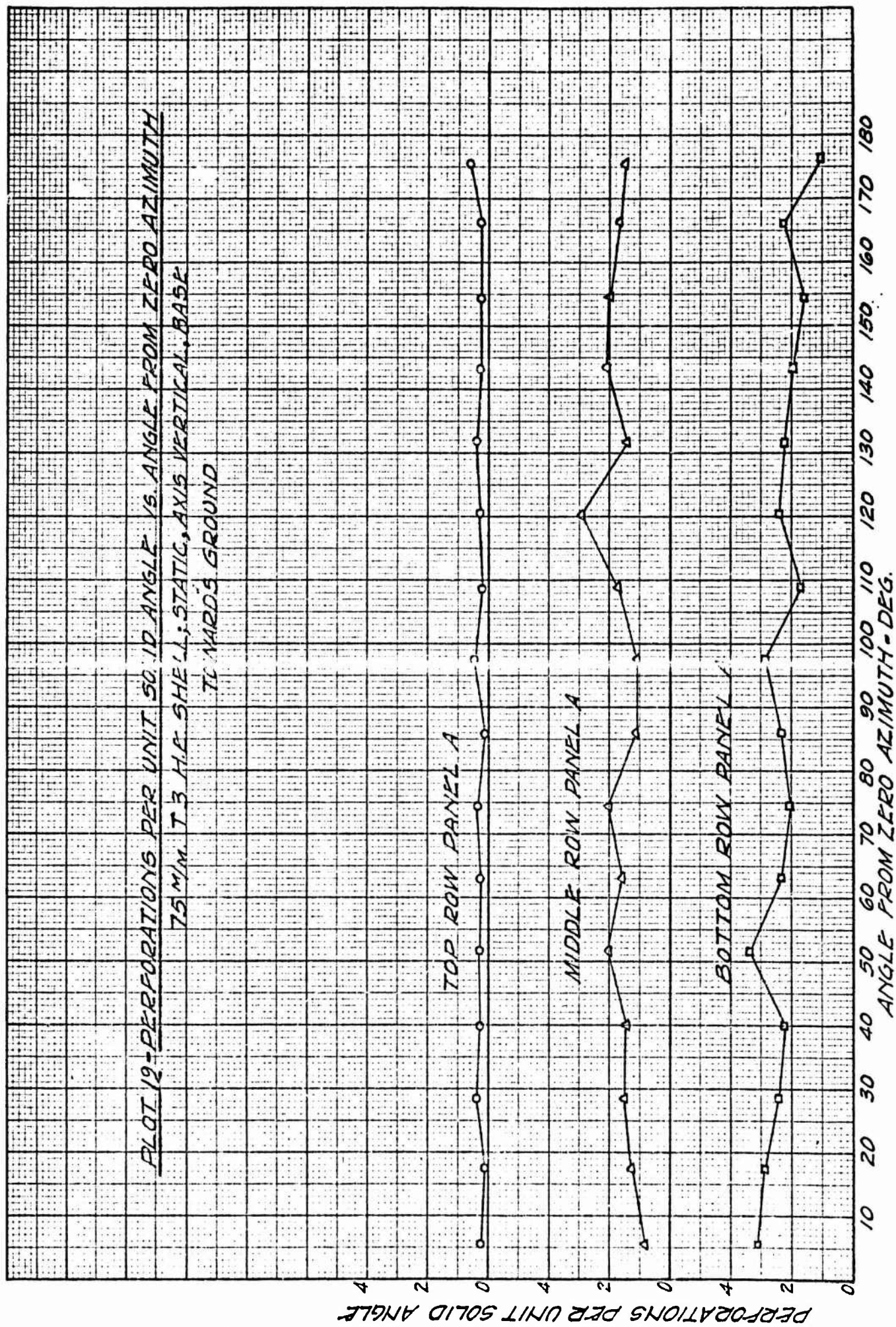
Since the fragment densities on the panels with shell axis vertical should be constant from zero to 180 deg. azimuth if a large number of rounds were fired, the results of the other conditions of test are not shown in the form of plots, but instead are listed in a table giving the average fragment density over the panels as follows:

Number of perforations, penetrations, and dents, of the sidespray per unit solid angle, shell axis vertical.

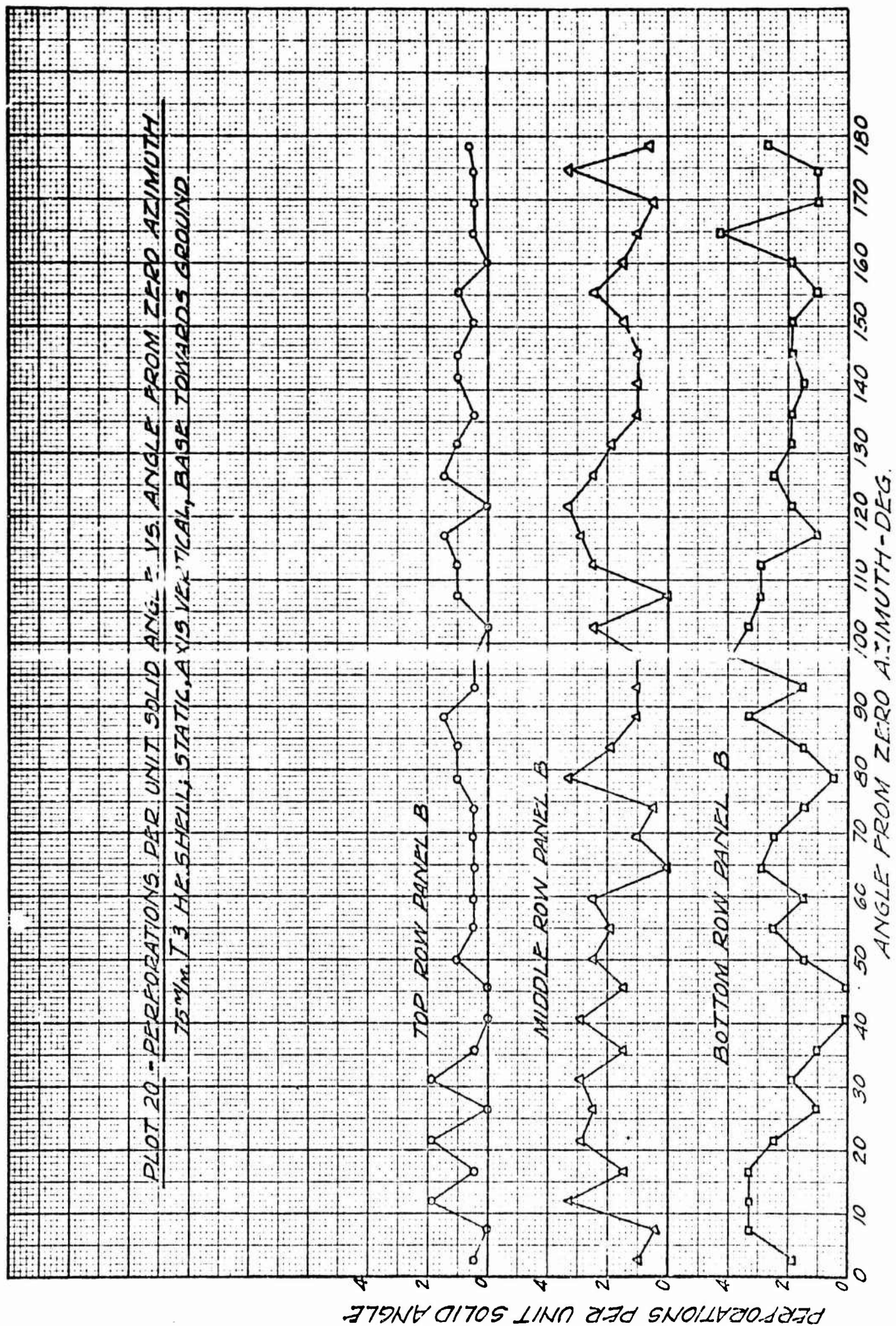
Panel	Panel Row	Base down			Base up*			Weighted Average of base down & base up		
		Perf.	Penets.	Dents	Perfs.	Penets.	Dents	Perfs.	Penets	Dents
		per u.s.a.	per u.s.a.	per u.s.a.	per u.s.a.	per u.s.a.	per u.s.a.	per u.s.a.	per u.s.a.	per u.s.a.
A	Top	.28	.38	.93	.39	.44	1.10	.32	.40	1.00
"	Middle	1.71	.91	.86	1.71	.72	1.52	1.71	.83	1.12
"	Bottom	2.31	1.00	1.11	2.37	.93	1.27	2.33	.97	1.17
	Mean	1.44	.76	.96	1.47	.70	1.29	1.45	.74	1.09
P.E. of Mean								.03	.06	.13
B	Top	.69	1.00	1.19	1.28	.73	.46	.93	.89	.90
"	Middle	1.74	1.39	.86	1.70	1.41	.76	1.72	1.40	.82
"	Bottom	1.99	1.14	.72	3.51	1.47	1.56	2.60	1.27	1.06
	Mean	1.47	1.18	.93	2.16	1.20	.93	1.75	1.19	.93
P.E. of Mean								.14	.04	.08
C	Top	2.71	1.31	.68						
"	Bottom	1.01	.68	.28						
	Mean	1.86	.99	.48						
D	Top	1.92	1.07	.67						
"	Bottom	3.44	1.16	.66						
	Mean	2.67	1.12	.66						

* The top and bottom rows are transposed in the table for comparison with base down results.

472



B 42



From the above table and from a table of sidespray densities given earlier in the report, a comparison of the sidespray obtained on Panel A by vertical and horizontal firings is made as follows:

Type of Fragment	Static, axis horizontal		Static, axis vertical	
	Ave. No. per u.s.a.	P.E. of Mean	Ave. No. per u.s.a.	P.E. of Mean
Perf.	1.49	.08	1.45	.03
Penet.	.97	.08	.74	.06
Dent.	2.39	.62	1.09	.13

From these results, it appears that the agreement between the two methods is satisfactory. The perforations and penetrations per unit solid angle check as closely as might be expected and while the dents were about twice as numerous with horizontal firings, the difference is probably not significant considering the probable errors. With vertical firings, Panel A cuts out about 1/2 of the total sidespray, while with horizontal firings about 1/10 of the total sidespray is obtained making the sample size with axis vertical 5 times greater. In view of the sample size and the probable errors, the fragment densities obtained with axis vertical should be the more reliable.

A fairly good approximation of the most dense portion of the sidespray as a function of the distance is obtained by considering the bottom row of squares of Panel B, the top row of Panel C, and the average of both rows of Panel D. Under the conditions of the firings, these panel sections subtend approximately 5 deg. of arc measured with the axis of the shell and are centered at approximately 95 deg. from the nose end. The sample is thus taken at about the middle of the sidespray band. Panel A is excluded because none of the sections are symmetrical with those selected on the other panels. On this basis, the number of fragments per unit solid angle are arranged in a table as follows.

Type of Fragment	Panel B (Bottom row)		Panel C (Top row)		Panel D (Ave. of Top & Bottom row)	
	Hits per u.s.a.	P.E. of Mean	Hits per u.s.a.	P.E. of Mean	Hits per u.s.a.	P.E. of Mean
Perf.	2.60	.31	2.71	.19	2.67	.27
Penet.	1.27	.09	1.31	.21	1.12	.40
Dent.	<u>1.06</u>	.17	<u>.68</u>	.03	<u>.66</u>	.13
All	4.93		4.70		4.45	

According to these results, there is not much loss in fragment density between Panels B and D. However, the probable errors are large enough that the loss of perforating fragments might be about 20%, the penetrations about 50%, and the dents about 60%.

Total Number of Fragments

The total number of fragments throughout the space surrounding the burst was computed using the fragment densities obtained on the panels. The total number of fragments N in space is given by the equation

$$N = 2\pi \times 100 \int_0^\pi \sigma(\theta) \sin\theta d\theta$$

In this equation, θ is the angle with the shell axis and $\sigma(\theta)$ the number of fragments per unit solid angle as a function of θ for a given panel distance. The factor of 100 is used in the equation because, in our computations, the unit solid angle is 1/100 of the large unit.

If the total number of fragments is divided by the number of unit solid angles in a sphere, the number of fragments per unit solid angle averaged over all directions from the burst is obtained, which is designated $\bar{\sigma}$. Since there are 400π unit solid angles in a sphere, one obtains

$$\bar{\sigma} = \frac{N}{400\pi}.$$

Values of N and $\bar{\sigma}$ were computed for 3 distances from the burst as shown in the following table:

Number of fragments, N , and average number per unit solid angle, $\bar{\sigma}$, at various distances from the burst.

Remain- ing Vel. f/s	Dist- ance ft.	Perfs.		Penet.		Dents		Total Hits	
		No.	$\bar{\sigma}$	No.	$\bar{\sigma}$	No.	$\bar{\sigma}$	No.	$\bar{\sigma}$
Static	15	722	.57	927	.74	3411	2.71	5060	4.03
"	36	660	.53	1016	.81	1253	1.00	2929	2.33
"	75	521	.41	343	.27	118	.09	982	.78
1085	15	681	.54	842	.67	2702	2.15	4225	3.36
"	36	626	.50	921	.73	1063	.85	2610	2.08
"	75	491	.39	375	.30	121	.10	987	.79
2130	15	689	.55	941	.75	2312	1.84	3942	3.14
"	36	683	.54	1255	1.00	1062	.84	3000	2.39
"	75	635	.51	378	.30	213	.17	1226	.98

From the results at 15 ft. distance, which is the nearest to the burst at which data were secured, it appears that the shell breaks up on detonation into about 5000 fragments, composed of about 700 perforating, 900 penetrating, and 3400 denting fragments. In pit fragmentation tests, about 750 fragments were recovered per round. As shown later in the report, it appears that practically all of the fragments obtained in pit tests would be perforating fragments in panel tests at 15 ft. distance.

The average number of fragments per unit solid angle, $\bar{\sigma}$, decreases with the distance from the burst. $\bar{\sigma}$ decreases more rapidly for the dents than for either the perforations or penetrations.

Fragment density as dependent on the distance from the burst

Plots 1 to 18 show the observed perforations, penetrations, and dents per unit solid angle as obtained on the panels. In these plots, the data for each panel distance are plotted on separate coordinate axes. In using the data it is desirable that the fragment densities for all panel distances for a given remaining velocity be plotted on the same coordinate axis so that computations may be made for almost any desired condition of firing. If the original data for four panel distances were plotted on the same axis there would be considerable crossing and overlapping of the curves because of accidental variations in the data. Consequently the observed results were adjusted or smoothed in order to present the data in a convenient and usable form.

Considering the perforations first, the data were adjusted with respect to the remaining velocity. Since the number of fragments in the base spray were observed to decrease with the remaining velocity, the decrease was made uniform. The fragment density in the nose spray was adjusted to increase uniformly with the shell velocity because the average density was observed to increase. The angle the sidespray makes with the axis of the shell was adjusted to decrease uniformly as a function of the remaining velocity. No change was made in the magnitude of the sidespray as dependent on shell velocity since the observed data show no definite trend in this respect. However, where the observed sidespray was particularly variable, curves were fitted to the data by the method of least squares. The perforations were next adjusted with respect to distance from the burst. In making this adjustment, the observed average reductions

in the density of the side spray as a function of the distance were used in smoothing the individual values at any particular angle with the axis of the shell. A similar method was employed for the base and nose spray.

The data for the penetrations were smoothed by the same method as the perforations. However, the adjustment of the dents was somewhat different. For the dents, the densities of the nose and base sprays were adjusted with respect to shell velocity. Then for the remaining angles with the shell axis, smooth curves were simply drawn through the original data.

Plots 21 to 23 show the adjusted perforations per unit solid angle for the four panel distances for static firing, 700 f/s, and 1035 f/s remaining velocity. Plots 24 to 26 give the adjusted penetrations for the same conditions while Plots 27 to 29 show the dents.

The information given by the plots as to fragment density as dependent on the angle with the axis of the shell, the distance from the burst, and the remaining velocity of the shell were discussed earlier in the report on the basis of the observed data. The main purpose of the adjusted plots is to show the data in a more convenient and usable form for future reference.

Number of fragments per sq. yd.

In reports made by the Ballistic Research Laboratory it has been customary to express fragment densities in number per unit solid angle and this unit has been used in the discussion and plots given in this report. However, fragment densities in terms of number per sq. yd. have been used to some extent in the past. Consequently, a number of plots* have been made on a per sq. yd. basis for purposes of comparison.

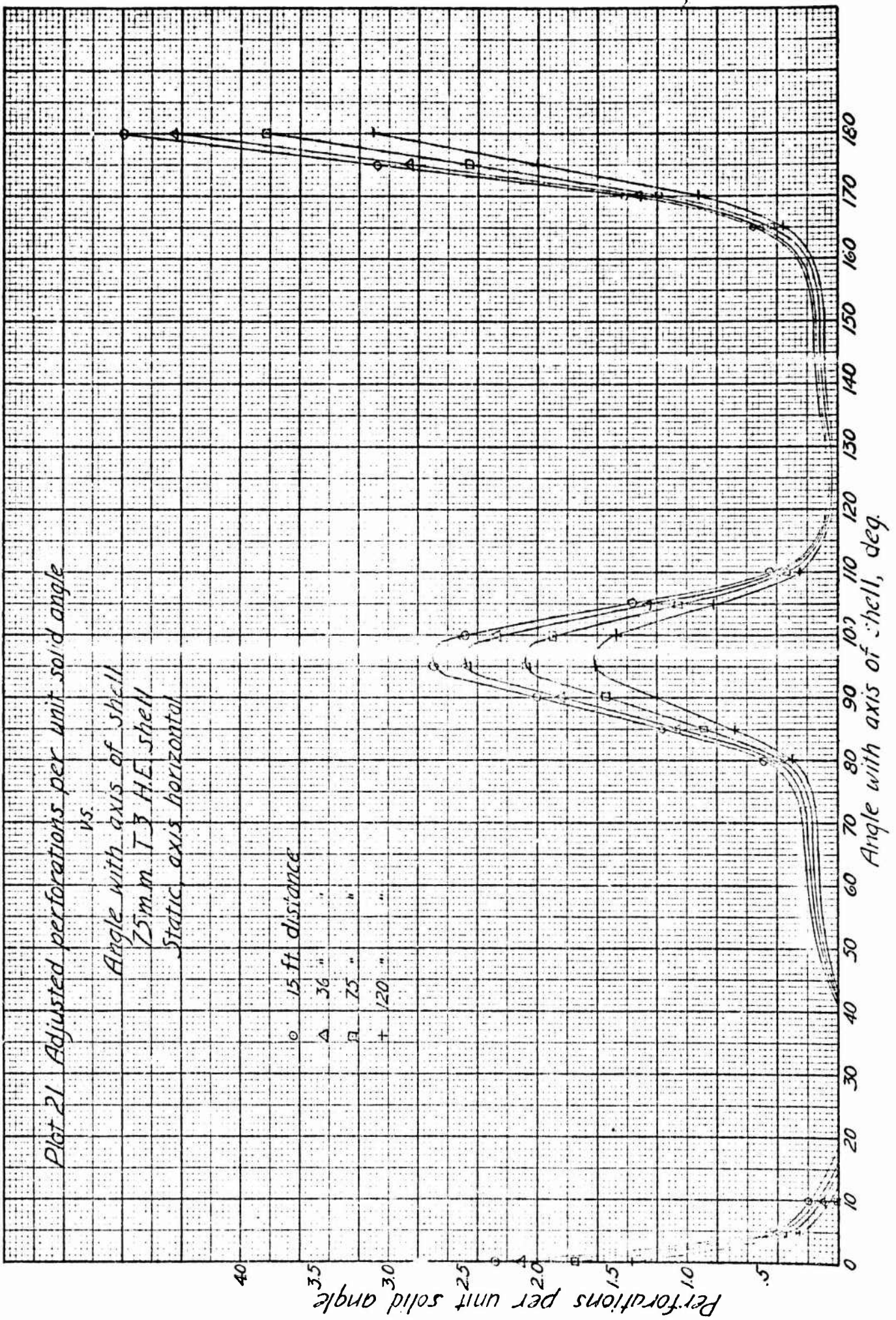
* The area inclosed by the 1 fragment per sq. yd. locus has sometimes been called the effective area of a round. It is desired to point out that the effective area so determined is not a true measure of the efficiency of the shell since it includes only a part of the total number of casualties. For a complete determination of efficiency, it is necessary to know $\sigma(R, \theta)$, that is, the fragment density as dependent on the distance from the burst, and the angle with the shell axis.

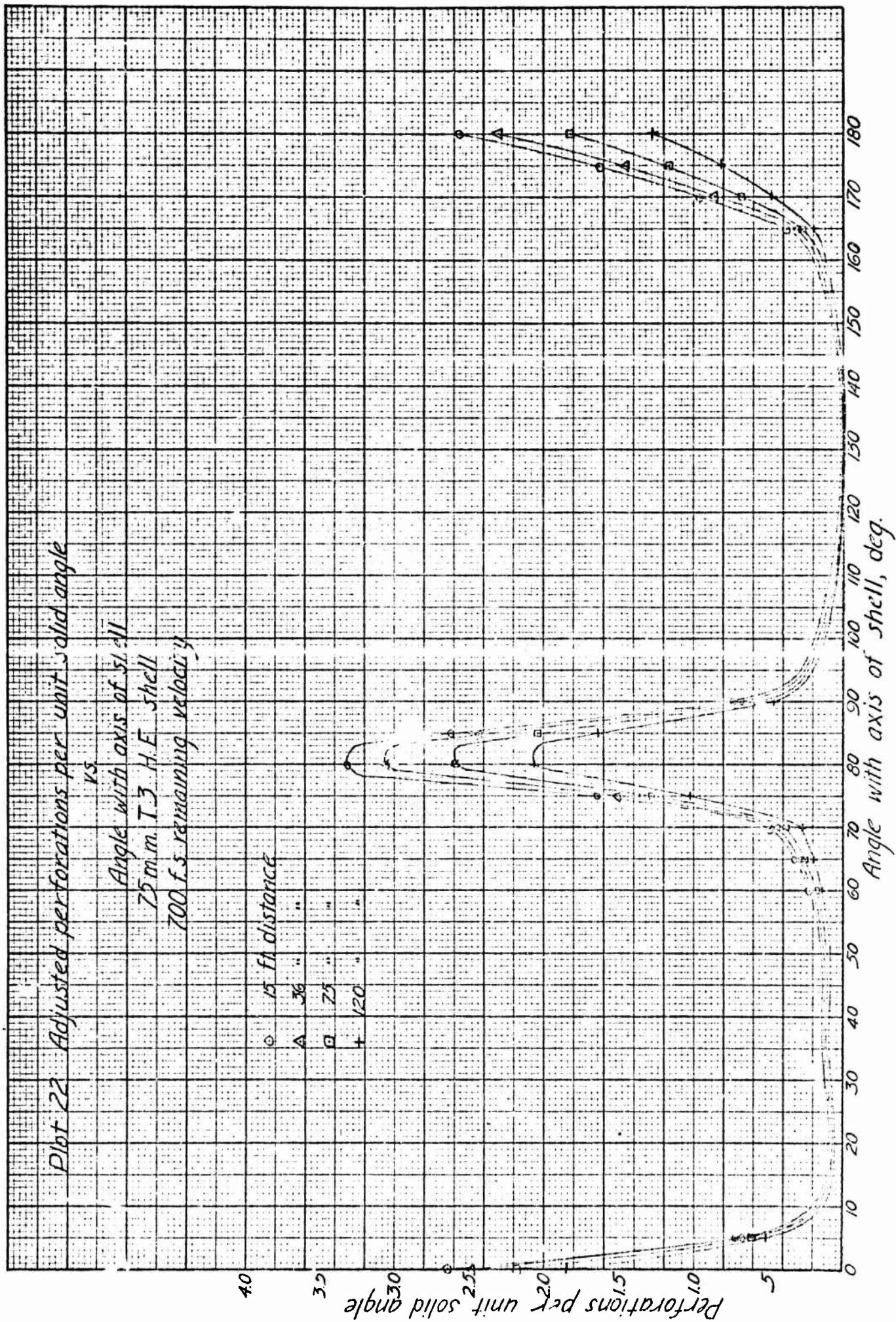
Pict 21 Adjusted perforations per unit solid angle
vs.

Angle with axis of shell
75mm T3 HE shell
Static axis horizontal

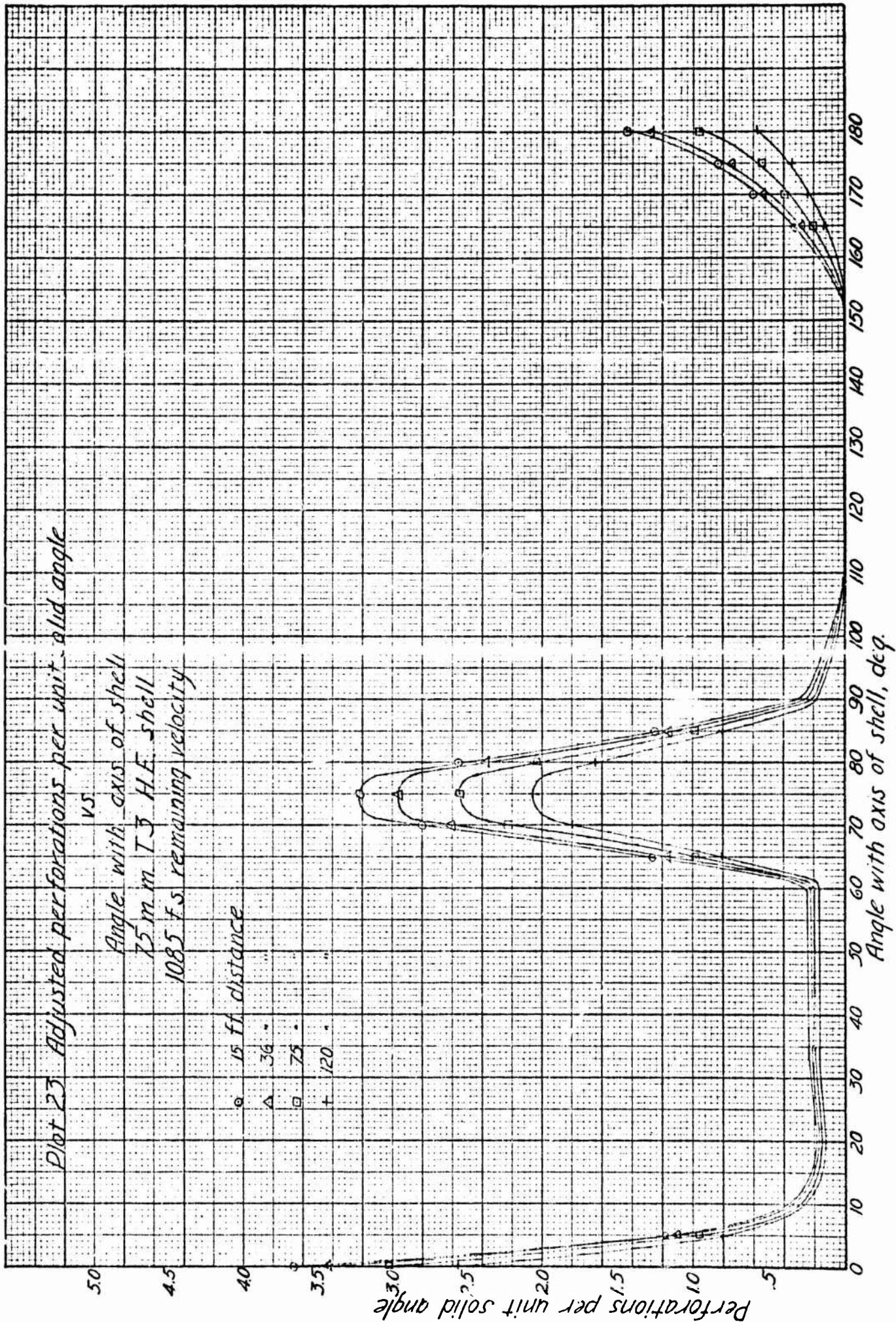
15 ft distance

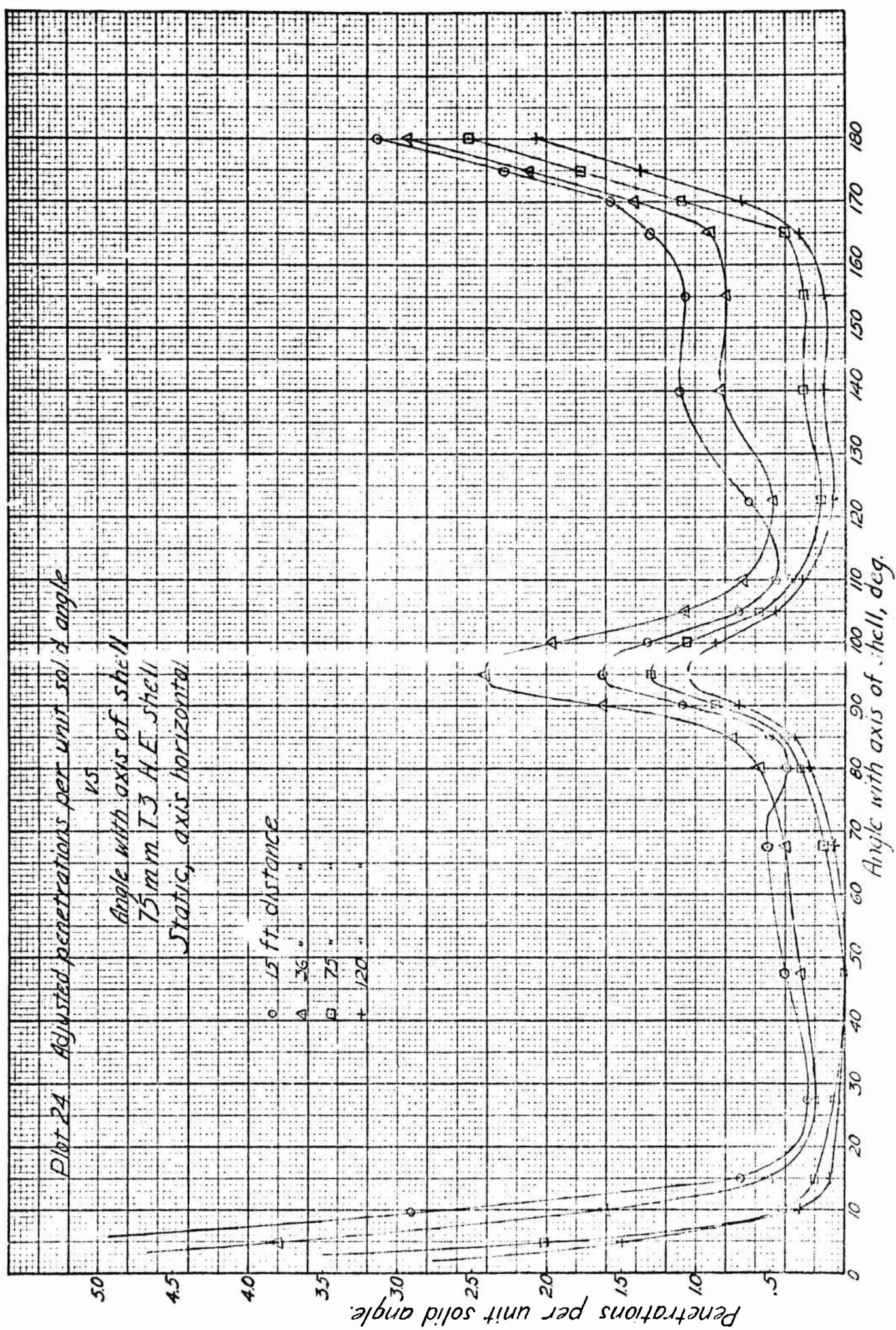
○ 36 "
△ 75 "
□ 120 "





382



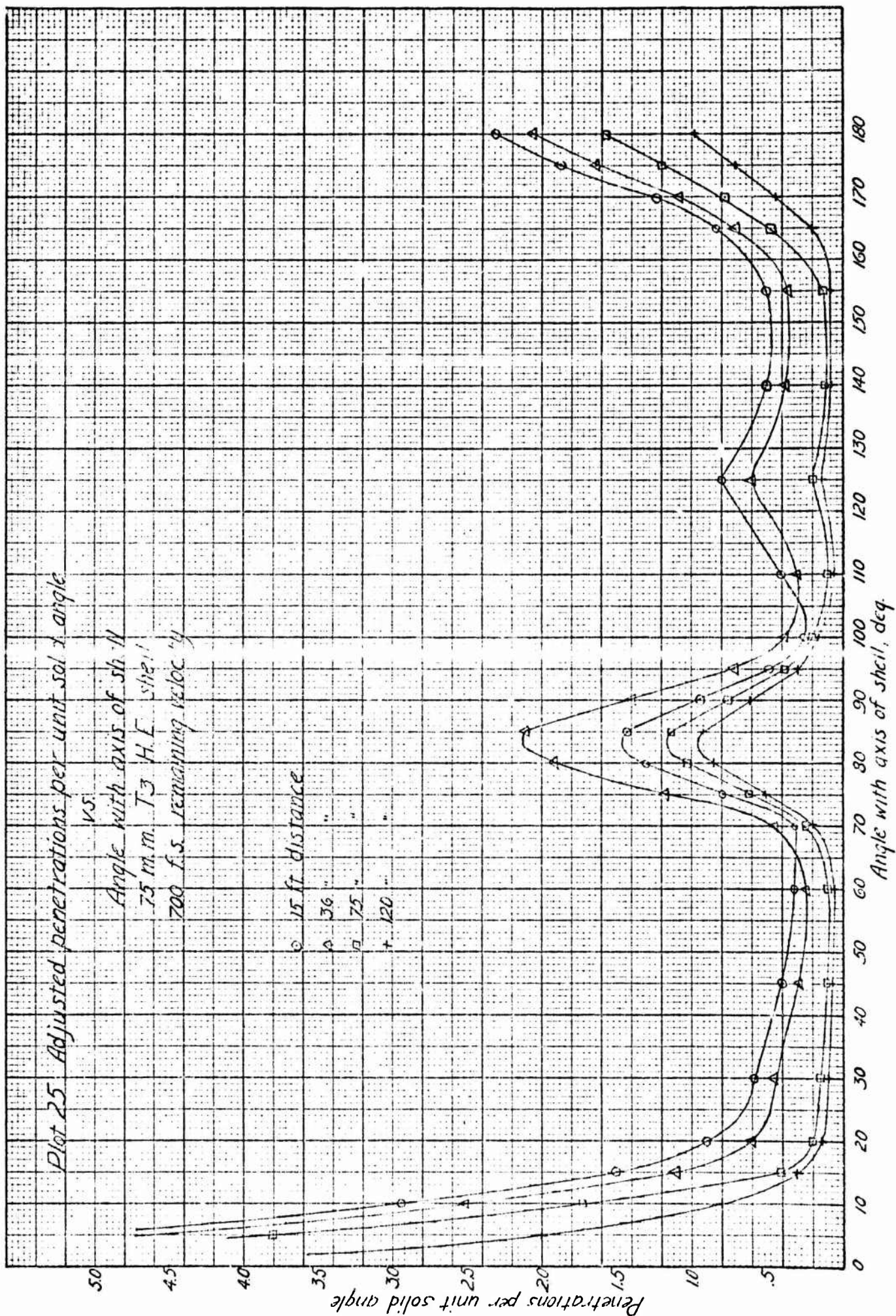


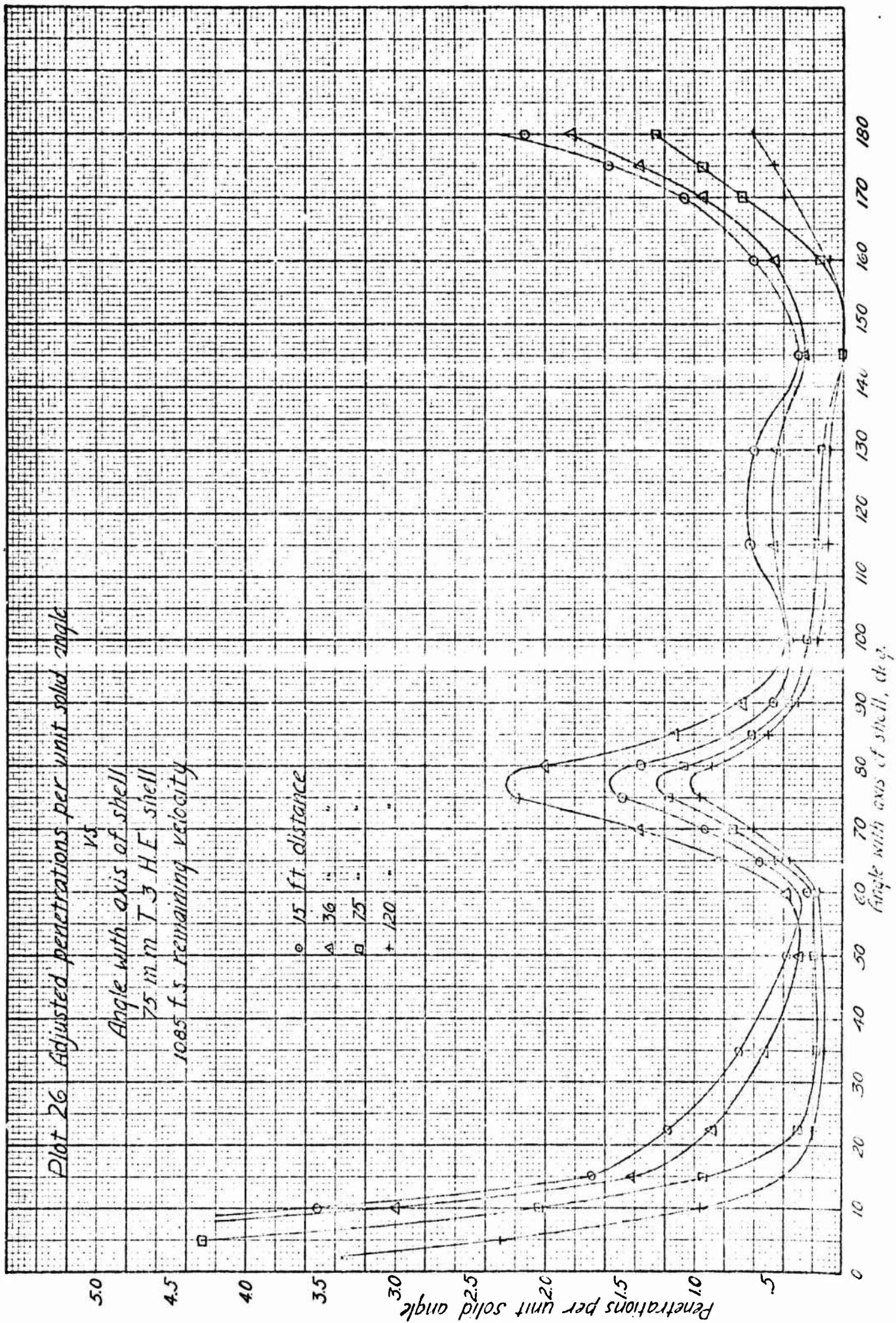
Plot 25 Adjusted penetrations per unit solid angle

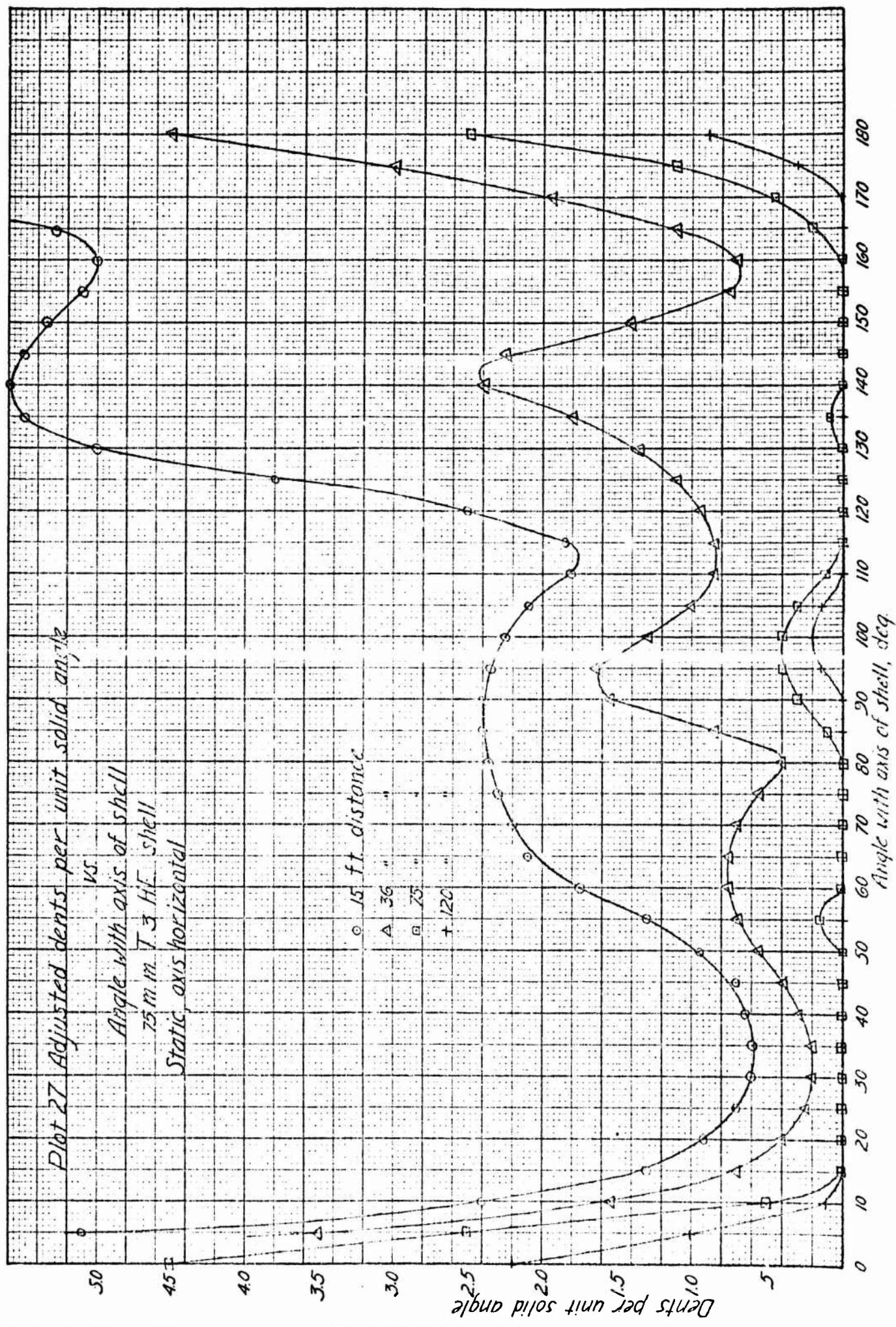
vs.
Angle with axis of shell
75 m.m. T3 H.E. shell
700 f.s. remaining velocity

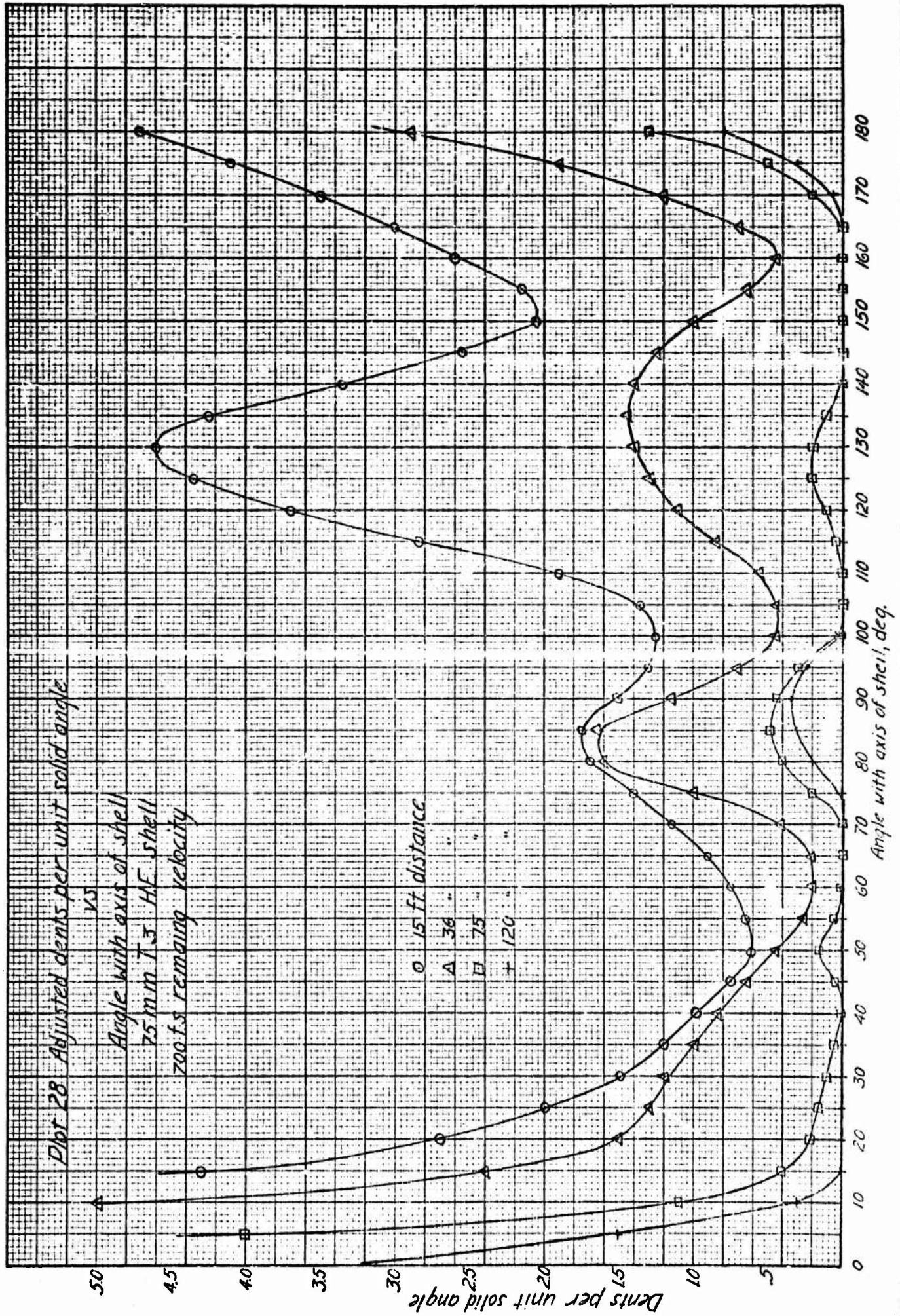
15 ft distance

36 "
75 "
120 "



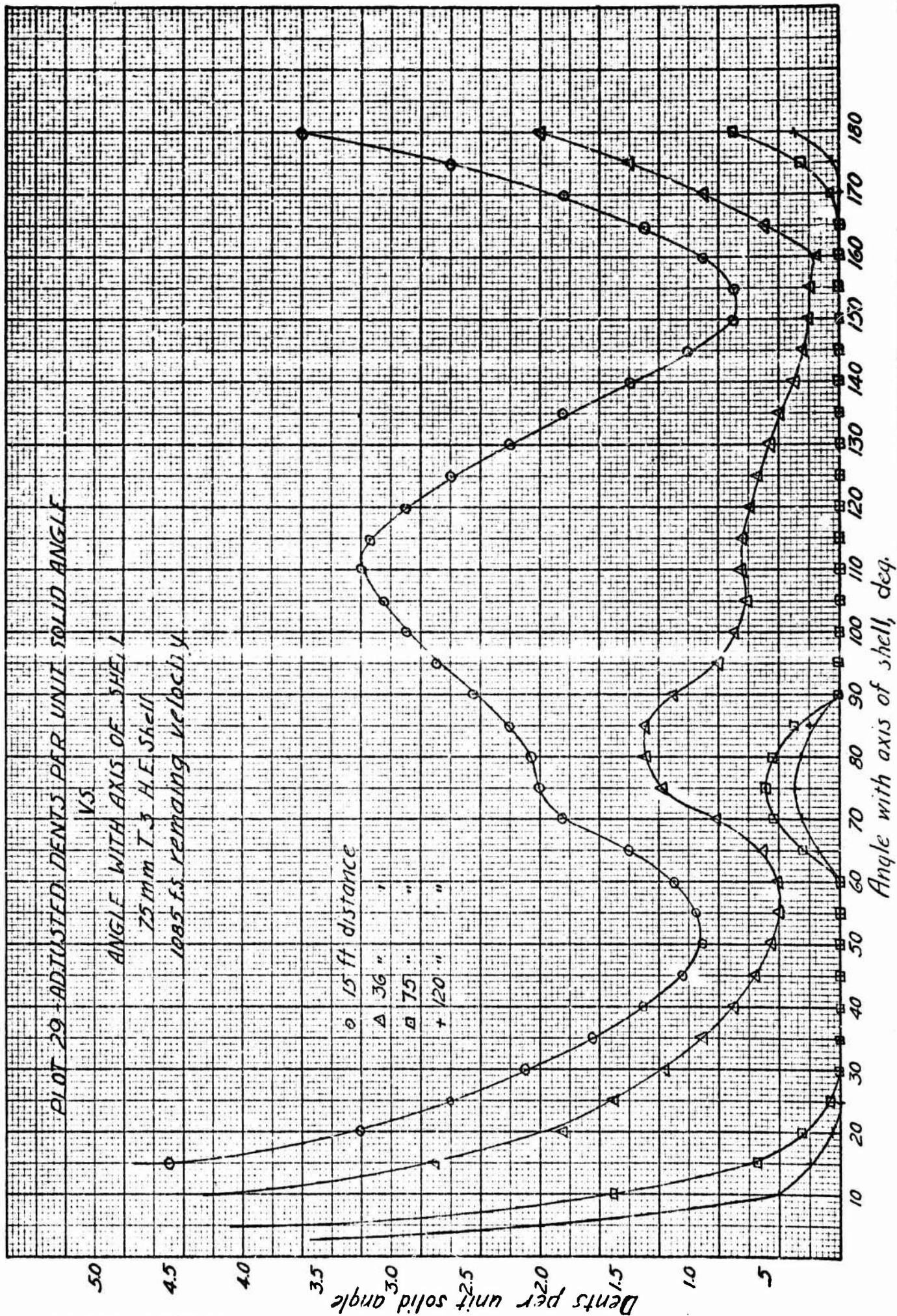






PLOT 29 - ADJUSTED DENTS PER UNIT SOLID ANGLE

VS
 ANGLE WITH AXIS OF SHELL
 75 mm T-3 H.E. Shell
 1085 ft remaining velocity



Usually the distance to a certain constant number of fragments per sq. yd. of surface as a function of the angle with the axis of the shell is desired rather than the number as a function of the distance. A sq. yd. of surface is here defined as one normal to the trajectories of the fragments.

Having given $\sigma(R)$, the fragment density per unit solid angle as a function of R , the distance at which there are N hits per sq. yd. is given by the equation

$$R^2 = \frac{100 \sigma(R)}{N}$$

Since $\sigma(R)$ was assumed to be a linear function of R with a negative slope the equation is in the form of a quadratic. Because $\sigma(R)$ was in the form of data rather than equations, it was convenient to plot

$\frac{NR^2}{100}$ and $\sigma(R)$ as functions of R on the same coordinate axis. Then, where the curves intersect, a root of the equation was determined.

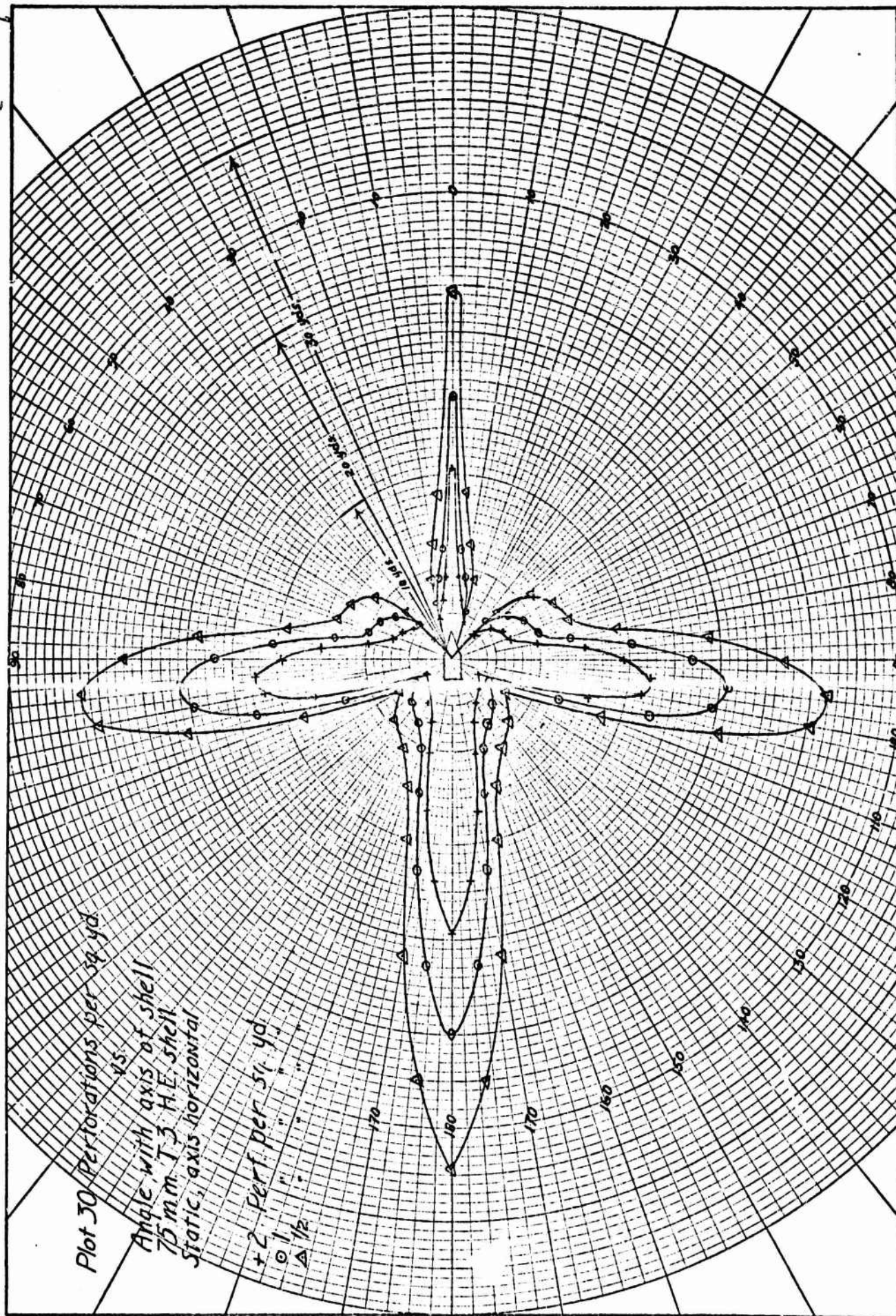
Values of N of 2, 1, and $1/2$ fragments per sq. yd. were assumed. The adjusted or smoothed fragment densities shown in Plots 1 to 18 were used for $\sigma(R)$.

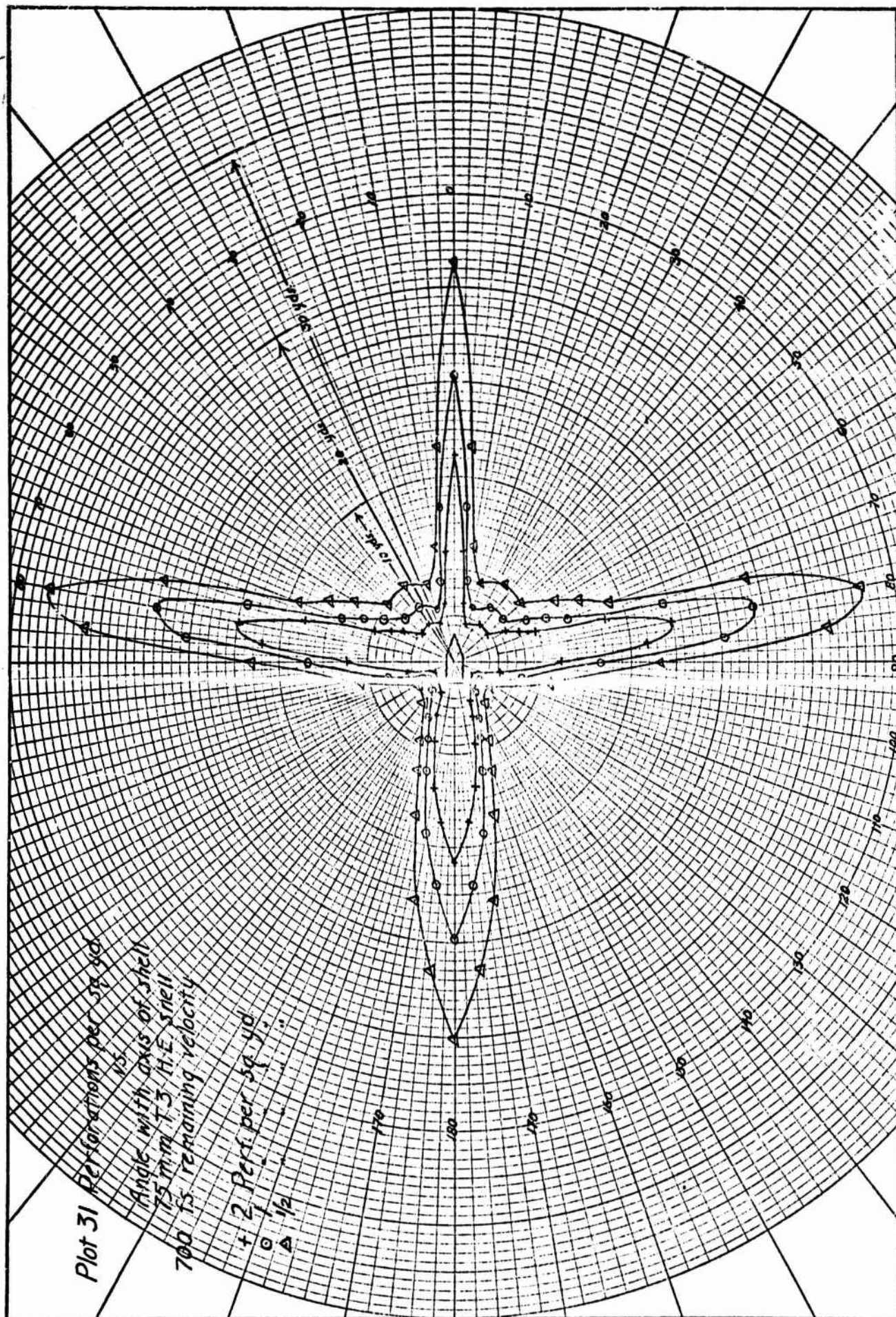
Plots 30 to 32 show the perforations per sq. yd. as a function of the angle with the axis of the shell for static firing, and for remaining velocities of 700 and 1085 f/s. Plots 33 to 38 show the data for the penetrations and dents under the same conditions of fire.

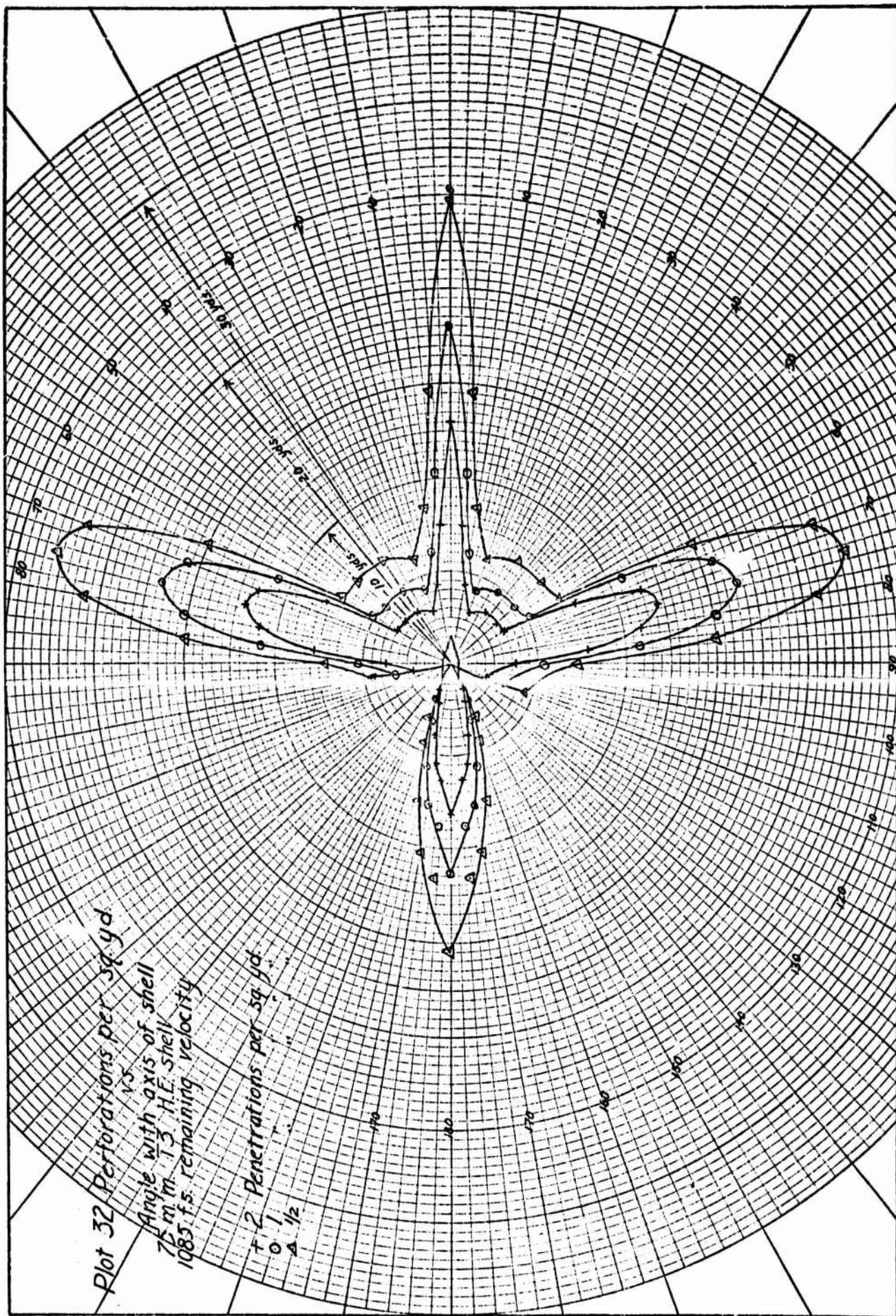
In view of the discussion earlier in the report regarding number of fragments per unit solid angle as dependent on the angle with the axis of the shell, the distance from the burst, and the remaining velocity of the shell, a discussion of the plots of number per sq. yd. would be a duplication of work. The plots are intended for future reference on the basis of number per sq. yd.

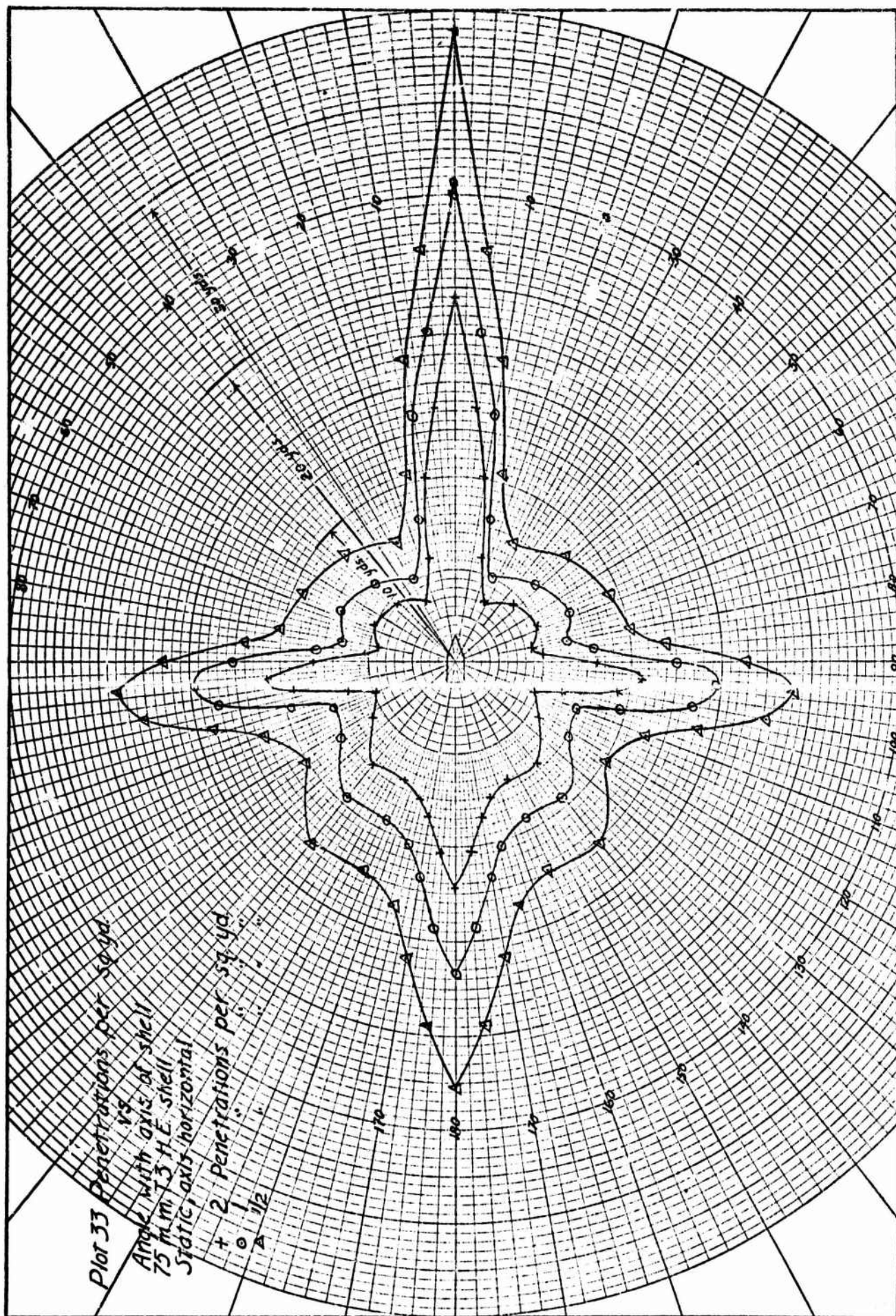
Sectional areas of fragments

The dimensions of the perforations and penetrations on the panels were measured as a part of the fragmentation tests. It was impractical, however, to measure the dents because of their small size. The sectional areas of the perforations and penetrations were computed and then grouped according to size. Plots 39 to 44 show for

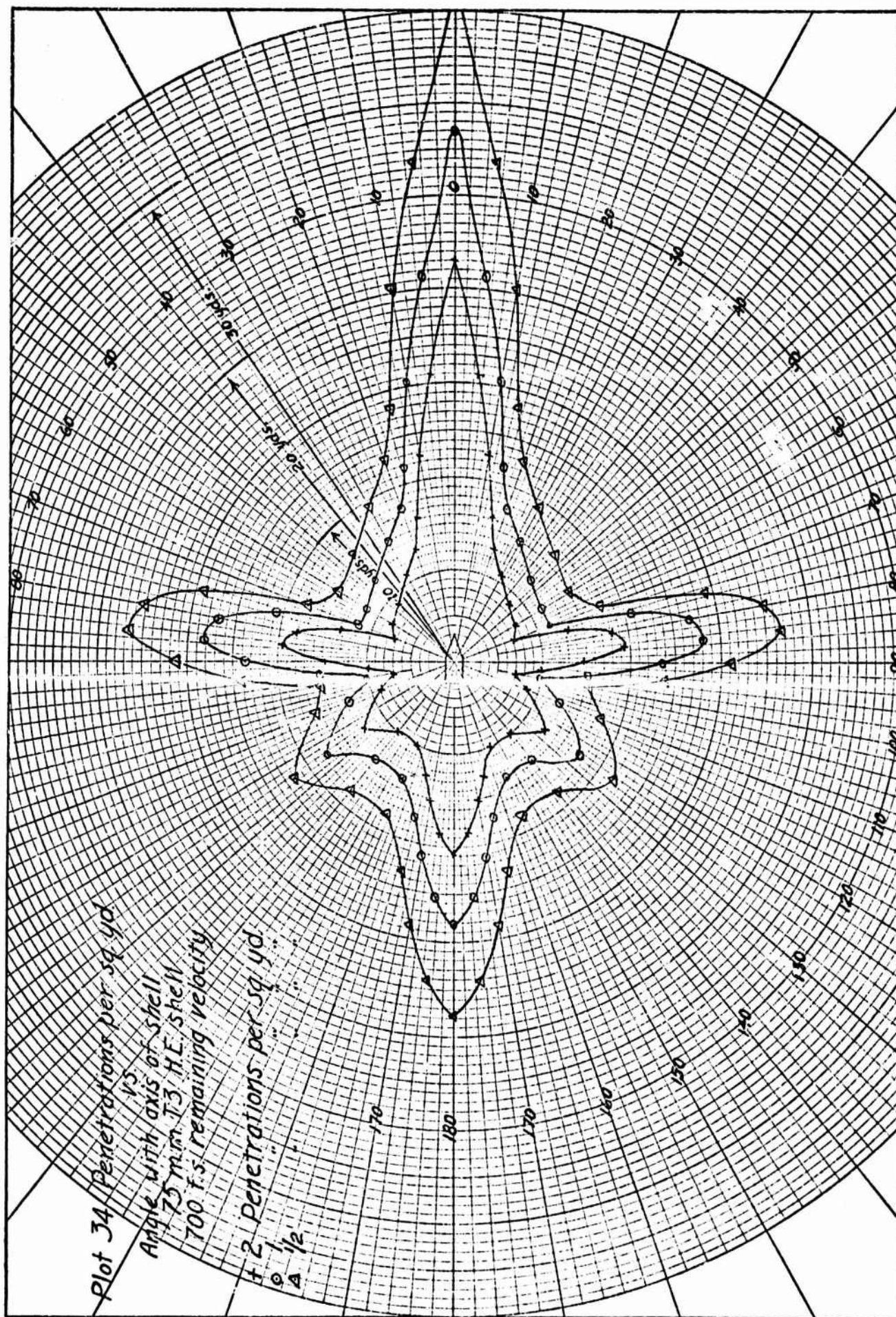


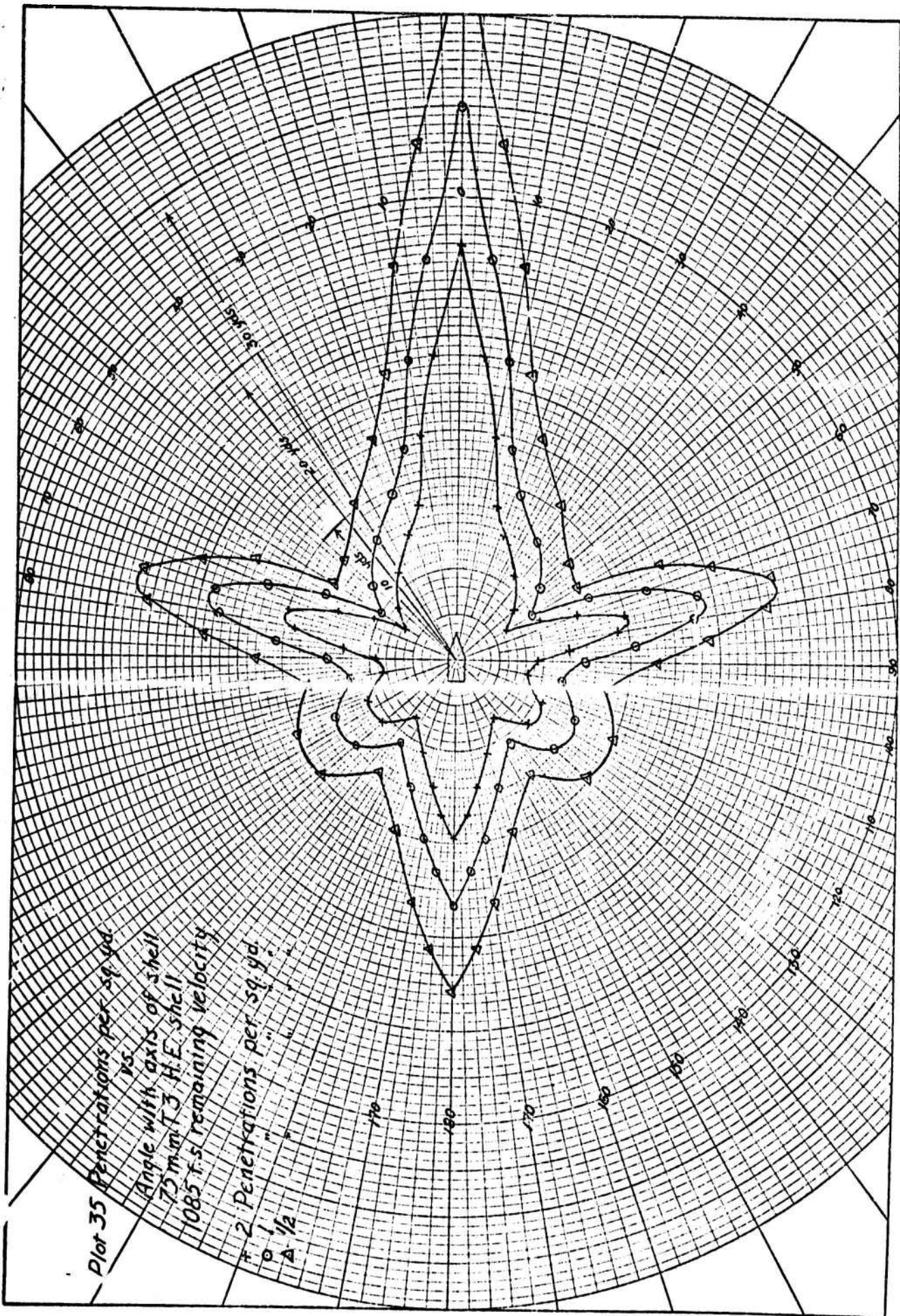




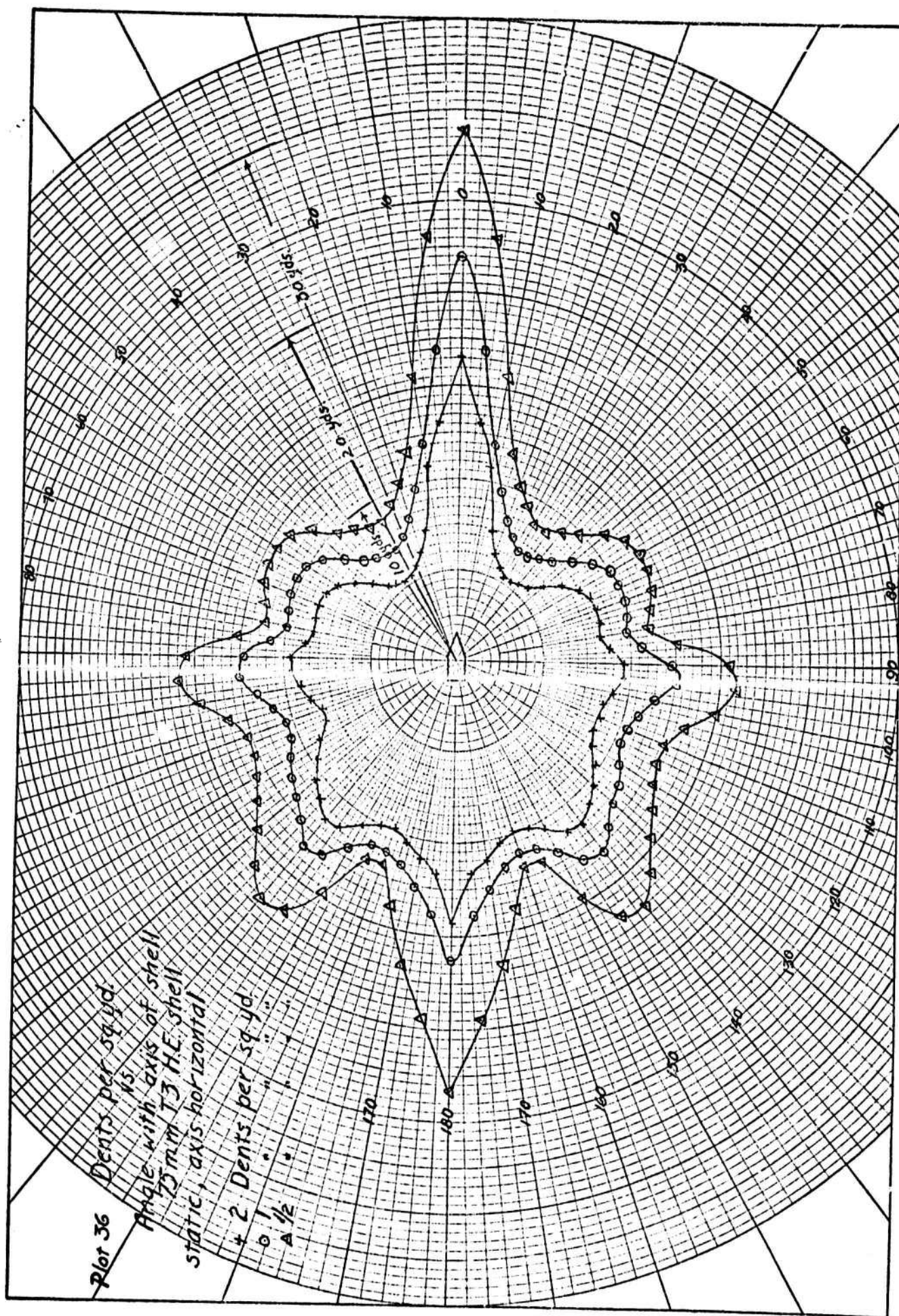


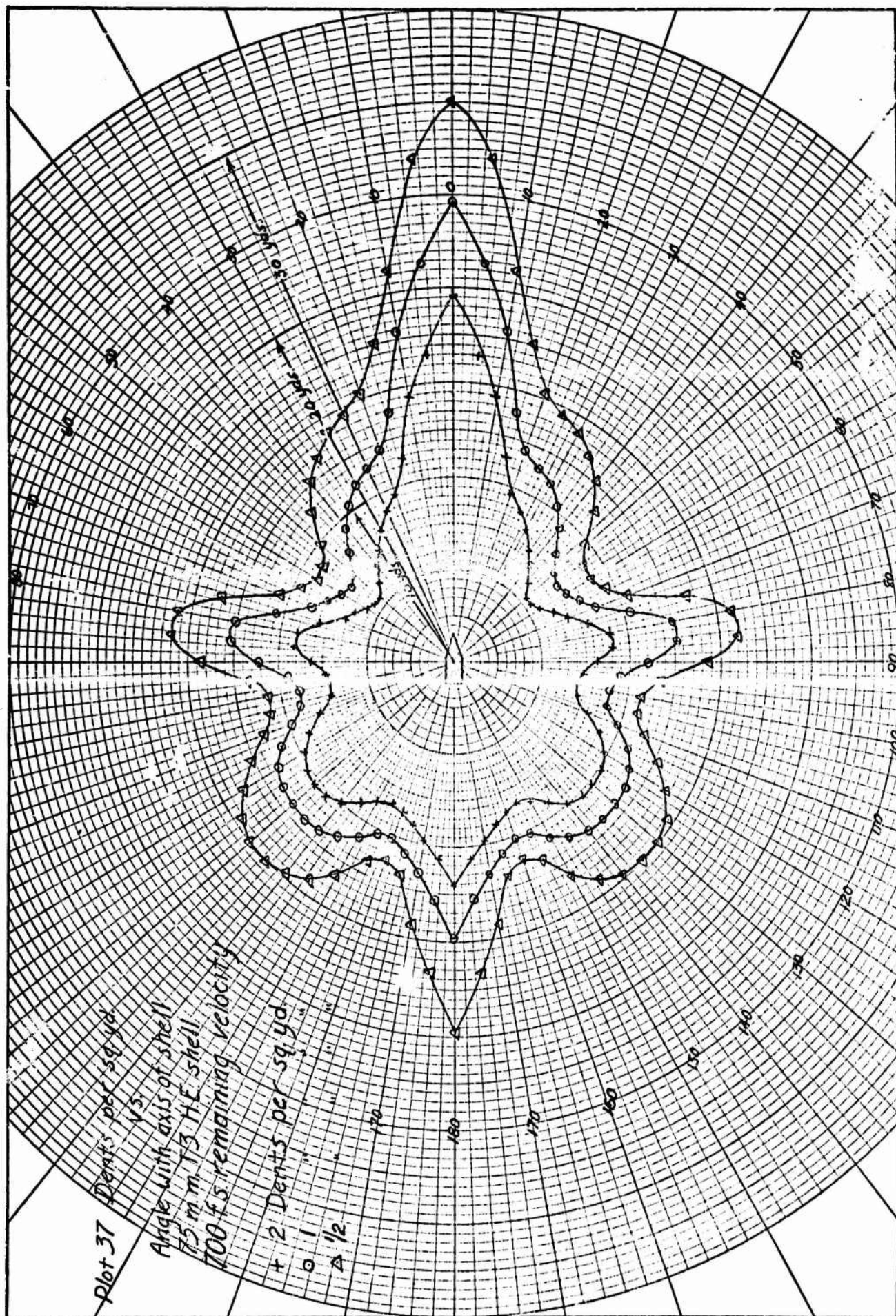
290

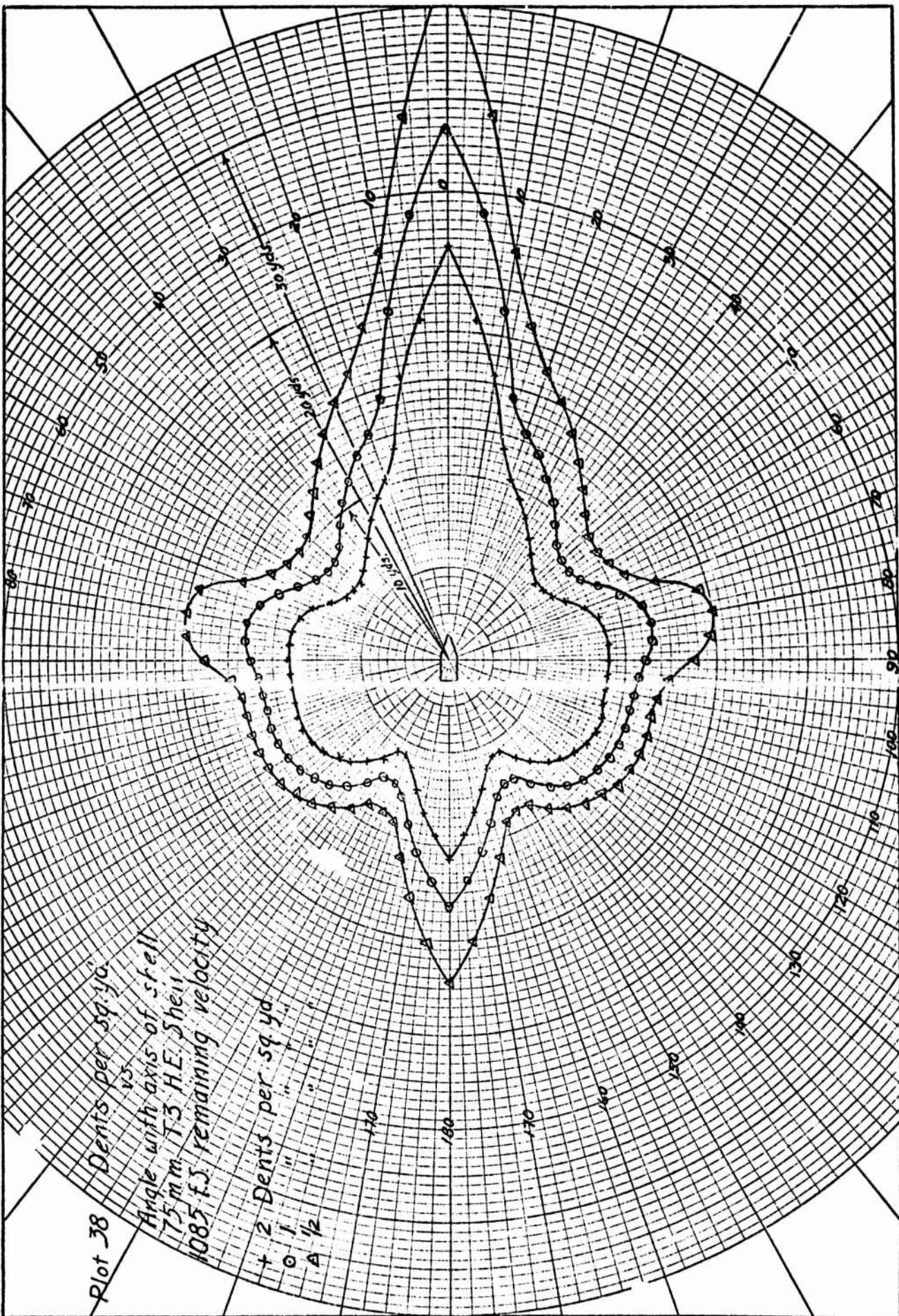




29F



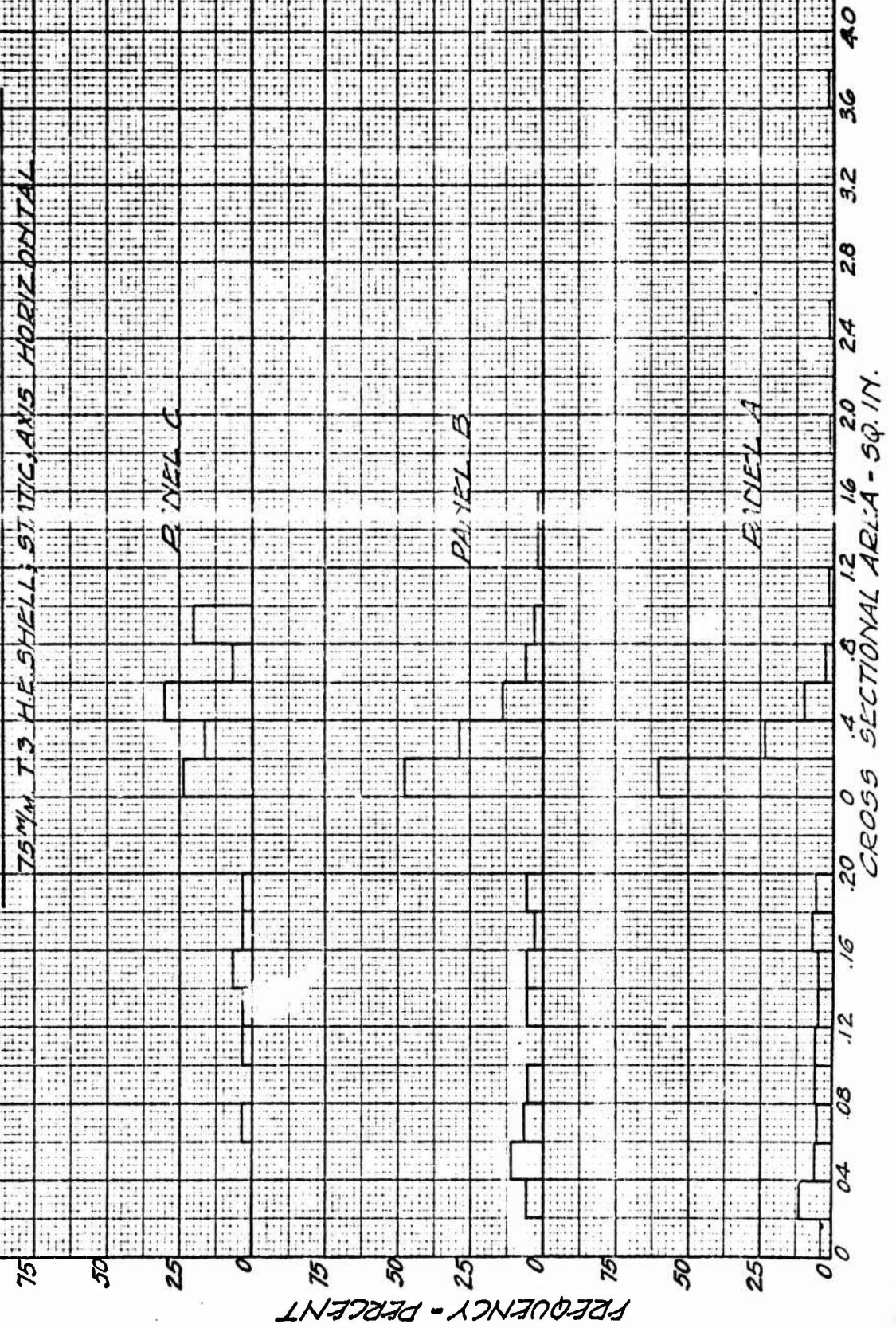


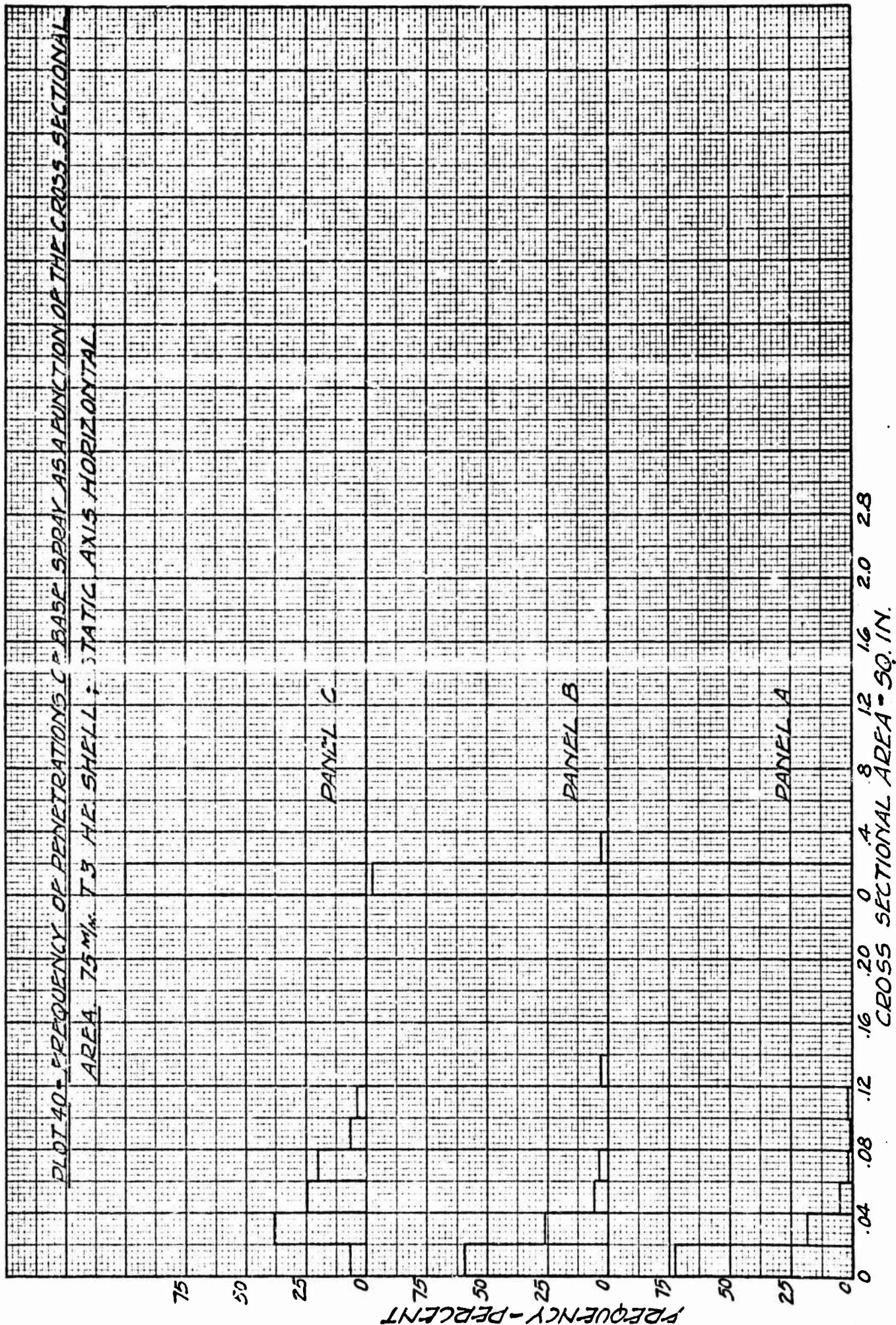


PLOT 39 - FREQUENCY OF PERFORATIONS OF BASE SPRAY

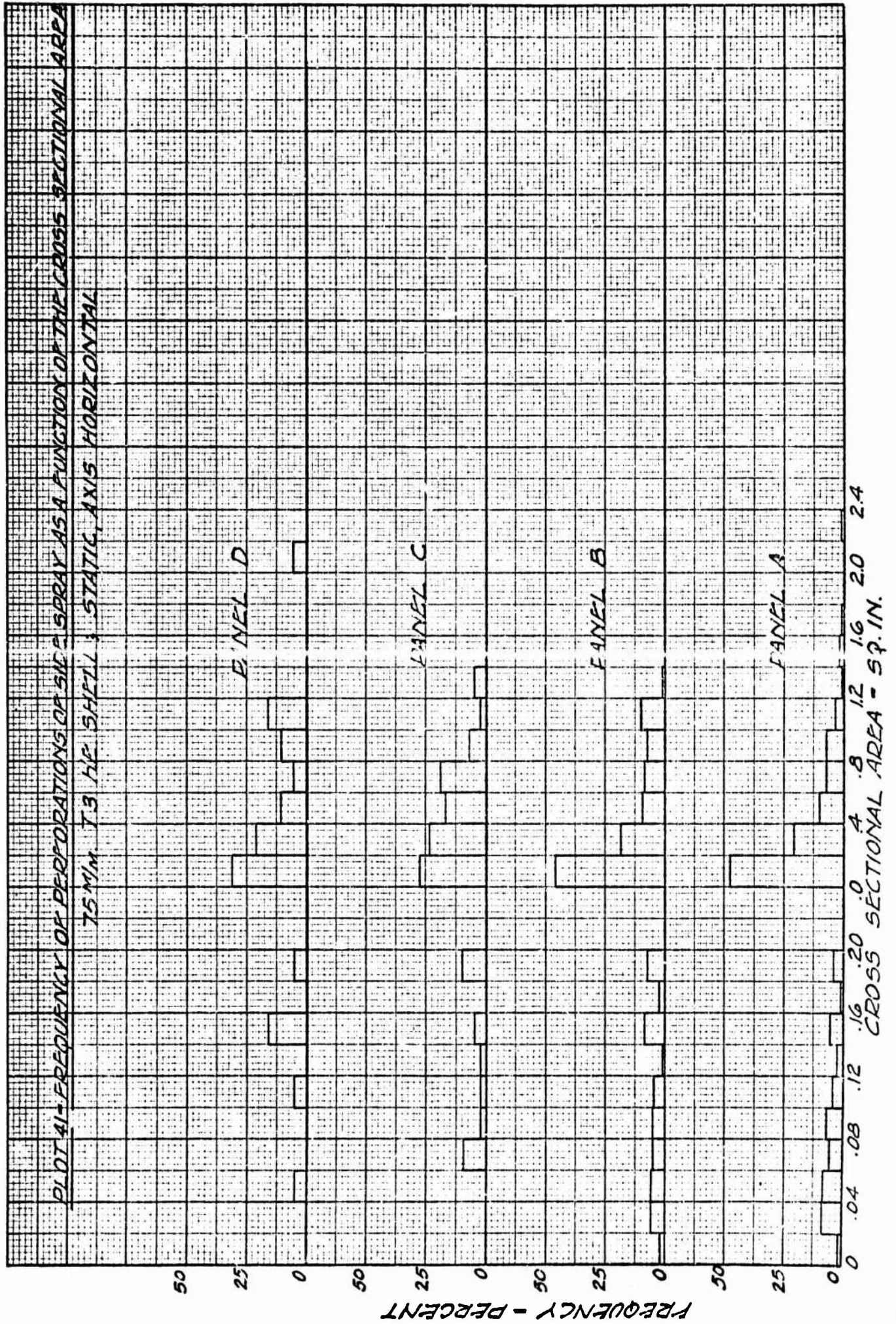
AS A FUNCTION OF THE CROSS SECTIONAL AREA

75 MM T-3 HE SHELL; STATIC AXIS HORIZONTAL

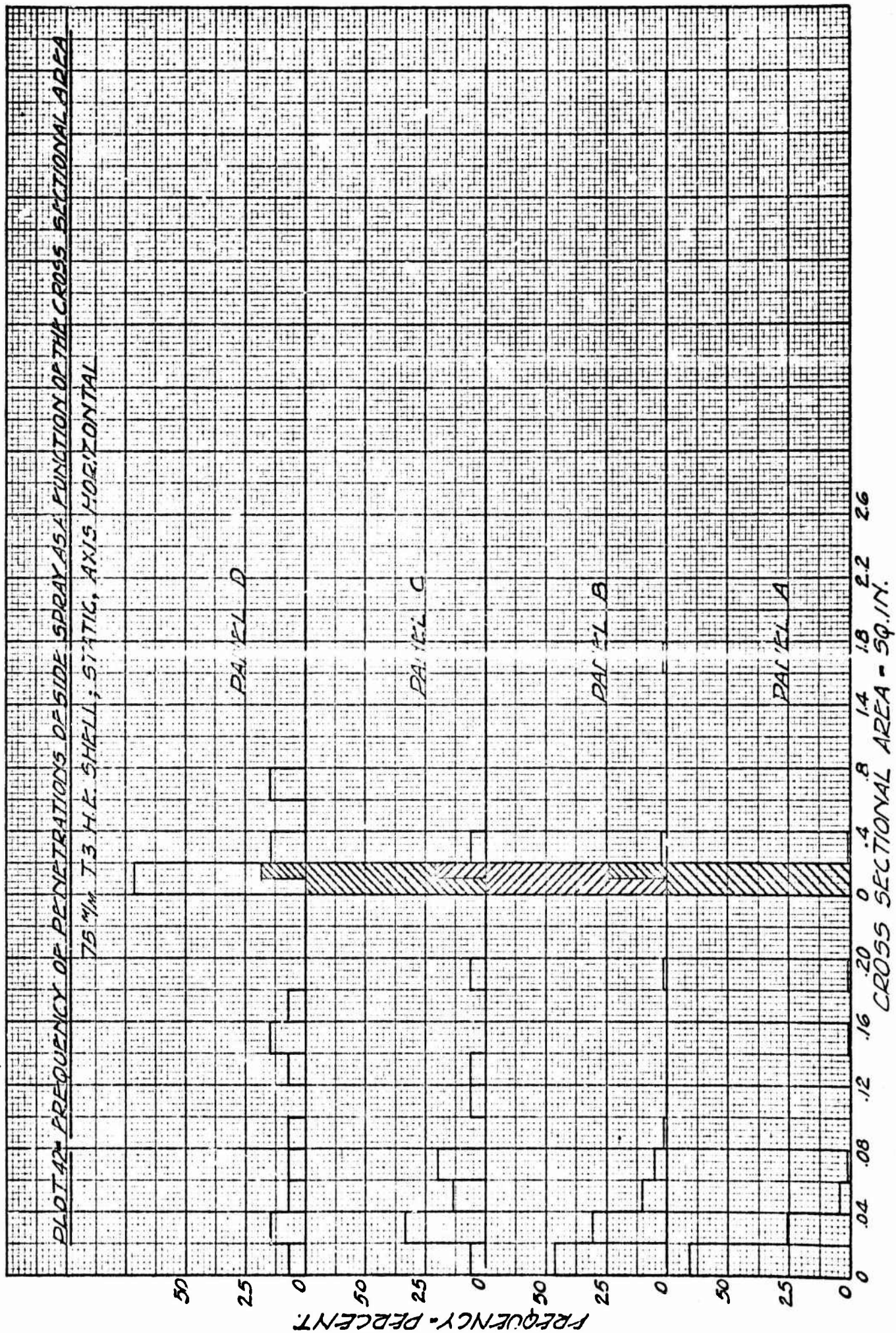




W/62



N62



PLOT 43 - FREQUENCY OF PERFORATIONS OF NO. 16 SPRAY AS A FUNCTION OF THE CROSS SECTIONAL

AREA 75 M²/IN. T. 3 H.E. SHELL; STATIC; AXIS HORIZONTAL

PANEL C

(38% BETWEEN 5.0 AND 7.0 SQ. IN.)

PANEL B

(20% BETWEEN 6.2 AND 6.4 SQ. IN.)

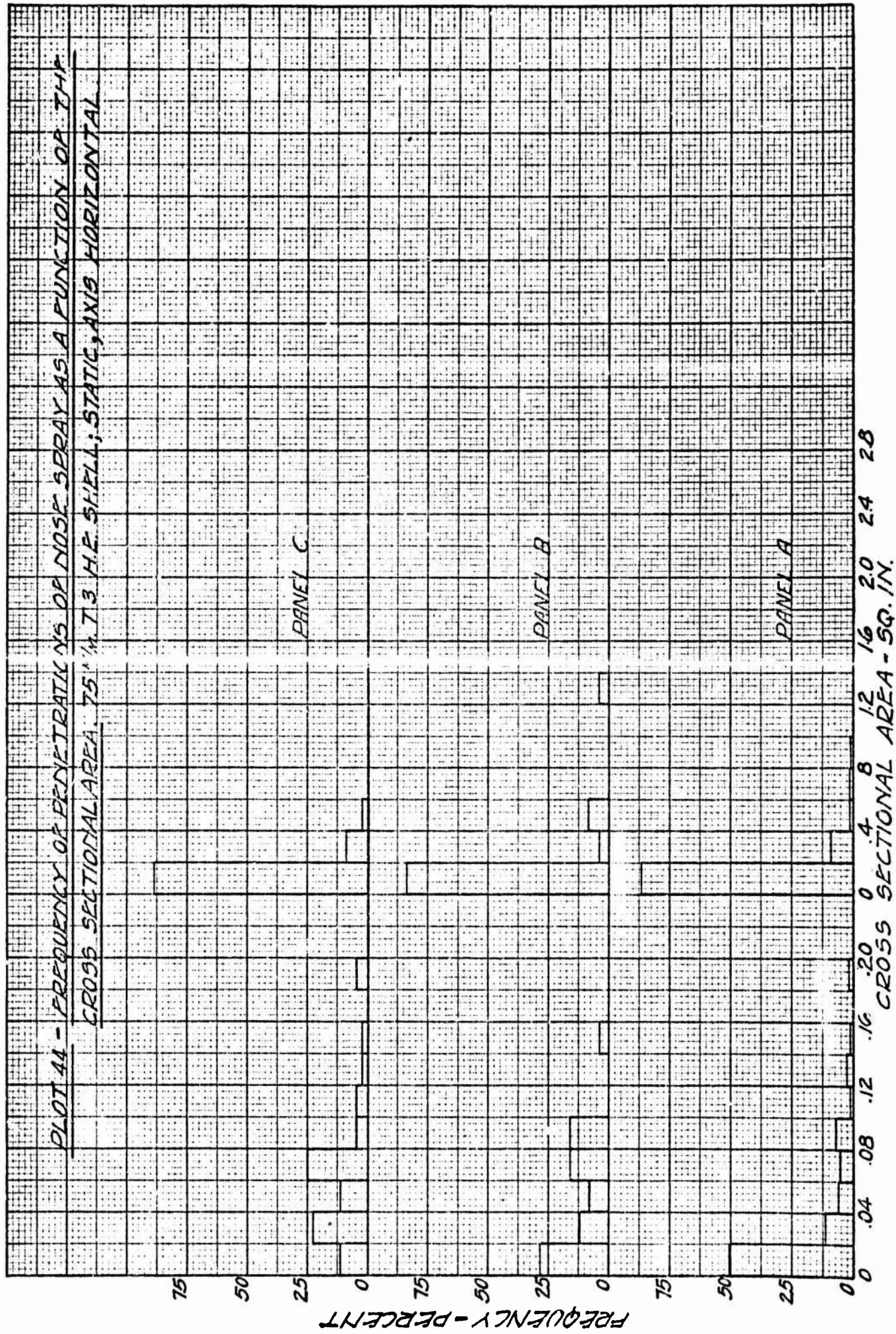
PANEL A

(15% BETWEEN 6.6 AND 6.8 SQ. IN.)

FREQUENCY - PERCENT

CROSS SECTIONAL AREA - SQ. IN.

462



static firing the frequency or the per cent of the total number of fragments as a function of the sectional area. For example, in Plot 39, 3.5% of the total number of the perforations in the base spray on Panel A had areas between 0 and .02 sq. in., 10.8% had areas from .02 to .04 sq. in., and so on. Two different scales were used for the areas in order to show the distribution of the small sizes.

As a class, it appears that the nose fragments are distinctly larger than either the base or side fragments. The base and side fragments have approximately the same distribution according to size.

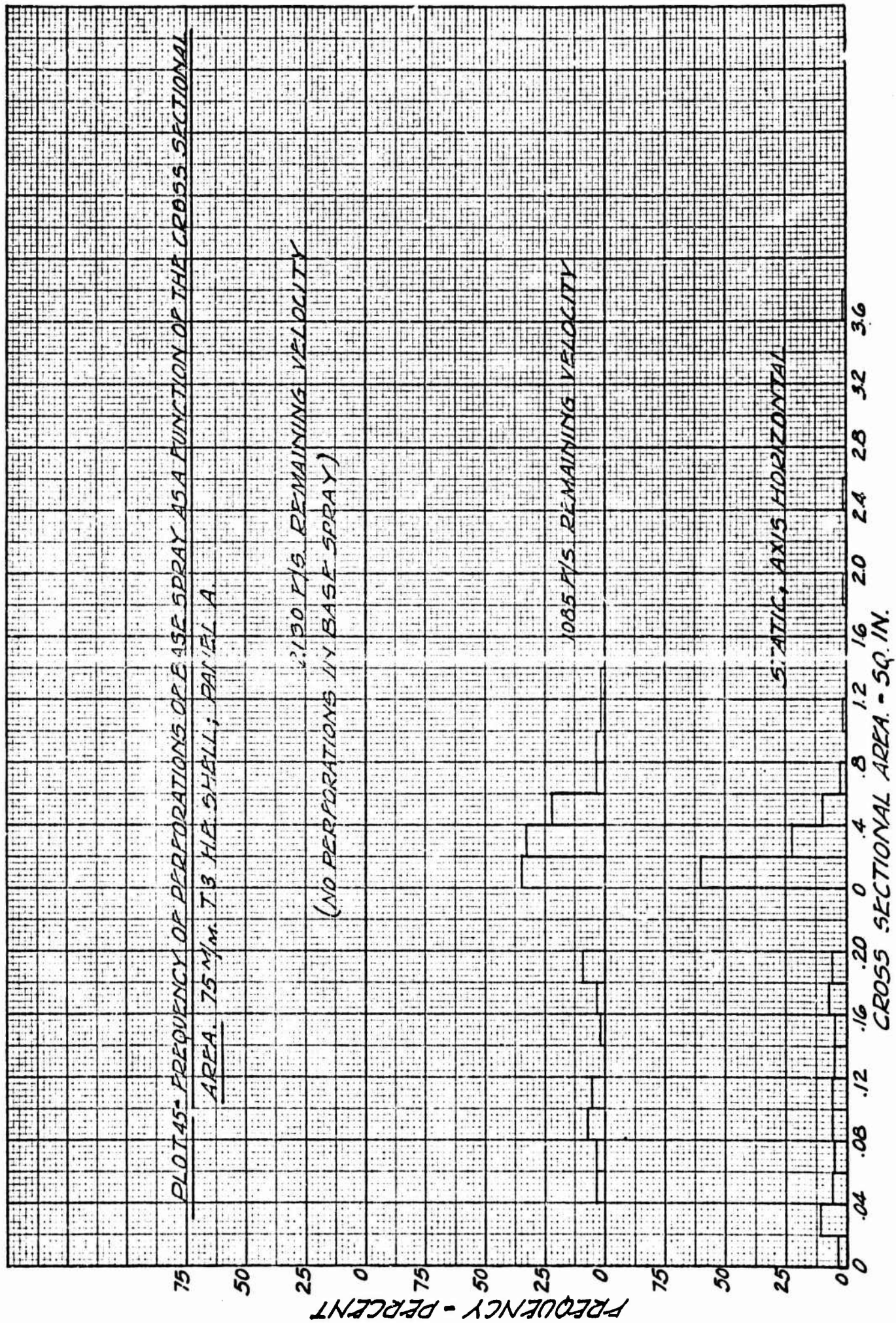
Comparing the sizes of the perforations with the penetrations, the former are much larger. Weighting the proportions according to the number represented it is computed that 2% of all the perforating fragments issuing from the shell have sectional areas less than .02 sq. in., while 10% have areas less than .04 sq. in. It is computed that 66% of all the penetrations have sectional areas less than .02 sq. in. while 89% have areas less than .04 sq. in.

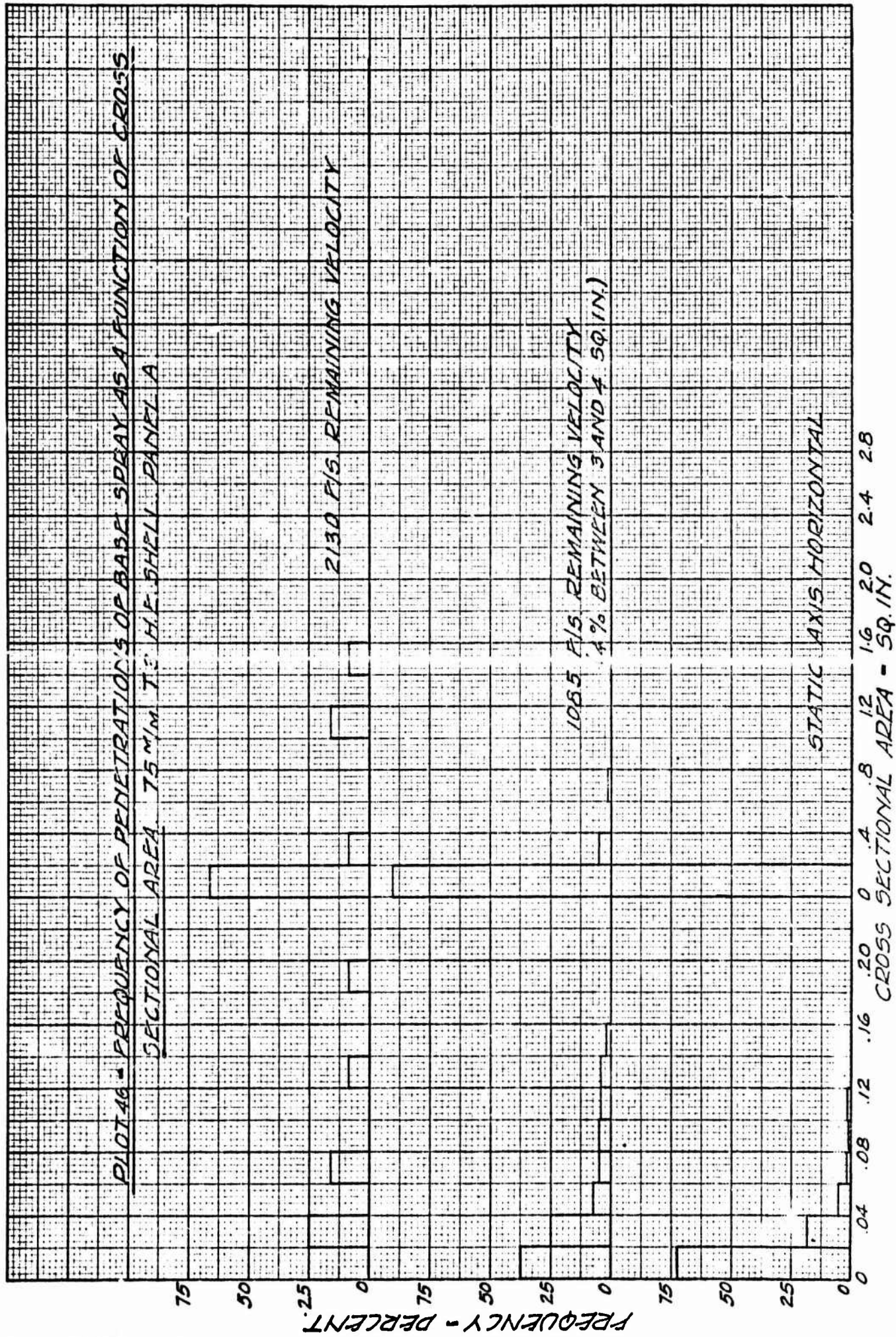
Considering the frequencies as a function of the distance from the burst, the proportion of large sizes increases with the distance.

The effect of remaining velocity is illustrated in Plots 45 and 46, showing the perforations and penetrations of the base spray on Panel A at 3 different velocities. The base spray was selected for this purpose because shell velocity has a great effect in reducing the number of these fragments. As the shell velocity is increased, the frequency of the larger sizes tends to increase. Since small fragments have small ballistic coefficients, it is assumed that as the fragments lose velocity due to shell velocity, the smaller base fragments are no longer able to mark the panel. The increase in proportion of large sizes with shell velocity does not appear to be due to greater initial velocity of the large sizes when fired statically.

In the pit fragmentation tests, an average of 779 fragments per shell were obtained, accounting for 95.6% of the weight of metal. As a result of panel tests it was computed that there are about 700 perforating, 900 penetrating, and 3400 denting fragments making a total of about 5000 fragments. In the pit tests, the fragments are separated from the sand by a screen having square

30A





openings .22 inches on a side, area of opening .048 sq.in. It is plausible to assume that practically all of the fragments having sectional areas of less than .02 sq.in. on the panels would pass through the screen. Since 66% of the penetrating fragments had sectional areas on the panels of less than .02 sq.in., it appears that practically all of these sizes would pass through the screen and be unaccounted for in the pit tests. Also, about 23% of the penetrations on the panels had sectional areas between .02 and .04 sq.in. and it may be assumed that a lot of these fragments would not be accounted for in pit tests. Hence, it appears that substantially all of the fragments obtained in pit tests appear as perforating fragments in panel tests at 15 ft. distance, while most of the penetrating fragments in panel tests are unaccounted for in pit tests.

Results of tests with armor plate

In conjunction with the fragmentation tests on wood panels, a few pieces of armor plate were placed on the panels for purposes of comparison. The plates were 12" x 12" x 1/4" in size, Brinell hardness averaging about 418. One plate was hung in the base spray and two in the side spray on both Panels A and B. The plates were on the panels for a total of 21 rounds, which were fired statically and at various remaining velocities. The sidespray plates were moved forward on the panels as the shell velocity was increased in order to keep within the band. The hits on the plates were classified as perforations, penetrations, and dents in the same manner as for the wood panels.

The fragment density per unit solid angle on the armor plates were computed for the various conditions of fire. Also, the fragment densities in the wood panel section surrounding the plates were computed for purposes of comparison. The following table shows the average density of the hits of the sidespray on Panel A for various remaining velocities.

Comparison of fragment densities of the sidespray on 1/4" armor plate and on wood panels.

Ave. vel. of Shell	Type of fragment	Number per unit solid angle On Armor Plate	On panel section sur- rounding plates
Static*	Perf.	0	1.71
	Penet.	.75	.96
	Dents.	.15	-
700	Perf.	.84	2.81
	Penet.	2.81	.96
	Dents.	1.12	-
1085	Perf.	1.12	3.85
	Penet.	.56	1.76
	Dents.	2.81	-
1450	Perf.	.56	2.41
	Penet.	1.12	.48
	Dents.	1.12	-
1625	Perf.	0	.96
	Penet.	0	.48
	Dents.	.56	-
2130	Perf.	0	3.05
	Penet.	1.68	2.40
	Dents.	1.68	-

While the results are rather erratic due to the small sample sizes, certain trends are evident. It appears that the sum of the perforations, penetrations, and dents on the plates is generally greater than the perforations on the wood panel, indicating that some of the penetrations on the wood become penetrations or dents on the plates. Comparing the perforations on panels and plates, it appears that on the average about one perforating fragment in 6 on the wood panels would be perforating against 1/4" plates at 15 ft. distance from the burst.

* Shell axis vertical, plates on middle row of panel squares.

Considering the results on Panel B, there were only 5 hits on armor plate in the sidespray consisting of 1 perforation, 1 penetration, and 3 dents. It appears that the sample size on Panel B was too small to show much in regard to fragment density. However, the results show that the sidespray is capable of perforating 1/4" armor plate at least to 36 ft. distance from the burst.

With regard to the plate suspended in the base spray, only two hits were secured, a penetration and a dent at 700 f/s velocity. It may be that at shell velocities above 700 f/s the base spray fragments will not perforate armor plate.

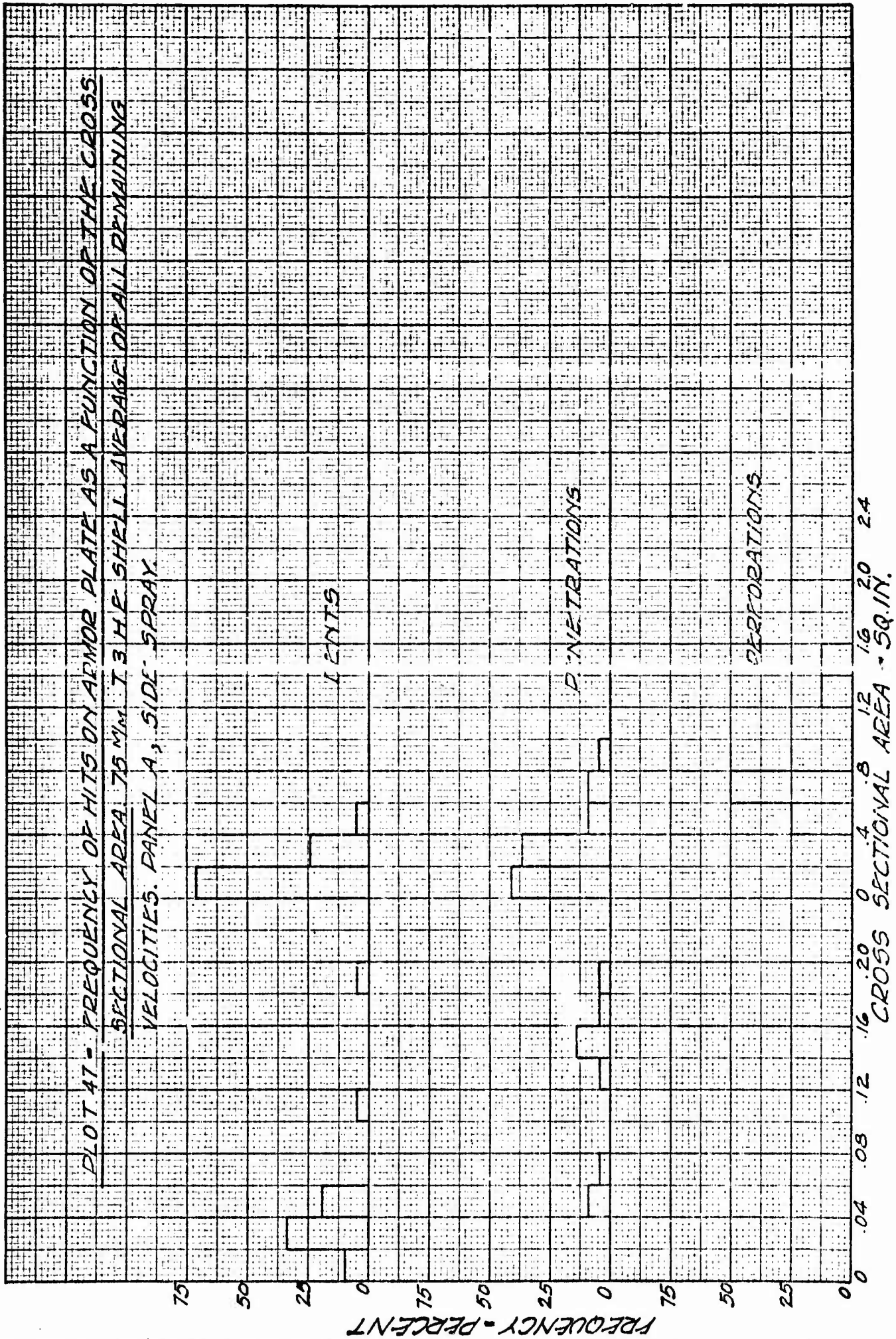
The dimensions of the hits on armor plate were measured and the cross-sectional areas computed. Plot 47 shows the frequency of the fragments as a function of the cross sectional areas for the sidespray, Panel A.

As a group, the perforations are much the largest in sectional area, since 100% were greater than .40 sq. in. while only 23% of the penetrations and 5% of the dents were greater than .40 sq. in.

Plot 47, showing the distribution of sizes of the sidespray on armor plate, Panel A, may be compared with Plots 41 and 42 showing the distribution of the perforations and penetrations of the side spray on the wood on Panel A. It is noted that all the perforations on plate are greater than .40 sq. in. while about 30% of the perforations on wood are greater than .40 sq. in. showing that the perforations on plate are included within the largest 1/3 of the sidespray fragments that perforate the wood panel. On the average, the dents on armor plate are somewhat larger than the penetrations on wood panels.

As a part of the test, small sand butts were placed back of the panel inline with the armor plates in order to recover the perforating fragments. Since there were only 9 fragments that perforated the plates, the individual weights and dimensions are shown in the following table:

33A



<u>Dimensions of perforations on plate, inches</u>	<u>Area, sq. in.</u>	<u>Wt. of fragment, grains</u>
1-1/2 x 5/8	.937	350
1-5/16 x 9/16	.737	84
1-5/16 x 1/2	.656	112
1-1/16 x 9/16	.597	203
2-1/4 x 11/16	1.546	301
2 x 11/16	1.374	602
1 x 5/8	.625	231
1-3/16 x 7/16	.519	140
7/8 x 3/4	.656	<u>273</u>

Ave. 255

Velocity of fragments in the sidespray

When a shell is fired statically, the sidespray band is centered at a little more than 90 deg. with the axis of the shell. However, when a shell is burst with some remaining velocity, the sidespray band is displaced forward of the static position, the amount depending on the remaining velocity. The change in the angle of the sidespray with shell velocity was utilized in computing the average velocity of the sidespray.

The average positions of the sidespray with respect to the axis of the shell were obtained by computing the centroids of the areas under the curves shown in the plots of hits per unit solid angle. Then, for a given remaining velocity, the side spray angles on the four panels were averaged together. The angles were computed for the perforations and penetrations but not for the dents, because the beginning and ending of the side spray of dents was not well defined.

The following table shows the computed average velocities of the sidespray.

Average remaining velocity shell, f/s	Type of fragments	Average angle of sidespray with shell axis, deg.	Computed vel. side-spray due to explosive charge, f/s	Computed resultant vel. of sidespray, f/s
Static	Perf.	95.2	-	-
700	"	81.5	2930	2950
1085	"	73.9	2880	2980
1450	"	64.2	2530	2800
1685	"	62.0	2720	3070
2130	"	54.5	<u>2660</u>	3250

Ave. 2740

Static	Penet.	95.5	-	-
700	"	83.7	3400	3400
1085	"	76.8	3300	3370
1450	"	65.9	2680	2920
1685	"	65.3	3040	3330
2130	"	55.7	<u>2750</u>	3310

Ave. 3030

The average velocity of the perforations due to the explosive charge computed from the change in the sidespray angle is 2740 f/s while that of the penetrations is 3030 f/s. It appears plausible to assume that the greater initial velocity of the penetrations may be due to the difference in size, the penetrating fragments attaining a higher velocity because of smaller ballistic coefficients. While a measurement of the velocity of the dents was not obtained, they are presumably somewhat faster than the penetrations.

The resultant velocity of the sidespray is simply the vector sum of the velocity due to the charge and the remaining velocity of the shell. The remaining velocity does not contribute much to the resultant velocity up to shell velocities of 1085 f/s but at 1450 f/s and higher, the resultants are appreciably greater. It should be noted, however, that the resultant velocities were computed from the average angle of the sidespray with the shell axis. The highest resultant velocities would occur in the front part of the side spray band.

As the remaining velocity is increased the angular width of the side spray should decrease. For example, suppose that for static firing the sidespray of perforations is 25 deg. wide, is centered at 95 deg. with the shell axis, and that all the fragments have a velocity of 2740 f/s. Then, at 2130 f/s remaining velocity of the shell, it is calculated that the side spray band should be 16 deg. wide, a reduction of about 1/3. Referring to plots 1 to 6 showing perforations per unit solid angle, it appears that, although somewhat erratic, the width of the sidespray is just about the same on the average for all remaining velocities. It is suggested that the explanation may be spread in velocity of the fragments, because the slow fragments would be displaced more by remaining velocity than those having high velocity, which would tend to widen the side spray. In the example just cited, a variation of the ± 400 f/s from the average would be sufficient to keep the width of the band at 25 deg. at 2130 f/s shell velocity.

Resume

1. Four rounds were fragmented in sand pit tests, of which 2 rounds were fired with 3 calibers air space, 2 with 6 calibers. No appreciable difference in fragmentation effect was observed with regard to the air spacing. On the average, there were 779 fragments recovered per shell distributed as follows: 6 on the No. 1 screen, 272 on No. 2, 255 on No. 3, 142 on No. 4, and 104 through No. 4. The per cent of metal recovered averaged 95.6

2. The fragment densities in the sidespray as determined by panel tests were averaged over 35 deg. of arc. Considering the sidespray on Panel A, shell static, axis horizontal, there were about 1.5 perforations, 1.0 penetrations, and 2.4 dents per solid angle, making a total of 4.9 hits per unit solid angle. The number of hits per unit solid angle decreased with the distance, averaging 4.9, 3.9, 1.8, and 1.5 on the 15, 36, 75, and 120 ft. panels.

3. The average fragment densities in the base spray, Panel A, shell static, axis horizontal, were 1.8 perforations, 1.6 penetrations, and 6.3 dents per unit solid angle. The fragment densities in the nose spray under the same shell conditions were .4 perforations, 3.5 penetrations, and 12.2 dents per unit solid angle.

4. The general effect of remaining velocity as regards fragment density, appears to be as follows: Most of the base spray drops out due to reduced resultant velocity. The average density of the sidespray on the panels appears to be approximately constant with increase in shell velocity, although there should be some increase because of the crowding of the fragments into a smaller number of solid angles as the side spray is shifted forward. The fragment density in the nose spray increases somewhat with shell velocity which appears to be due to the displacement of adjacent fragments into the nose spray zone.

5. The fragment densities of the side spray on the panel of 15 ft. radius obtained with shell axis vertical check closely with those obtained with shell axis horizontal. Although firings with shell axis vertical appear to be excellent for obtaining the sidespray on a panel relatively close to the shell, the panel heights required are too large to be feasible as the distance becomes large.

6. The total number of fragments issuing from the shell computed from the fragment densities on the panels was about 5000, consisting of about 700 perforations, 900 penetrations, and 3400 dents. As the remaining velocity was increased, the total number of fragments determined by panel tests decreased appreciably.

7. As determined by the areas of the hits on the panels, it appears that the fragments of the base and side sprays have about the same distribution according to size. The nose spray fragments are distinctly larger than either the base or side sprays. The perforating fragments are considerably larger than the penetrations.

8. Comparing the number and sizes of fragments obtained in pit fragmentation tests with the panel tests, it appears that practically all the fragments obtained in pit tests would be perforating fragments in panel tests at 15 ft. distance, while the penetrations and dents in panel tests are unaccounted for in pit tests.

9. Considering the hits on the small sections of 1/4" armor plate hung in the sidespray on the 15 ft. panel, it appears that about 1/6 of the perforations on panels would be perforating against plates at 15 ft. distance. One perforation was obtained at 36 ft. distance indicating that the limiting distance of complete protection with 1/4" plate is greater than 36 ft.

10. The average velocity of the fragments in the side spray was computed from the change in the angle of the sidespray with remaining velocity. The computed velocity of the perforating fragments due to the explosive charge averaged 2740 f/s while that of the penetrations was 3030 f/s. The greater initial velocity of the penetrations is assumed to be due to their smaller ballistic coefficients.

N. A. Tolch

N. A. Tolch